THE MECHANISM OF TRIGLYCERIDE PARTITIONING – HOW THE ANGPTL3-4-8 SYSTEM OF PROTEINS ORCHESTRATES TISSUE ENERGY DISTRIBUTION

by

Thomas G. Pottanat

A Dissertation

Submitted to the Faculty of Purdue University

In Partial Fulfillment of the Requirements for the degree of

Doctor of Philosophy

Department of Biology at IUPUI

Indianapolis, Indiana

December 2020

THE PURDUE UNIVERSITY GRADUATE SCHOOL
STATEMENT OF COMMITTEE APPROVAL

Dr. Nicolas Berbari, Chair

Department of Biology

Dr. Robert Konrad, Co-Chair

Laboratory for Experimental Medicine, Eli Lilly & Company

Dr. Benjamin Perrin

Department of Biology

Dr. David Skalnik

Department of Biology

Approved by:

Dr. Theodore R. Cummins

To my Mira: You are never too old to create something new – forge ahead and change the world.

"Do not go where the path may lead, go instead where there is no path and leave a trail."

- *Ralph Waldo Emerson*

ACKNOWLEDGMENTS

As with any great accomplishment, many individuals have contributed to help me achieve this doctorate. Those that are listed here have always gone above and beyond to help me along this journey. To everyone, even if you are not listed, thank you for your support, encouragement, and help along the way.

I would first like to thank Jason Troutt and Jeff Cramer, who have had the privilege of being my directors at Lilly during the time I have spent working on this PhD. If not for both of you helping me to organize and balance my time between work, school, and home, I would never have gotten this far. You two have been inspiring leaders who I hope to emulate one day.

I would like to thank my coworkers in the Scientific Implementation Group at Eli Lilly & Company. All of you have always been ready to assist me when my work and school load became unbalanced or to support me in earnest when I needed words of encouragement. You are the best coworkers and friends I could have asked for.

I would like to thank Dr. Michael Hodsdon, Dr. Daniel Peterson, and Dr. Robert Siegel. Not only have you contributed to my dissection of scientific data or writing in one way or another, but you have been invaluable mentors to me. I have truly benefited from your mentorship both at school and at work.

I would like to thank Eugene Zhen, Ajit Regmi, and Dr. William Roell for your instruction and collaboration as we pursued an understanding of triglyceride metabolism. To Yan Q Chen, I owe you so much for all your help and instruction in learning how to dissect scientific literature and generate data. Your assistance in crafting my experiments during my attempts with primary hepatocytes greatly improved the value of the data generated from each experiment. Your skill in the lab is phenomenal, but your ability to distill and teach information is even greater.

I would like to thank Dr. Simon Atkinson and Dr. Bruce Molitoris. Without your initial trust in my scientific abilities, I would not have been able to start this journey towards earning my doctorate. Dr. Molitoris, I truly thank you for always making time to join committee meetings despite not being required to do so. I have always felt that your feedback during the meetings was crucial to knowing where to take the next steps and where to not step. Without heeding your guidance, I would still be spending my near future crafting data for a thesis. You have been instrumental in helping me focus my work.

I want to thank Dr. Nicolas Berbari for taking over when Dr. Atkinson left IUPUI. You have been a steady hand who has always been ready to not only provide guidance on the science I presented you, but you have also been quick to answer a phone call from a nervous graduate student who didn't work on campus. I have relied on you heavily to ensure my successful completion of this program. Without your quick responses, I would not have gathered the remainder of the committee on such short notice to be able to allow for a successful preliminary examination.

To Dr. David Skalnik and Dr. Benjamin Perrin, thank you for participating in my committee without ever having met me. I have appreciated our discussions about my work. I have also felt that questions from both of you have made me assess specific experiments with care – specifically my affinity studies using the Octet system.

To Dr. Robert Konrad, your encouragement for me to start this graduate program and continual support throughout my career and this educational journey has been instrumental in my development. While you have always been a teacher to me, my time as your graduate student has allowed me to learn even more from you about how to conduct science. You have taught me to focus on the big picture, to think critically about experiments, to dissect literature with some skepticism, and to always share science through a gripping story. Thank you for everything you have done for me and for allowing me to be part of the team which helped to create a unified model for triglyceride metabolism.

To my wife Neha, thank you for your support through this journey. From reading my writings, to taking care of dinner, and now taking care of Mira, while I seclude myself to keep working – I would not have been able to do this without your help.

Lastly, I would like to thank the Eli Lilly – IUPUI LGRAD program for providing me the means and opportunity to pursue a graduate degree. Without having the financial backing and support from this company, I may not have decided upon this path in my life and career. The LGRAD program has indeed changed my future.

TABLE OF CONTENTS

LIST OF TABLES

LIST OF FIGURES

LIST OF ABBREVIATIONS

ANGPTL3	Angiopoietin-like protein 3
ANGPTL3/8	Angiopoietin-like protein 3/ angiopoietin-like protein 8 complex
ANGPTL4	Angiopoietin-like protein 4
ANGPTL 4/8	Angiopoietin-like protein 4/ angiopoietin-like protein 8 complex
ANGPTL8	Angiopoietin-like protein 8
ANGPTL	Angiopoietin-like proteins
Apo	Apolipoproteins
BIL	Basal insulin peglispro
BCA	Bicinchoninic acid
BMI	Body Mass Index
BSA	Bovine serum albumin
CVD	Cardiovascular disease
cm	Centimeter
CTAD	C-terminal domain-containing
CMV	Cytomegalovirus
dL	Deciliter
DNA	Deoxyribonucleic acids
DMP	Dimethyl pimelimidate
DTT	Dithiothreitol
DMEM	Dulbecco's Modified Eagle Media
EU	Endotoxin units
ELISA	Enzyme linked immunosorbent assays
EGIR	European Group for The Study of Insulin Resistance
FA	Fatty acids
FBS	Fetal bovine serum
GR	Glucocorticoid receptor
GIP	Glucose-dependent insulinotropic peptide

GPIHBP1	Glycosylphosphatidylinositol-anchored high-density lipoprotein-binding protein 1
IC_{50}	Half maximal inhibitory concentration
HDL	High density lipoprotein
HDL-C	High density lipoprotein cholesterol
hrs	Hours
HAS	Human serum albumin
HTG	Hypertriglyceridemia
Ig	Immunoglobulin
kD	Kilodalton
kV	Kilovolt
KO	Knockout
LDLR	LDL receptor
LPL	Lipoprotein lipase
LC-MRM	Liquid chromatography–multiple reaction monitoring
LXR	Liver x receptor
LOF	Loss-of-function
LDL	Low density lipoprotein
LDL-C	Low density lipoprotein cholesterol
m/z	Mass to charge ratio
Hg	Mercury
MSD	Mesoscale discovery
mRNA	Messenger ribonucleic acid
MetS	Metabolic syndrome
µg	Microgram
µl	Microliter
µm	Micrometer
µM	Micromolar
ms	Millisecond
mg	Milligram
mL	Milliliter

mm	Millimeter
mM	Millimolar
min	Minutes
M	Molar
ng	Nanogram
nm	Nanometer
nM	Nanomolar
Ni-NTA	Nickel-nitrilotriacetic acid
n	Number
ppm	Parts per million
PBS	Phosphate buffered saline
PECF	Phosphoethanolamine-n-carboxyfluorescein
PTM	Post-translational modifications
PPAR	Proliferator-activated receptor
RNA	Ribonucleic acids
s	Second
SE1	Specific epitope 1
SEC	Size exclusion chromatography
siRNA	Small interfering RNA
SIL	Stable-isotope-labeled
SEM	Standard error of the mean
TG	Triglyceride (or triglycerides)
TBS	Tris buffered saline
T2DM	Type 2 diabetes mellitus
VH	Variable heavy
VL	Variable light
VLDL	Very low-density lipoproteins
VLDLR	VLDL receptor
WHO	World Health Organization

LIST OF SYMBOLS

α	Alpha
~	Approximately
β	Beta
°C	Degrees Celsius
γ	Gamma
μ	Micro

ABSTRACT

The incidence of Metabolic Syndrome (MetS) is increasing worldwide and accompanied by elevated risks for cardiovascular disease (CVD) and other subsequent comorbidities. MetS is associated with increased circulating triglycerides. A key enzyme involved in triglyceride (TG) clearance is lipoprotein lipase (LPL) whose activity is modulated by a variety of factors.

Recent literature has identified the importance of angiopoietin-like proteins (ANGPTL) as regulators of LPL activity and has hypothesized a model in which three of these proteins interact with LPL to regulate the partitioning of TG metabolism from adipose to skeletal muscle. The work detailed in this dissertation adds to the model of ANGPTL regulation of LPL by establishing how ANGPTL8 modulates the ability of ANGPTL3 and ANGPTL4 to inhibit LPL activity in the bloodstream and localized environments, respectively.

In the updated model, elevated insulin concentrations result in increased hepatic ANGPTL3/8 secretion and increased ANGPTL4/8 in adipose tissue. ANGPTL3/8 works as an endocrine molecule to inhibit skeletal muscle LPL from hydrolyzing circulating TG. Simultaneously, ANGPTL4/8 works in a paracrine mechanism to bind LPL on the endothelial vasculature adjacent to adipose tissue to alleviate ANGPTL4-mediated LPL inhibition and also prevent ANGPTL3/8 inhibition of localized LPL. Thus, in the postprandial state free fatty acids (FFA) from the hydrolysis of TG are directed into adipocytes for storage.

Under fasting conditions, ANGPTL8 production is decreased in adipocytes and hepatocytes. This decreased production results in diminished ANGPTL4/8 and ANGPTL3/8 secretion from their respective tissues. As a result, ANGPTL4 inhibits adipocyte localized LPL activity while ANGPTL3 at physiological concentrations has minimal effect on LPL activity. Furthermore, any ANGPTL3/8 which is produced has its LPL-inhibitory ability diminished by the circulating apolipoprotein ApoA5. LPL is more active in skeletal muscle compared to adipose tissue where energy is shunted towards utilization in the muscle and away from storage in adipose tissue. A complete understanding of LPL regulation by ANGPTL proteins can potentially provide therapeutics targets for MetS.

CHAPTER 1. INTRODUCTION

1.1 Triglycerides

Triglycerides (TG), also known as triacylglycerols, are comprised of three fatty acids connected via ester bonds to a glycerol backbone (1). TG play an important role in maintaining human homeostasis – especially for the storage of excess energy. In fact, up to 85% of stored energy is in the form of TG (1). More importantly, fatty acids (FA) in TG provide around 70% of the energy needs for the heart (2). Because of their hydrophobicity, TG circulate as part of triglyceride rich lipoprotein particles (TRL) – most commonly as very low density lipoprotein (VLDL) and chylomicrons (3). VLDL is produced in the liver whereas chylomicrons are TRL derived from dietary fats (4-6). However, in certain conditions, such as Metabolic Syndrome (MetS), dysregulation of TG homeostasis is associated with cardiovascular disease (CVD).

1.2 Metabolic Syndrome and associated hypertriglyceridemia

MetS is a compilation of risk factors, such as hypertension, elevated TG, and reduced high-density lipoprotein cholesterol (HDL-C), which have all been directly correlated to CVD (7). MetS, also known as Syndrome X or Insulin-resistance Syndrome, has been shown to increase the risk for CVD by 235% (8) Identified over six decades ago, MetS has only recently garnered attention from public health professionals as the consequences of MetS slowly expand into a worldwide epidemic (8).

Over the past three decades, the definition for MetS has changed multiple times. While first called Syndrome X in 1988, MetS or Insulin-resistance Syndrome was clinically defined by the World Health Organization (WHO) in 1998. Subsequently, this initial definition was modified by the European Group for the Study of Insulin Resistance (EGIR) (9, 10). EGIR identified insulin resistance as the major cause of MetS and required it for diagnosis (10). The EGIR definition included elevated circulating insulin levels along with two additional comorbidities (abdominal obesity, hypertension, elevated TG, reduced HDL-C, or elevated glucose) (9). The National Cholesterol Education Program's Adult Treatment Panel III altered this definition by no longer requiring the presence of insulin-resistance in all cases, but rather needing three factors concomitantly (abdominal obesity, elevated TG, reduced HDL-C, elevated blood pressure, and

increased fasting glucose) (7). In 2003, the American Association of Clinical Endocrinologists further altered the definition to re-instate insulin resistance as the primary cause. Then in 2005, the International Diabetes Foundation determined that abdominal obesity was required for diagnosis of MetS along with two other comorbidities (elevated TG, reduced HDL-C, elevated blood pressure, and increased fasting glucose) (7). Currently, diagnosis of MetS requires TG above 150 mg/dL, blood glucose above 100 mg/dL, HDL-C below 40 mg/dL in men or below 50 mg/dL in women, systolic blood pressure above 130 mm Hg with a diastolic blood pressure above 85 mm Hg, and waist circumference greater than 40 inches in men or greater than 35 inches in women (3, 7, 11).

Obesity, as found in MetS and which strongly correlates with insulin resistance, has been increasing in the United States where approximately two-thirds of the population is obese and a third of the population have MetS (6, 7, 9). Moreover, as obesity becomes more endemic in adolescents (17% prevalence), current trends in the United States demonstrate that MetS is also increasing in adolescents – a risk which only increases with age (11-13).

MetS treatments are specifically targeted to reduce the risk for CVD and decrease obesity (7). The primary approach is implementation of lifestyle changes designed to reduce consumed calories and to increase regular physical activity (11, 14). The recommended dietary guidelines call for reductions in fat and simple sugars combined with increases in dietary fiber (11). If such changes are insufficient, therapeutic approaches to reduce hyperlipidemia, diabetes, and hypertension are attempted (7). Pharmacologic approaches have utilized fibrates and nicotinic acid which can raise HDL-C and reduce TG. In extreme cases, bariatric surgery may provide beneficial improvements (15).

Within MetS, hypertriglyceridemia (HTG) is a common finding (6). In essence, HTG is a result of a decrease in TG-rich lipoprotein lipolysis, an increase in TG-rich production, or a combination of both (3). The Endocrine Society has defined moderate HTG as fasting TG levels from 200 to 999 mg/dL and severe HTG for 1000 to 1999 mg/dL. Anything above 2000 mg/dL is defined as very severe HTG (3, 6). HTG can be defined as primary or secondary HTG. In relation to obesity and insulin resistance, HTG is categorized as secondary (3). While most measurements of HTG are performed when the patient is fasting, recent publications have demonstrated that non-fasting HTG is more predictive of CVD and its associated events, including death (16, 17).

Similar to the treatment of MetS, HTG treatment focuses on lifestyle changes prior to the addition of therapeutics. Of the possible therapeutics, fibrates, niacin, and n-3 fatty acids are pursued (3). Fibrates can reduce TG somewhat but have not demonstrated a reduction in CVD events or deaths (3). Fibrates increase lipoprotein lipase (LPL) synthesis and decrease very low VLDL (3). n-fatty acids have been found to reduce CVD risk in two trials (Cardiovascular Events with Icosapent Ethyl–Intervention Trial [REDUCE-IT] and Japan EPA Lipid Intervention Study [JELIS]) (18, 19).

1.3 Lipoprotein Lipase

TG are hydrolyzed by LPL to produce monoacylglycerol and non-esterified free fatty acids (FA) (2, 5, 20-22). Originally, described in dogs given heparin, active LPL, or clearing factor lipase, is a dimer of two glycosylated 55 kilodalton (kD) subunits arranged in a head-to-tail manner (2, 23-30). LPL consists of a signal sequence at the N-terminus, a catalytic domain consisting of Ser159, Asp183 and His226, a lid covering the active site, and a C-terminal domain (29-32). LPL is produced in parenchymal cells which include myocytes, adipocytes, and fetal hepatocytes. However, in the human adult liver, LPL is not produced (2, 29, 30). Lipase maturation factor promotes the maturation of LPL within the endoplasmic reticulum and is necessary for its post-translational activation (6, 14, 33). Upon maturation, LPL is transported to the luminal side of capillary endothelium by glycosylphosphatidylinositol-anchored high-density lipoprotein-binding protein 1 (GPIHBP1) (5, 6, 20, 34, 35). GPIHBP1 stabilizes LPL but does not activate it (36). LPL on the capillaries of skeletal and cardiac muscle allows for hydrolysis of TG-rich lipoproteins for energy utilization and, in adipose tissue, integration for energy storage (5).

In adipose tissue, LPL is upregulated by cortisol, dexamethasone, insulin, peroxisome proliferator-activated receptor gamma (PPARγ), and gastric inhibitory peptide (GIP) (5, 37-39). However, during fasting, LPL activity in skeletal and cardiac muscle is increased (5, 37-39). An increase in endothelial LPL is found throughout the body during times of fasting (37, 40).

LPL expression has also been shown to be elicited by insulin during the cephalic phase of insulin secretion. Insulin does not change LPL messenger ribonucleic acid (mRNA) expression dose dependently. However, insulin demonstrates a dose-dependent effect on LPL enzymatic activity (41, 42). The changes in LPL localization during fasting and postprandial states are not necessarily due to increased mRNA expression, but rather due to sequestration of circulating

unbound LPL (43). The mechanism for how insulin alters LPL enzymatic activity is the underlying focus of this dissertation.

The first human mutation in LPL was identified in 1989, and since then over 114 mutations have been described. Most commonly, LPL related genetic disorders occur in exons coding the catalytic domains and result in the elimination of LPL activity and subsequent development of HTG (2, 44). Some of these loss-of-function (LOF) variants have also been linked to increased risk for CVD events (6, 45). For example, the Asn291Ser mutation has been linked to a 31% increase in TG and a reduction in HDL-C (2). In line with such findings, animal models which have null mutations in LPL have HTG (30- to 50-fold above normal) and die shortly after birth (46-48). Conversely, overexpression of LPL reduces TG by 75% and prevents diet-induced HTG (49, 50). S447X is a mutation which initially was believed to be a gain of function mutation with respect to TG metabolism. Individuals with this mutation have reductions in circulating TG, lower VLDL, increased HDL-C, and a reduced risk for CVD events (51-55). However, S447X does not affect the TG hydrolysis activity of LPL, but rather enhances hepatic lipoprotein cholesterol uptake (55). The decrease in cholesterol containing particles likely drives the reduction of CVD risk.

GPIHBP1, the protein required for translocation of LPL to the endothelial luminal surface, has been shown to be important for LPL localization and function (34, 56-59). Knockout (KO) GPIHBP1 mice exhibit chylomicronemia, severe HTG, and reduced LPL activity (60, 61). Reported in 15 families, the Q115P GPIHBP1 mutation, is associated with HTG due to chylomicronemia (62, 63). This mutation alters how GPIHBP1 is able to bind with LPL (36, 63). Other mutations in GPIHBP1 have been shown to be associated with increased HTG (61, 63). GPIHBP1 transcription was found to be increased in heart and adipose tissue during fasting and reduced after refeeding (60, 61). High fat diets tend to increase GPIHBP1 expression in adipose, skeletal, and hepatic tissues (60). These findings have suggested that while GPIHBP1 is increased during fasting, other mechanisms must control how the associated LPL functions in these different tissues (60).

Most regulation of LPL activity appears to be post-transcriptional with striking differences occurring upon fasting, postprandial uptake, and exercise (5, 64, 65). This regulation is most apparent in skeletal and adipose tissue (64, 66, 67). Of the proteins which can regulate LPL, apolipoproteins (Apo) C1, C2, C3, A5, and E are currently being studied. ApoC2 activates LPL and is a component of VLDL (4, 68-70). ApoC1 and ApoC3 are inhibitors of LPL (3, 6, 71).

Another group of proteins named the angiopoietin-like proteins (ANGPTL) also regulate LPL – specifically ANGPTL3, ANGPTL4, and ANGPTL8 and are the focus of my research (5, 6).

1.4 Angiopoietin-like Proteins

1.4.1 ANGPTL3 and ANGPTL4

ANGPTL3 and ANGPTL4, have both been shown to be inhibitors of LPL. They are secreted proteins with 31% homology (72-76). They both contain an N-terminal coiled-coil domain containing the specific epitope 1 (SE1) region known to inhibit LPL enzymatic activity (77, 78). They also both contain a C-terminal fibrinogen-like domain and are found both as full length and truncated N-/C- terminal fragments in plasma (72, 73, 78-80). Both proteins circulate as higher order oligomers (79, 81, 82).

ANGPTL3 and ANGPTL4 KO mice display hypotriglyceridemia due to increased LPL activity and hydrolysis of VLDL from the circulation (74, 76, 78, 83-86). In contrast, overexpression of ANGPTL3 or ANGPTL4 led to HTG and increased cholesterol (75, 87, 88). LPL activity is elevated in both ANGPTL3 KO (postprandially) and ANGPTL4 KO mice (fasting and postprandial) (74, 80, 89). However, each protein, works via an independent mechanisms as ANGPTL4 KO demonstrated lower TG when a monoclonal antibody to ANGPTL3 was administered (mAb 5.50.3) and an ANGPTL3 KO demonstrated similar results with a monoclonal antibody to ANGPTL4 (14D12) (90). Based on *in vitro* assays, ANGPTL4 is a more potent inhibitor of LPL (~100x) compared to ANGPTL3 (90). In fact, the concentrations of ANGPTL3 required for substantial inhibition of LPL are supraphysiological (91). This conundrum regarding the relatively weak inhibition of ANGPTL3 in comparison to ANGPTL4 will be addressed in Chapter 2 of this dissertation.

GPIHBP1 decreases the inhibition from ANGPTL3 and ANGPTL4 (36). It reduces the ANGPTL4 inhibition by 20% and ANGPTL3 by 40% (36). GPIHBP1 KO mice have elevated TG levels as LPL is likely destabilized. However, when one functional ANGPTL4 allele is knocked out in these mice, TG levels drop by 33% relative to the GPIHBP1 KO mice. When both ANGPTL4 alleles are nonfunctional in the GPIHBP1 KO mice, TG drop 93% relative to the GPIHBP1 KO mice with two functional ANGPTL4 alleles. Taken together, this data suggests that without GPIHBP1, ANGPTL4 can suppress LPL enzymatic activity to a large extent and that

GPIHBP1 acts as a protector against ANGPTL4 mediated LPL inhibition. (36). However, the TG concentrations of ANGPTL3 and GPIHBP1 double KO animals were only slightly lower than GPIHBP1 KO alone suggesting that ANGPTL3 is not as profound of an inhibitor of LPL. Administration of neutralizing antibodies to ANGPTL3 or ANGPTL4 in GPIHBP1 KO mice reinforced the findings from analysis of the genetic models (36). When double ANGPTL3 and ANGPTL4 KOs are generated, there is a loss in progeny and an increase in perinatal mortality. Surviving double KO mice did not live past 2 months and had nearly undetectable TG levels (74).

ANGPTL3 was discovered through investigation of the KK/San obese mouse. These mice display abnormally low lipid levels despite an obese/diabetic profile (83, 92). ANGPTL3 is a 460 amino acid protein which, as stated above, contains the N-terminal SE1 domain, a linker region, and a C-terminal fibrinogen binding domain (72). ANGPTL3 appears to be constitutively expressed in the liver and is inducible by liver X receptor (LXR) ligands (93-95). ANGPTL3 mRNA does not appear to be altered by nutritional state but is upregulated in human subjects with insulin-resistance (96). Interestingly, ANGPTL3 does not appear to correlate with circulating TG, but it does appear to regulate TG uptake in peripheral tissues postprandially (97, 98).

Two ANGPTL3 mutations have been associated with hypolipidemia: E129X and S17X. Individuals with either of these mutations exhibit losses in low density lipoprotein cholesterol (LDL-C), HDL-C, and low TG (99, 100). The presence of a loss of function ANGPTL3 variant provides a 34-41% lowered risk of CVD, depending on the study (101-103). In the Dallas Heart Study population, individuals (5% of African Americans in the study) expressing the M259T mutation had lower TG. Moreover, this M259T variant failed to suppress LPL activity (100). Mimicking human findings, ANGPTL3 KO mice have lower TG and post-heparin LPL activity (104). Mice overexpressing ANGPTL3 demonstrate postprandial HTG(74, 104). In ANGPTL3 KO mice, peripheral LPL activity was 9-fold higher postprandially – this effect was not seen during fasting (74). Two monoclonal antibodies against ANGPTL3, REGN1500 and mAb 50.5.3 reduced serum TG in a manner similar to ANGPTL3 KO mice (77, 105). Together, these data on ANGPTL3 demonstrate its role in inhibiting LPL; however, these data do not address why ANGPTL3 therapeutic interventions and knockouts predominantly affect postprandial TG levels.

ANGPTL4 has gone by other monikers including peroxisome proliferator-activated receptor (PPAR) angiopoietin related protein, fasting-induced adipose factor, and hepatic fibrinogen angiopoietin-related protein (73, 76, 106, 107). ANGPTL4 is predominantly expressed in the

intestine and adipose tissue with some expression detected in cardiac, hepatic, and renal tissues (73, 106, 107).

Fasting increases ANGPTL4 in adipose tissue where it is released as a full-length protein (82, 108). ANGPTL4 mRNA is upregulated by PPAR agonists and by hypoxia whereas its mRNA is repressed by leptin (73, 106, 107, 109-112). Interestingly, ANGPTL4 expression increases in acute exercise in non-exercised tissue to shunt fatty acid energy utilization to exercising tissue (113, 114).

The reduction in adipose LPL activity during fasting is a direct result of ANGPTL4 expression (115). The mechanism whereby ANGPTL4 inhibits LPL is still debated. Some research points to ANGPTL4 inducing a conformational unfolding of the catalytic hydrolase domain (80, 116). Other researchers have identified that ANGPTL4 dissociates the LPL dimer creating inactive monomers (90, 117). Still others have said that ANGPTL4 is a reversible, non-competitive inhibitor of LPL (118). Regardless, the mechanism of how ANGPTL4 inhibits LPL predominantly during the fasting state remains unclear and will be addressed in Chapter 2 of this dissertation.

ANGPTL4 associations with circulating TG are debatable – often due to discrepant commercial enzyme linked immunosorbent assays (ELISA) (119). However, genetic studies have identified correlations. One ANGPTL4 mutation, E40K, which is present in approximately 3% of European Americans, is associated with lower TG and higher HDL-C. Depending on the study, the E40K mutation was associated with a 15-30% reduction in circulating TG (120). Upon *in vitro* investigation, the E40K mutation blunts the ability of ANGPTL4 to associate with and inhibit LPL (77, 90, 116).

Overexpression of ANGPTL4 in animal models results in increased TG regardless of mechanism (e.g. adenoviral or transgene) (74, 76, 81, 87, 121, 122). Overexpression of ANGPTL4 resulted in decreased clearance of chylomicrons 24 hours postprandially and increased TG-rich VLDL (74, 81, 87, 88). Similarly, infusion with recombinant ANGPTL4 increases TG by 3- to 5-fold after 30 minutes. Interestingly, organ specific overexpression of ANGPTL4 has suggested a paracrine effect for ANGPTL4 inhibition of LPL (74, 121).

ANGPTL4 KO mice demonstrate a 65-90% lowering in fasting TG and a 70% postprandial TG reduction (74, 84, 123). Animals treated with 14D12, a monoclonal neutralizing antibody against ANGPTL4, lowered fasting TG by 50% (77, 84). However, both ANGPTL4 KO mice and

those receiving the therapeutic antibody demonstrated lipogranulomatous lesions in intestinal lymph nodes (84).

It is important to note that ANGPTL4 is expressed throughout the small intestine where it may be involved in the regulation of luminal intestinal/pancreatic lipase by ANGPTL4 (124). Pancreatic lipase hydrolyzes dietary TG to allow released FA to be absorbed by enterocytes where they will be repackaged into TG and subsequently packaged into chylomicrons containing ApoB48 (125, 126). Afterwards, chylomicrons are released into surrounding lymph to enter circulation at the thoracic duct (125, 126).

Taken together, it appears that ANGPTL4 may inhibit pancreatic lipase to regulate the influx of FA into the enterocytes (124). ANGPTL4 KO mice demonstrated enhanced intestinal lipase activity. However, these mice exhibited no change in TG release from the intestine into circulation. Thus, inhibition or deletion of ANGPTL4 results in enhanced dietary TG uptake by the intestine without a corresponding change to TG secretion – in turn, leading to the accumulation of fat in intestinal lymph nodes.

1.4.2 ANGPTL8

In 2012, three separate groups identified another protein responsible for modulating LPL activity, ANGPTL8 (also known as TD26, hepatocellular carcinoma associated gene, C19orf80, refeeding-induced fat and liver betatropin, and lipasin) (127-129). ANGPTL8 shares 20% of its N-terminal domain with ANGPTL3 and ANGPTL4 but lacks the C-terminal fibrinogen-binding domain (127, 129). ANGPTL8 is expressed in hepatic and adipose tissue. Its expression appears to be nutritionally regulated as reductions are seen upon fasting and raised by refeeding (128, 129). However, correlations of ANGPTL8 with MetS parameters has been difficult to ascertain (130-133).

Insulin increases ANGPTL8 mRNA in both adipocytes and hepatocytes in a dose dependent manner at concentrations as low as 1 nM (127, 134). Insulin combined with elevated glucose increased ANGPTL8 mRNA more dramatically than insulin only (134). ANGPTL8 expression in hepatocytes is also increased with palmitic acid, tunicamycin, and T0901317 (liver X receptor alpha [LXRα] agonist) (134, 135). ANGPTL8 mRNA, however, is very unstable and expression is altered rapidly when fasting and postprandially. While LXRα induces mRNA expression,

glucocorticoid receptor (GR) appears to downregulate mRNA transcription (135). The effect of LXR agonism on TG levels will be investigated in Chapter 3 of this dissertation.

In 2013, ANGPTL8, then termed betatrophin, was identified as a hormone which induced pancreatic beta cell proliferation (136). This paper was later retracted after multiple studies demonstrated that both KO mice and mice overexpressing hepatic ANGPTL8 maintained normal beta cell expansion (137, 138). These studies, however, did identify that ANGPTL8 KO animals have lower TG levels whereas overexpression of hepatic ANGPTL8 increases TG (128, 137, 138). For animals in which ANGPTL8 was overexpressed, the increase in TG was more pronounced during fasting (139). Using different methods to induce ANGPTL8 KO animals, it has been demonstrated that the reduction in body weight and plasma TG coincide with increases in β-oxidation in skeletal muscle (140).

Further validation of these animal models came from human genetic studies which identified a rare (~1 in 1000 individuals) loss of function mutation Q121X (141). Carriers of this mutation demonstrated a 15% reduction in TG and increased HDL; however, it is unclear if the mutation is cardioprotective due to the study being underpowered (141). Moreover, no change in fasting glucose or risk for type 2 diabetes mellitus (T2DM) was seen in these individuals possibly for the same aforementioned reason (142). Another mutation, R59W, was identified in three populations and correlated with reduced LDL-C and HDL-C. However, this mutation is not associated with circulating TG (129).

Antibodies which neutralize ANPGTL8 have been shown to reduce TG. In 2017, Regeneron demonstrated that its ANGPTL8 antibody (REGN3776) decreased TG, body weight, and fat content in mice expressing humanized ANGPTL8 and duplicated the effect in dyslipidemic cynomolgus monkeys (143, 144). Specifically, REGN3776 reduced serum TG by 60% in the humanized mice and 65% in dyslipidemic monkeys (143, 144). Another antibody, AB-2, was found to reduce postprandial TG by 40% via increased LPL activity in the heart and skeletal muscle (139).

Interestingly, recombinant ANGPTL8 fails to inhibit LPL to a great degree despite containing a similar SE1 region as ANGPTL3 and ANGPTL4 (144, 145). However, ANGPTL8 has been shown to circulate as a part of a large protein complex (129). In line with these findings, when LPL binding fragments of ANGPTL8 and ANGPTL3 are refolded together, a 3-fold increase is seen on LPL inhibition when compared to ANGPTL3 alone. Conversely, when fragments of

ANGPTL8 and of ANGPTL4 are refolded together,ANPGTL4 had less ability to inhibit LPL activity (117). Interestingly, the ANGPTL3 and ANGPTL8 complex (ANGPTL3/8) inhibits LPL activity by 80% - the same magnitude as ANGPTL4 alone (117). It is suggested that ANGPTL3 changes the confirmation of ANGPTL8 so that the ANGPTL8 SE1 region is available to inhibit LPL or that ANGPTL8 activates ANGPTL3 (129, 144). This ANGPTL3/8 complex appears to be formed within the cell and then secreted into the circulation (91). Further clarification of ANGPTL8 and its interactions with other ANGPTL proteins will be investigated in Chapter 2 of this dissertation.

While overexpression of ANGPTL8 increases TG, ANGPTL8 expression in ANGPTL3 KO mice fails to elicit any change in TG (129, 144). Interestingly, expression of ANGPTL3 in ANGPTL8 KO mice slowly increased plasma TG due to ANGPTL3's latent LPL inhibitory potential (144). Overexpression of both ANGPTL3 and ANGPTL8 induce HTG to a greater extent than that seen with ANGPTL3 overexpression alone (144). Liver- and adipose-specific ANGPTL8 KO mice display different phenotypes (146). When hepatically knocked out, ANGPTL8 does not appear in circulation – a finding similar to that found in systemic ANGPTL8 KO mice (146). TG were also reduced in the liver-specific ANGPTL8 KO mice. However, postprandial TG levels were increased in the adipose-specific KO mice despite post-heparin LPL activity remaining similar to that of wildtype animals (146). Together these complex genetic and pharmacological data surrounding the functions of ANGPTL8 suggest a role in which ANGPTL8 activity is preferential for muscle or adipocyte localized LPL depending on nutritional status. It also strongly suggests that ANGPTL3 may be a key component necessary for the LPL inhibition result from ANGPTL8 overexpression. The work outlined in Chanter 2 of this dissertation will further explore the nutritional regulation of ANGPTL8.

1.5 Conclusions

Taken together, the data presented in the literature hints at a regulated system for postprandial TG metabolism through interactions with the ANGPTLs and LPL. Postprandially, ANGPTL8 appears to act in concert with ANGPTL3 to circulate and inhibit LPL in an endocrine manner (4, 146, 147). Conversely, in the fasted state, ANGPTL4 appears to be upregulated but only inhibits adipose LPL. The purported ANGPTL3/8 complex is downregulated during fasting

allowing skeletal and cardiac utilization of circulating TG/VLDL (4, 127, 146, 147). A complete understanding of this system remains unknown.

The work outlined in this thesis details experiments which expound upon the function and regulation of ANGPTL8 during both fasting and fed states. In Chapter 2, we will demonstrate with certainty that ANGPTL8 interacts with ANGPTL3 and ANGPTL4 separately postprandially. Increased by postprandial insulin and glucose-dependent insulinotropic peptide (GIP), the ANGPTL4 and ANGPTL8 complex inhibits LPL in a localized manner around adipocytes due to interactions with heparin proteoglycans. This complex also appears to prevent circulating ANGPTL3 complexed with ANGPTL8 from inhibiting adipocyte localized LPL. In Chapter 3, we will expound upon how another protein apolipoprotein A5 can interact with the ANGPTL3-4-8 system to further regulate the partitioning of fatty acids. We will also explore how LXR agonists cause HTG after administration.

CHAPTER 2. ANGIOPOIETIN-LIKE PROTEIN 8 DIFFERENTIALLY REGULATES ANGPTL3 & ANGPTL4 DURING POSTPRANDIAL TISSUE PARTITIONING OF FATTY ACIDS

A modified version of this chapter has already been published in the Journal of Lipid Research. [Chen YQ, Pottanat TG, Siegel RW, Ehsani M, Qian YW, Zhen EY, Regmi A, Roell WC, Guo H, Luo MJ, Gimeno RE, Van't Hooft F, Konrad RJ. Angiopoietin-like protein 8 differentially regulates ANGPTL3 and ANGPTL4 during postprandial partitioning of fatty acids. J Lipid Res. 2020 Aug;61(8):1203-1220. doi: 10.1194/jlr.RA120000781.]

2.1 Introduction

As humans evolved, the greatest survival threat was insufficient caloric intake (148-152). Our predecessors therefore relied on mechanisms that during times of starvation could direct fatty acids (FA) toward skeletal muscle to provide energy to hunt for food. Similarly, they relied on mechanisms that, during relatively rare periods of caloric availability, could reduce FA uptake into skeletal muscle and shift FA toward adipose tissue for storage as triglycerides (TG) to prepare for future periods of famine. These mechanisms allowed hominids to survive food scarcity. In a modern world of caloric abundance, however, the result is an unprecedented increase in metabolic syndrome and its related co-morbidities (153-156).

Metabolic syndrome includes elevated TG, decreased high density lipoprotein (HDL), obesity, hypertension, and insulin resistance/impaired glucose tolerance (156). This constellation of abnormalities predisposes not only to type 2 diabetes and increased cardiovascular disease, but also to an increased risk of peripheral vascular disease, non-alcoholic fatty liver disease, and several types of cancer (157-164). It is currently estimated that two-thirds of the US population is overweight, and that one-third suffers from metabolic syndrome (165-170). At its most basic level, metabolic syndrome manifests as dysregulated lipid metabolism resulting in increased TG with excessive FA storage (as TG) in adipose tissue (171). Increased TG are associated with decreased HDL, although the exact mechanisms have not been fully elucidated (172, 173). The excess adiposity causes insulin resistance (mainly in skeletal muscle through incompletely understood mechanisms) and hypertension (by increasing the arterial resistance) (174-184).

In the present study, we examine the role that angiopoietin-like protein 8 (ANGPTL8), a novel protein implicated in TG metabolism (4, 91, 127, 128, 138-140, 143, 144, 185, 186), plays

in metabolic syndrome. ANGPTL8 is the most recently discovered member of the ANGPTL3/4/8 family of proteins involved in lipoprotein lipase (LPL) regulation (91, 128, 129, 139, 144, 145). LPL is the enzyme responsible for conversion of TG (contained in lipoproteins) into FA that can be taken up into tissues such as skeletal muscle and fat (22, 187-190). In general, increased LPL activity is thought to be beneficial as it would decrease circulating TG. ANGPTL3 and ANGPTL4 have been previously described as LPL inhibitors, and their inhibitory mechanisms have been at least partially characterized (4, 36, 77, 116, 129, 191-198). In addition, ANGPTL3 has been shown to be an inhibitor of endothelial lipase (EL), the enzyme which hydrolyzes phospholipids (PL) in PL-rich HDL (86, 191).

ANGPTL3 knockout mice have been characterized as having decreased circulating TG (97, 104). In humans, ANGPTL3 knockout mutations are associated with decreased TG, decreased HDL (possibly due to increased EL activity), and decreased low-density lipoprotein cholesterol (LDL-C) via unknown mechanisms (99, 102, 199). Humans with ANGPTL3 mutations have a reduced risk of cardiovascular events, presumably due to decreased TG and LDL-C (199, 200). ANGPTL4 knockout mice demonstrate decreased TG and an increased risk of intestinal lymphatic toxicity when placed on a high fat diet (likely due to ANGPTL4 protecting against excessive saturated fatty acid uptake) (84, 201, 202). In humans, the ANGPTL4 E40K mutation has been associated with decreased TG, increased HDL, and a decreased risk of cardiovascular events (203-206). In a large human genetic study, review of medical records found no evidence of intestinal lymphadenopathy in 17 individuals homozygous for the ANGPTL4 E40K mutation, while no subjects were identified that were either homozygotes or compound heterozygotes for ANGPTL4 complete loss of function mutations (207).

ANGPTL8 was originally described as an atypical ANGPTL protein lacking the fibrinogen-like C-terminal domain present in other ANGPTL members (129). Subsequent reports showed that its overexpression in mice resulted in increased TG and that the effect was dependent upon ANGPTL3, indicating that the two proteins may work together in some way (91, 144). ANGPTL8 knockout mice were described as having decreased circulating TG (especially after re-feeding) as well as reduced fat mass (138, 140). In humans, an ANGPTL8 knockout mutation has been associated with decreased TG, decreased LDL-C, and increased HDL. However, because the mutation is very rare, the study was not sufficiently powered to assess cardiovascular protection (141). Recently, Zhang described an elegant ANGPTL3/4/8 model in which the three proteins are

postulated to work together to move FA either toward the adipose tissue or skeletal muscle under feeding or fasting conditions, respectively (4). Using a mammalian expression system, Chi and colleagues demonstrated that ANGPTL8 complexed with ANGPTL3, greatly enhanced the ability of ANGPTL3 to bind to and inhibit LPL, and required complex formation to be secreted efficiently (91). Very recently, Kovrov and colleagues built upon these concepts by further exploring possible ideas for how ANGPTL8 might work together with both ANGPTL3 and ANGPTL4 to partition FA between adipose tissue and skeletal muscle (117).

In our current study, we examine the mechanisms by which ANGPTL8 acts as a key regulator of both ANGPTL3 and ANGPTL4 to direct FA toward adipose tissue after feeding. We show that in humans, ANGPTL8 increases with feeding and is present in ANGPTL3/8 and ANGPTL4/8 complexes, which can be measured in serum. Levels of these complexes correlate inversely with HDL and directly with all other markers of metabolic syndrome. In addition, we demonstrate that these complexes have dramatically opposite effects on LPL activity, with ANGPTL3/8 being over 100 times more potent than ANGPTL3 alone, while ANGPTL4/8 was more than 100-fold less potent than ANGPTL4 alone. We also show that ANGPTL4/8 can prevent ANGPTL3/8 from inhibiting LPL, thereby providing a mechanism to allow for LPL in the adipose tissue to be protected from increased postprandial circulating ANGPTL3/8 levels. Together, our data demonstrate how increased ANGPTL8 levels that occur following feeding can decrease LPL activity in the skeletal muscle while increasing LPL activity in the fat, thus directing postprandial uptake of FA into adipose tissue.

2.2 Results

Result sections denoted with ***** *after the subsection heading were addressed through my personal contributions*.

2.2.1 Characterization of ANGPTL complexes*

Based on reports that ANGPTL8 may interact with other ANGPTL proteins (91, 117, 129, 144), we immunoprecipitated ANGPTL8, ANGPTL3, and ANGPTL4 (using an N-terminal ANGPTL4 antibody) from human serum and identified co-immunoprecipitating proteins via Western blotting. As Figure 2.1A shows, ANGPTL3 and ANGPTL4 did not co-immunoprecipitate

with each other, while each co-immunoprecipitated with ANGPLT8, indicating the presence of ANGPTL3/8 and ANGPTL4/8 complexes. The existence of these complexes was confirmed via mass spectrometry. As Figure 2.1B demonstrates, the amount of ANGPTL8 present in the ANGPTL3/8 and ANGPTL4/8 complexes was similar to the total amount of ANGPTL8 observed, suggesting that most ANGPTL8 in serum was present in either ANGPTL3/8 or ANGPTL4/8 complexes. While human serum contained ANGPTL3 at roughly 200 ng/mL, much less N-terminally intact (active) ANGPTL4 was present. Other than N-terminally intact ANGPTL4 present in ANGPTL4/8 complex, very little non-complexed (free), active ANGPTL4 was observed. The main free circulating form of ANGPTL4 was subsequently determined by separate immunoassay experiments (Figure 2.2B) to be C-terminal domain-containing (CTDC) ANGPTL4.

We also utilized a mass spectrometry LC-MRM method with stable-isotope-labeled peptides (SIL) to ascertain the molar ratios of the respective proteins in the recombinant ANGPTL3/8 and ANGPTL4/8 complexes. The protein ratios in the ANGPTL3/8 and ANGPTL4/8 complexes were found to be 3:1 and 1:1, respectively (Table 1). In addition, endogenous ANGPTL3/8 and ANGPTL4/8 complexes were immunoprecipitated from human serum and similarly characterized. The protein ratios in the endogenous ANGPTL3/8 and ANGPTL4/8 complexes were also found to be 3:1 and 1:1 respectively (Table 1), consistent with the ratios for the recombinant complexes.

2.2.2 Measurement of ANGPTL proteins & complexes in human serum*

We used recombinant ANGPTL proteins and complexes (Figure 2.2A) to develop dedicated immunoassays to measure human serum levels of ANGPTL3, ANGPTL4, ANGPTL8, ANGPTL3/8 complex, and ANGPTL4/8 complex. For ANGPTL4, an assay using two N-terminal ANGPTL4 antibodies enabled measurement of full-length ANGPTL4 and N-terminal ANGPTL4 fragment (collectively referred to as active ANGPTL4). Likewise, an assay using C-terminal ANGPTL4 antibodies enabled measurement of full-length ANGPTL4 and (inactive) ANGPTL4 C-terminal fragment, collectively referred to as C-terminal domain-containing (CTDC) ANGPTL4. As Figure 2.2B shows, active ANGPTL4 levels of roughly 0.1 ng/mL were more than three log orders lower than the ANGPTL3 concentrations and more than two log orders lower than those for C-terminal domain-containing ANGPTL4.

Figure 2.1. ANGPTL8 circulates in ANGPTL3/8 and ANGPTL4/8 complexes.

A: Anti-ANGPTL8, anti-ANGPTL4, and anti-ANGPTL3 antibodies covalently coupled to beads, with heavy and light chains further cross-linked, were used to immunoprecipitate (IP) human serum. Proteins were separated on a 12% Bis-Tris gel and transferred to PVDF. Co-immunoprecipitating proteins were visualized via Western blotting. Results are representative of two independent experiments.

B: ANGPTL8, ANGPTL4, and ANGPTL3 were immunoprecipitated from human serum. Beads were washed using PBS, and bound proteins were reduced with DTT and alkylated. Following digestion, digests were acidified, and co-immunoprecipitating proteins were quantified using a mass spectrometry LC-MRM method. Results are shown as the mean ± SEM (n = 3) from one experiment representative of two independent experiments.

FIGURE 2.1

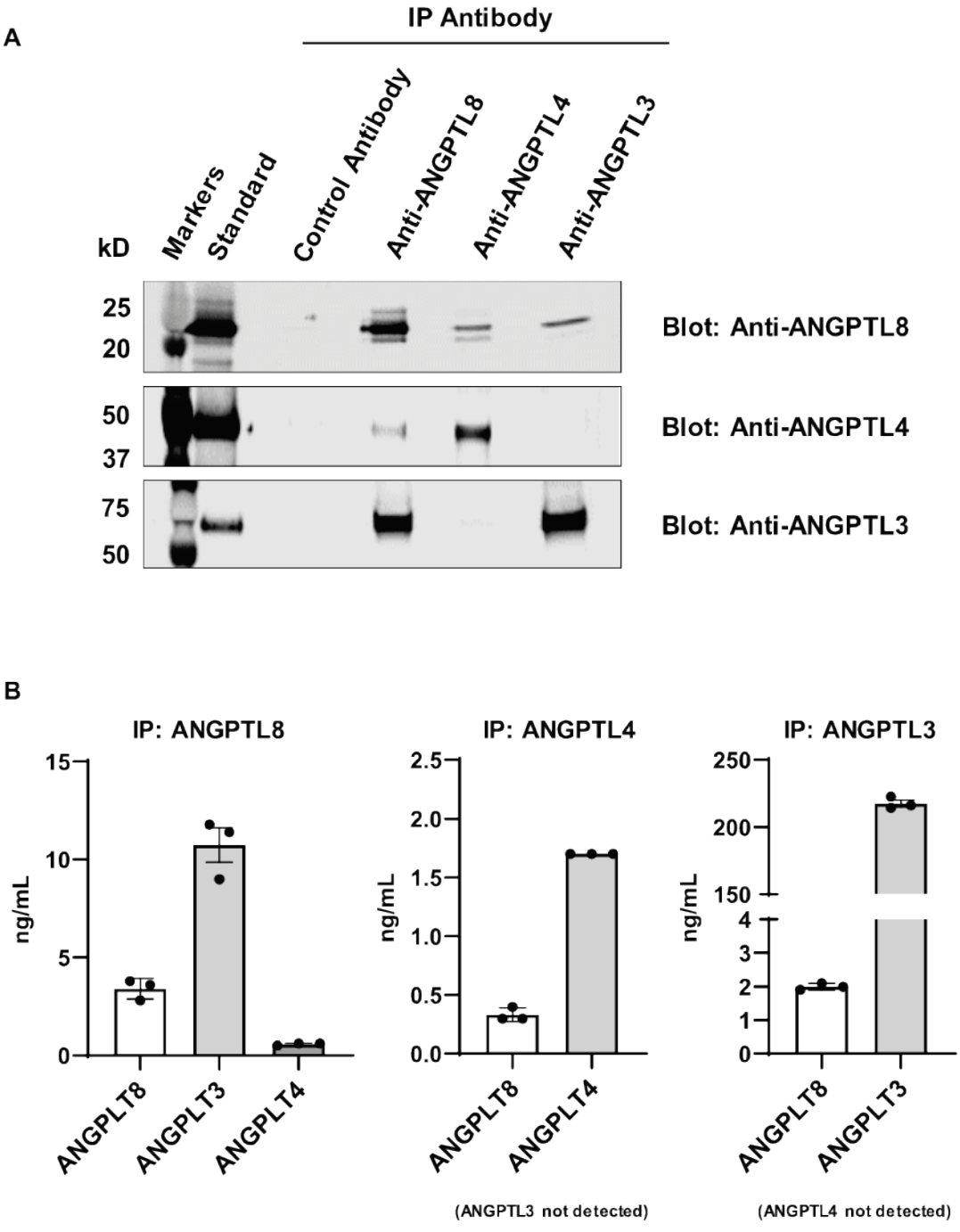
A
IP Antibody
Markers
Standard
Control Antibody
Anti-ANGPTL8
Anti-ANGPTL4
Anti-ANGPTL3
kD
25
20
50
37
75
50
Blot: Anti-ANGPTL8
Blot: Anti-ANGPTL4
Blot: Anti-ANGPTL3
B
IP: ANGPTL8
IP: ANGPTL4
IP: ANGPTL3
ng/mL
ANGPLT8
ANGPLT3
ANGPLT4
(ANGPTL3 not detected)
(ANGPTL4 not detected)

Table 1 Determination of ANGPTL3/8 and ANGPTL4/8 protein ratios by mass spectrometry.

ANGPTL3/8 and ANGPTL4/8 complexes were digested using trypsin and Lys-C. Identical molar amounts of stable-isotope-labeled (SIL) peptides were spiked into samples during digestion, and the ratio of unlabeled to labeled peptides was determined. Stoichiometries of protein complexes were determined by comparing the averaged ratios derived from 2 peptides per protein. Data for recombinant complexes were derived from a single preparation performed in triplicate. Data for endogenous complexes were derived from a serum pool from 20 healthy donors and performed in duplicate. Standard deviations (SD) are shown for each peptide in the technical replicates and for the protein ratios in the respective complexes

	Sample	Molar ratio of ANGPTL3 compared to labeled peptides			Molar ratio of ANGPTL4 compared to labeled peptides			Molar ratio of ANGPTL8 compared to labeled peptides			Protein ratio for each respective complex	
		Peptide #1	Peptide #2	Average	Peptide #1	Peptide #2	Average	Peptide #1	Peptide #2	Average	ANGPTL3/8	ANGPTL4/8
Recombinant complexes	ANGPTL3/8 Sample #1	9.60	12.96	11.28				3.64	2.92	3.28	3.4	
	ANGPTL3/8 Sample #2	9.19	13.74	11.47				3.64	3.04	3.34	3.4	
	ANGPTL3/8 Sample #3	8.06	13.45	10.75				3.23	2.92	3.08	3.5	
	ANGPTL3/8 SD	0.80	0.40	0.37				0.24	0.07	0.14	0.03	
	ANGPTL4/8 Sample #1				0.71	0.81	0.76	0.88	0.74	0.81		0.9
	ANGPTL4/8 Sample #2				0.54	0.67	0.60	0.68	0.57	0.62		1.0
	ANGPTL4/8 Sample #3				0.68	0.92	0.80	0.74	0.62	0.68		1.2
	ANGPTL4/8 SD				0.09	0.13	0.11	0.11	0.09	0.10		0.13
Endogenous complexes	ANGPTL3/8 Sample #1	1.27	1.34	1.31				0.37	0.38	0.37	3.5	
	ANGPTL3/8 Sample #2	1.25	1.27	1.26				0.37	0.36	0.36	3.4	
	ANGPTL3/8 SD	0.02	0.05	0.03				0.004	0.01	0.01	0.08	
	ANGPTL4/8 Sample #1				0.041	0.055	0.048	0.062	0.058	0.060		0.8
	ANGPTL4/8 Sample #2				0.043	0.052	0.048	0.059	0.062	0.061		0.8
	ANGPTL4/8 SD				0.002	0.002	0.00	0.002	0.003	0.01		0.01

Because levels of ANGPTL4 measured by this assay were so much less than ANGPTL4/8 levels, this assay likely did not detect ANGPTL4 present in ANGPTL4/8 complexes to any appreciable extent. These data confirmed our mass spectrometry-based observations and indicated that most free, circulating ANGPTL4 consisted of inactive C-terminal fragment, a concept consistent with our subsequent LPL activity data. Concentrations of ANGPTL8, ANGPTL3/8, and ANGPTL4/8, averaged 4 ng/mL, 20 ng/mL, and 23 ng/mL respectively.

Overall, the protein concentrations obtained using our immunoassays compared reasonably well to the mass spectrometry-based estimates, especially considering the multiple steps required for mass spectrometry assessments. Levels of each of the respective proteins and complexes were also compared with serum TG concentrations. Interestingly, only ANGPTL8, ANGPTL3/8, and ANGPTL4/8 were significantly positively correlated with circulating TG (R-values of 0.47, 0.51, and 0.36 respectively and *p*-values of 0.0007, 0.0002, and 0.01 respectively). There was no significant correlation of ANGPTL3, active ANGPTL4, or C-terminal domain-containing (CTDC) ANGPTL4 with serum TG.

Based on these findings, we used our immunoassays to measure levels of ANGPTL3, ANGPTL8, ANGPTL3/8, and ANGPTL4/8 in serum samples collected from normal subjects while fasting and one and two hours following a mixed meal challenge. As shown in Figure 2.2C, ANGPTL3 concentrations did not change meaningfully in the postprandial state. In contrast, ANGPTL3/8, and ANGPTL4/8 both increased significantly postprandially, consistent with increases observed in ANGPTL8.

We further explored circulating ANGPTL3/8 and ANGPTL4/8 levels by measuring these complexes in 352 control subjects from the SCARF cardiovascular outcomes study (208-210). The average ANGPTL3/8 level in the SCARF samples was 17 ng/mL, while the average ANGPTL4/8 level was 23 ng/mL. These levels were similar to those observed in the previously studied healthy subjects. As Table 2 shows, circulating ANGPTL3/8 and ANGPTL4/8 levels were inversely correlated with HDL-cholesterol (HDL-C) and directly correlated with TG, fasting glucose, fasting insulin, waist to hip ratio, and BMI, as well as systolic and diastolic blood pressure. In addition, ANGPTL3/8 concentrations (but not ANGPTL4/8 concentrations) were also positively correlated with total cholesterol (TC) and LDL-C. Finally, ANGPTL3/8 and ANGPTL4/8 were also directly correlated with each other ($R = 0.39$, $p < 0.0001$).

Figure 2.2 ANGPTL3/8 and ANGPTL4/8 complexes increase with feeding.

A: Recombinant human ANGPTL proteins and complexes used for immunoassays were characterized via electrophoresis. One microgram of each recombinant protein or complex was analyzed using gradient gel electrophoresis with a 4–20% Tris-glycine gel, followed by Coomassie Blue staining.

B: Active ANGPTL4 (defined as full length ANGPTL4 or the N-terminal fragment of ANGPTL4), CTDC ANGPTL4, ANGPTL3, ANGPTL8, ANGPTL3/8, and ANGPTL4/8 were measured in 50 normal donors using dedicated sandwich immunoassays.

C: ANGPTL3/8, ANGPTL4/8, ANGPTL3, and ANGPTL8 were measured using dedicated sandwich immunoassays in 10 normal donors during fasting conditions and 1 and 2 h following a mixed meal challenge. Results are shown as the mean ± SEM. Significance for the feeding effect on ANGPTL proteins and complexes was assessed using a paired t-test.

FIGURE 2.2

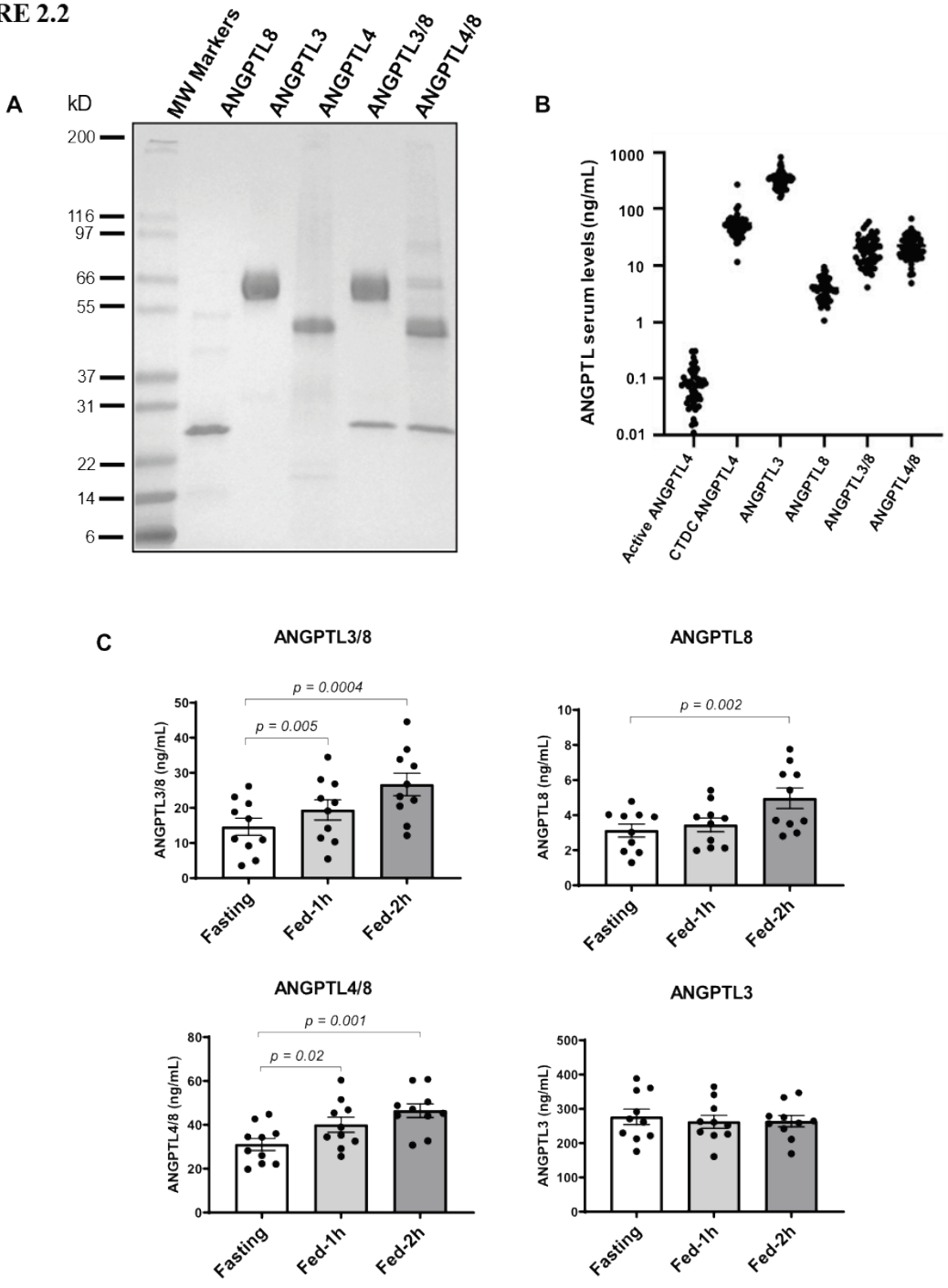
A
kD
MW Markers
ANGPTL8
ANGPTL3
ANGPTL4
ANGPTL3/8
ANGPTL4/8
200
116
97
66
55
37
31
22
14
6
B
ANGPTL serum levels (ng/mL)
1000
100
10
1
0.1
0.01
Active ANGPTL4
CTDC ANGPTL4
ANGPTL3
ANGPTL8
ANGPTL3/8
ANGPTL4/8
C
ANGPTL3/8
ANGPTL3/8 (ng/mL)
p = 0.0004
p = 0.005
ANGPTL8
ANGPTL8 (ng/mL)
p = 0.002
ANGPTL4/8
ANGPTL4/8 (ng/mL)
p = 0.001
p = 0.02
ANGPTL3
ANGPTL3 (ng/mL)
Fasting
Fed-1h
Fed-2h

Table 2 Circulating ANGPTL3/8 and ANGPTL4/8 are highly correlated with metabolic syndrome markers.

ANGPTL3/8 and ANGPTL4/8 complexes were measured in fasting serum samples from SCARF subjects (n=352), and their associations with various metabolic parameters were assessed.

Phenotype	ANGPTL3/8		ANGPTL4/8	
	R-value	*p*-value	R-value	*p*-value
Triglyceride (TG)	0.485	<0.0001	0.261	<0.0001
HDL-cholesterol (HDL-C)	-0.279	<0.0001	-0.247	<0.0001
LDL-cholesterol (LDL-C)	0.218	<0.0001	0.062	0.24 (NS)
Total cholesterol (TC)	0.233	<0.0001	0.072	0.18 (NS)
Body mass index (BMI)	0.484	<0.0001	0.377	<0.0001
Waist-hip ratio	0.351	<0.0001	0.240	<0.0001
Fasting glucose	0.282	<0.0001	0.215	<0.0001
Fasting Insulin	0.635	<0.0001	0.473	<0.0001
Systolic blood pressure	0.187	0.0005	0.196	0.0003
Diastolic blood pressure	0.286	0.0002	0.234	<0.0001

2.2.3 ANGPTL3/8 inhibition of LPL facilitated hepatic VLDL cholesterol uptake

After analyzing the SCARF samples and noting that ANGPTL3/8 was positively correlated with LDL-C, we turned our attention toward understanding why this might be the case. In so doing, we examined the ability of ANGPTL3/8 to affect LPL-facilitated hepatocyte VLDL-C uptake. We chose ANGPTL4/8 as the control for these experiments after observing that 1) ANGPTL3 showed no correlation with TG in clinical samples, 2) serum levels of active ANGPTL4 were negligible compared to those of ANGPTL3/8 and ANGPTL4/8, and 3) we could not detect any effect of ANGPTL8 alone on LPL activity. As Figure 2.3 shows, addition of LPL to VLDL-C-containing media significantly increased Huh7 hepatocyte uptake of VLDL-C, consistent with previous reports (51, 55, 189, 211). When ANGPTL3/8 was pre-incubated with LPL prior to addition of LPL to the media, however, hepatocyte VLDL-C uptake was reduced nearly to levels observed in the absence of LPL. In contrast, when ANGPTL4/8 was pre-incubated with LPL prior to addition of LPL to the media, there was no significant effect on LPL-facilitated VLDL-C uptake by the hepatocytes. Together, these results suggested that ANGPTL3/8 may inhibit the ability of LPL to facilitate hepatic uptake of cholesterol containing lipoproteins. An important caveat in interpreting

these data, however, is that the results reflect VLDL particle uptake by multiple different receptors (including LDLR and VLDLR), with several required steps (including lipolysis, attachment, and internalization). Therefore, reduced uptake in this assay could be due to both direct effects on particle uptake as well as indirect effects on VLDL clearance mechanisms.

FIGURE 2.3

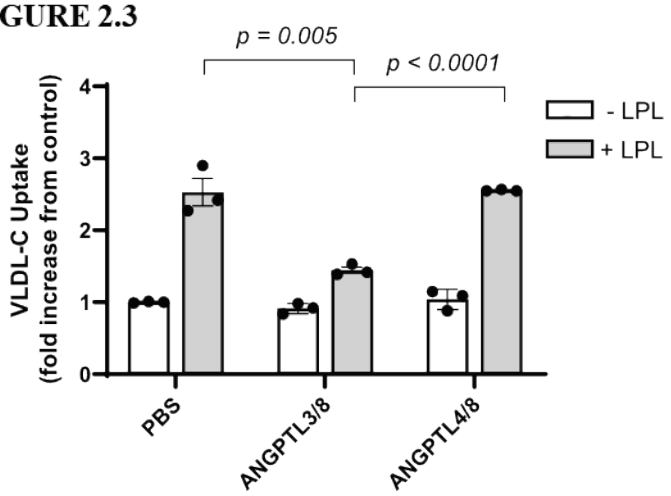

Figure 2.3 ANGPTL3/8 blocks LPL-facilitated hepatocyte VLDL-C uptake.

Cholesterol uptake in Huh7 hepatocytes was measured in the absence or presence of LPL pre-incubated with vehicle, ANGPTL3/8 complex, or ANGPTL4/8 complex for 1 h before mixing with fluorescent-labeled VLDL, followed by addition to the Huh7 hepatocytes for 30 min. The media was then replaced with fixative. Cells were fixed for 20 min, washed twice with PBS, and covered with PBS. Fluorescence at 495/525 nm was measured, with VLDL uptake calculated as relative fluorescent units at 525 nm. Results are shown as the mean ± SEM (n = 3).

2.2.4 Binding of ANGPTL complexes to LPL*

To understand better the potential differences in LPL interactions with ANGPTL3/8 and ANGPTL4/8, we examined the *in vitro* binding of purified ANGPTL3, ANGPTL4, ANGPTL3/8, and ANGPTL4/8 to LPL using bio-layer interferometry. As Figure 2.4A shows**,** ANGPTL3 demonstrated weak binding to LPL, whereas ANGPTL3/8 demonstrated markedly increased binding, similar to that observed with ANGPTL4 alone (Figure 2.4B). In contrast, ANGPTL4/8 demonstrated a very different binding pattern, with a much slower off-rate than what was observed for either ANGPTL3/8 or ANGPTL4. Table 3 shows a summary of the LPL-binding kinetics for ANGPTL3, ANGPTL3/8, ANGPTL4, and ANGPTL4/8.

FIGURE 2.4

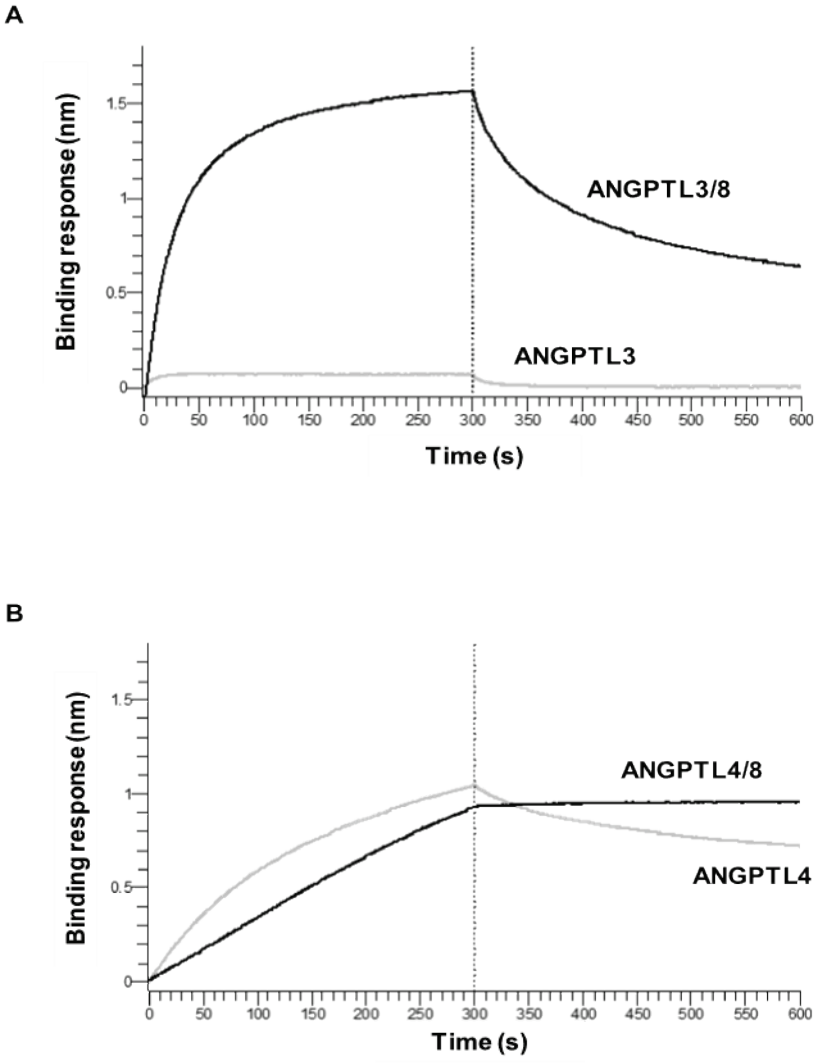

Figure 2.4 ANGPTL3/8 and ANGPTL4/8 manifest different binding patterns to LPL.

A: The ability of ANGPTL3 and ANGPTL3/8 to bind LPL was assessed with bio-layer interferometry. Avidin-tagged LPL was immobilized on streptavidin biosensors and incubated with ANGPTL3 or ANGPTL3/8 and transferred to buffer-only wells to monitor dissociation. The left side of the graph shows the association of ANGPTL3 and ANGPTL3/8 with LPL. The right side shows their respective dissociations. Results are representative of three independent experiments.

B: The ability of ANGPTL4 and ANGPTL4/8 to bind LPL was assessed with bio-layer interferometry. Avidin-tagged LPL was immobilized on streptavidin biosensors and incubated with ANGPTL4 or ANGPTL4/8 and transferred to buffer-only wells to monitor dissociation. The left side of the graph shows the association of ANGPTL4 and ANGPTL4/8 with LPL. The right side shows their respective dissociations. Results are representative of three independent experiments

Table 3 LPL-binding characteristics of ANGPTL proteins and complexes.

The K_d, k_{on} and k_{off} for ANGPTL3, ANGPTL3/8, ANGPTL4, and ANGPTL4/8 binding to LPL were determined using bio-layer interferometry.

ANGPTL protein or complex	K_d (nM)	K_{on} (1/Ms)	K_{off} (1/s)
ANGPTL3	343.0	3.2×10^4	1.2×10^{-3}
ANGPTL3/8	6.4	6.9×10^4	4.4×10^{-3}
ANGPTL4	17.7	9.7×10^5	1.7×10^{-3}
ANGPTL4/8	< 0.001	4.8×10^4	$< 1 \times 10^{-7}$

2.2.5 Effect of ANGPTL3, ANGPTL3/8, ANGPTL4, & ANGPTL4/8 on LPL activity*

We next examined the effect that ANGPTL8 had on the ability of ANGPTL3 to inhibit LPL enzymatic activity (188, 194). On its own, ANGPTL3 demonstrated inhibition of LPL with an IC_{50} of 26 nM (Figure 2.5A). When ANGPTL8 was present together with ANGPTL3 in an ANGPTL3/8 complex, however, the inhibition increased markedly, with ANGPTL3/8 demonstrating a 186-fold increase in potency compared to ANGPTL3 alone (IC_{50} of 0.14 nM). ANGPTL4 was then evaluated in the LPL activity assay (Figure 2.5B) and demonstrated inhibition with an IC_{50} of 0.29 nM (similar to that observed for ANGPTL3/8). In stark contrast to the results obtained with ANGPTL3, when ANGPTL8 was combined with ANGPTL4 to form ANGPTL4/8 complex, potency was reduced 128-fold (IC_{50} of 37 nM), indicating that ANGPTL8 was drastically decreasing the ability of ANGPTL4 to inhibit LPL. In light of the marked decrease in LPL inhibitory activity of ANGPTL4/8 versus ANGPTL4, we performed an additional VLDL substrate-based activity assay to confirm this result (Figure 2.5C). In this assay, ANGPTL4/8 showed a 239-fold decrease in potency of LPL inhibition compared to ANGPTL4 alone (IC_{50} of 105 nM versus 0.44 nM, respectively). Table 4 summarizes these results.

2.2.6 ANGPTL4/8 blocking of ANGPTL3/8 & ANGPTL4 mediated inhibition of LPL

The studies presented in Figure 2.5 indicated that binding of ANGPTL8 to ANGPTL3 markedly enhanced the inhibitory effect of ANGPTL3 on LPL activity In contrast, while ANGPTL4 alone had an inhibitory effect comparable to that of the ANGPTL3/8 complex on LPL activity, the binding of ANGPTL8 to ANGPTL4 markedly reduced this inhibitory effect of

Figure 2.5 ANGPTL8 markedly increases ANGPTL3 inhibition of LPL but dramatically decreases ANGPTL4 inhibition of LPL.

A: The ability of ANGPTL3 or ANGPTL3/8 to inhibit LPL was assessed using LPL-stable expression cells incubated with ANGPTL3 or ANGPTL3/8 prior to the addition of lipase substrate. Fluorescence was monitored at 1 and 30 min to correct for background. ANGPTL3/8 showed a 186-fold increase in LPL inhibition compared to ANGPTL3 alone (IC50 values of 0.14 nM versus 26 nM, respectively). Results are shown as the mean ± SEM (n = 5).

B: The ability of ANGPTL4 or ANGPTL4/8 to inhibit LPL was similarly assessed. ANGPTL4/8 showed a 128-fold decrease in LPL inhibition compared to ANGPTL4 alone (IC50 values of 37 nM versus 0.29 nM, respectively).

FIGURE 2.5

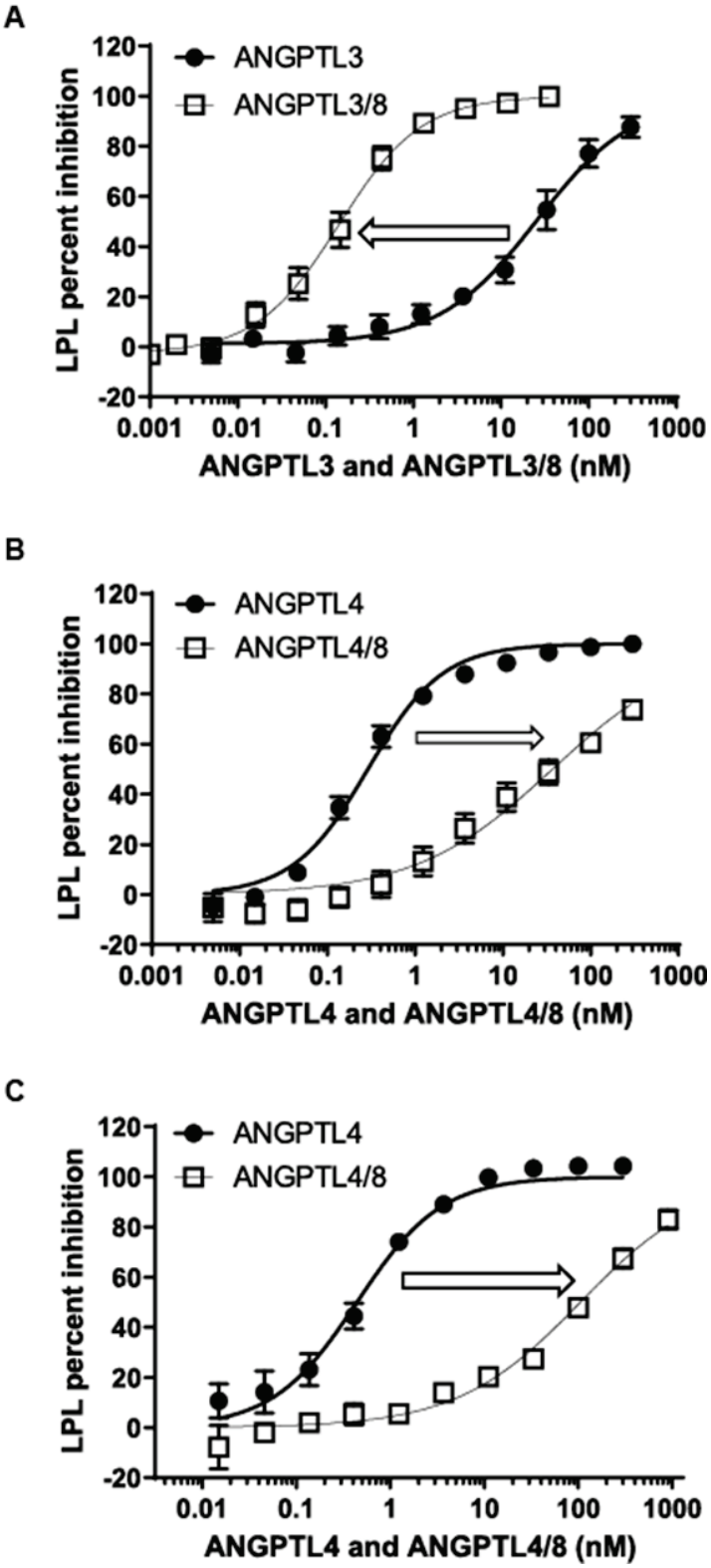
A
ANGPTL3
ANGPTL3/8
LPL percent inhibition
120
100
80
60
40
20
0
-20
0.001
0.01
0.1
1
10
100
1000
ANGPTL3 and ANGPTL3/8 (nM)
B
ANGPTL4
ANGPTL4/8
LPL percent inhibition
ANGPTL4 and ANGPTL4/8 (nM)
C
ANGPTL4
ANGPTL4/8
LPL percent inhibition
ANGPTL4 and ANGPTL4/8 (nM)

Table 4 LPL inhibition summary for ANGPTL3 versus ANGPTL3/8 and ANGPTL4 versus ANGPTL4/8.

IC_{50} concentrations were determined for ANGPTL3 versus ANGPTL3/8 and ANGPTL4 versus ANGPL4/8 in LPL activity assays.

Enzyme	Substrate	ANGPTL Protein	IC_{50} (nM)	ANGPTL Complex	IC_{50} (nM)	Change Direction	Fold Change
LPL	BODIPY-TG	ANGPTL3	26	ANGPTL3/8	0.14	Increase	(+) 186
LPL	BODIPY-TG	ANGPTL4	0.29	ANGPTL4/8	37	Decrease	(-) 128
LPL	VLDL	ANGPTL4	0.44	ANGPTL4/8	105	Decrease	(-) 239

ANGPTL4 on LPL activity. These data suggested that when bound to LPL, the ANGPTL4/8 complex might also act as a 'bodyguard' to protect LPL from the inhibitory effect of the ANGPTL3/8 complex.

We thus hypothesized that the tight binding of the ANGPTL4/8 complex to LPL and its slow dissociation rate might prevent LPL inhibition by ANGPTL3/8. This prompted us to assess the ability of ANGPTL3/8 to inhibit LPL activity after pre-incubation of LPL with ANGPTL4/8. In these experiments, increasing amounts of ANGPTL4/8 proportionally decreased the ability of ANGPTL3/8 to inhibit LPL (Figure 2.6A).

After obtaining these results, we performed experiments to determine if increasing amounts of ANGPTL4/8 could also decrease the ability of ANGPTL4 to inhibit LPL. As shown in Figure 2.6B, this proved to be the case. Together, these results indicated that ANGPTL4/8 can effectively compete with both ANGPTL3/8 and ANGPTL4 for binding to LPL and in so doing block the ability of ANGPTL3/8 and ANGPTL4 to inhibit LPL. In these experiments, pre-incubation of LPL with 10 nM of ANGPTL4/8 was required to completely block the inhibition of LPL by 1 nM ANGPTL3/8 (and 1 nM ANGPTL4), indicating that high local concentrations of ANGPTL4/8 may be required to prevent circulating ANGPTL3/8 from inhibiting LPL in the fat.

These observations suggested a mechanism by which ANGPTL4/8 localized in adipose tissue could block circulating ANGPTL3/8 from inhibiting LPL in the fat, thus ensuring that increased ANGPTL3/8 after feeding inhibits LPL mainly in skeletal muscle. This concept is consistent with the serum levels observed for ANGPTL3/8 and ANGPTL4/8.

FIGURE 2.6

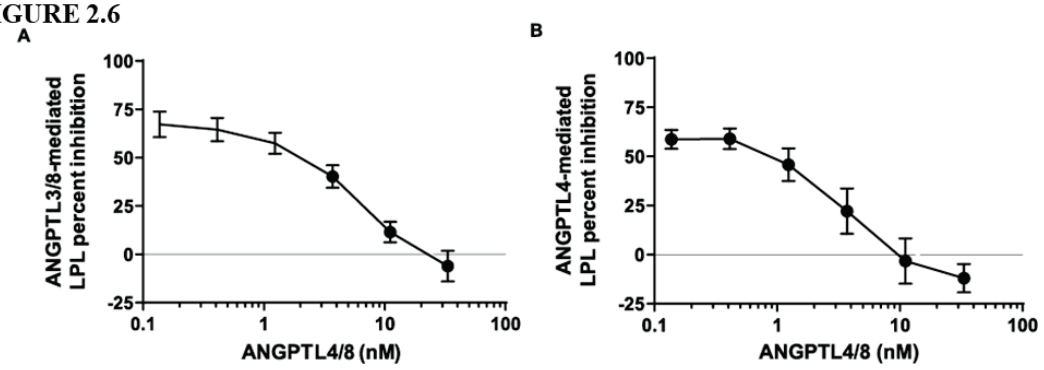

Figure 2.6 ANGPTL4/8 blocks ANGPTL3/8- and ANGPTL4-mediated inhibition of LPL.

A: To study the ability of ANGPTL4/8 to protect LPL from ANGPTL3/8 inhibition, various concentrations of ANGPTL4/8 were pre-incubated with LPL-stable expression cells for 1 h. Afterward, 1 nM of ANGPTL3/8 was added for a further 1 h incubation, prior to the addition of lipase substrate. Fluorescence was monitored as in Fig. 5A. Results are shown as the mean ± SEM (n = 4).

B: To study the ability of ANGPTL4/8 to protect LPL from ANGPTL4 inhibition, various concentrations of ANGPTL4/8 were pre-incubated with LPL-stable expression cells for 1 h. Afterward, 1 nM of ANGPTL4 was added for a further 1 h incubation, prior to the addition of lipase substrate. Fluorescence was monitored as in Fig. 5A. Results are shown as the mean ± SEM (n = 6).

ANGPTL3/8 would be expected to act in an endocrine manner as its serum level falls midway on its LPL inhibition curve. In contrast, circulating ANGPTL4/8 levels are far lower than those required to block the ability of circulating ANGPTL3/8 to inhibit LPL, consistent with ANGPTL4/8 acting more in an autocrine/paracrine manner.

2.2.7 Insulin stimulated release of ANGPTL3/8 from hepatocytes*

We next turned our attention to the source of increased postprandial ANGPTL3/8 that we observed in human serum. Based on previous reports that hepatic ANGPTL8 mRNA increases in the fed state, we hypothesized that insulin might stimulate the secretion of ANGPTL3/8 from the liver (138). To test this hypothesis, we measured ANGPTL3/8 at multiple time points in insulin-naïve patients treated for 52 weeks with basal insulin peglispro (BIL), a hepato-preferential insulin (212, 213). Mean baseline ANGPTL3/8 and ANGPTL4/8 levels in these type 2 diabetes patients were 19 and 45 ng/mL respectively. As Figure 2.7A shows, the hepato-selective insulin significantly increased ANGPTL3/8 circulating concentrations. In comparison, there was little change in circulating ANGPTL4/8 levels, suggesting that the source of increased postprandial

ANGPTL4/8 was not the liver. To confirm further that insulin stimulated the release of ANGPTL3/8 (but not ANGPTL4/8) from hepatocytes, we also incubated human primary hepatocytes in the absence or presence of 1 nM insulin and measured levels of secreted ANGPTL3/8 and ANGPTL4/8 complexes. As Figure 2.7B shows, insulin stimulation significantly increased hepatocyte release of ANGTL3/8, while not affecting the release of ANGPTL4/8. Together with the *in vivo* BIL data, these results confirmed that insulin stimulates hepatic secretion of ANGPTL3/8.

FIGURE 2.7

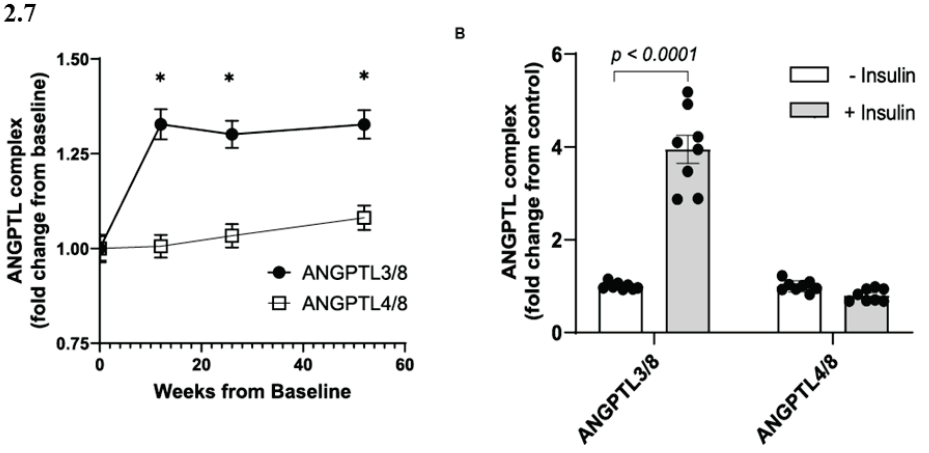

Figure 2.7 Insulin stimulates human hepatocyte secretion of ANGPTL3/8.

A: Insulin-naïve patients (n = 279) were administered the hepatic-preferential insulin BIL, and serum samples were obtained under morning fasting conditions over the course of 1 year of BIL treatment. ANGPTL3/8 and ANGPTL4/8 levels were measured at baseline and after 12, 26, and 52 weeks of BIL administration. Results are shown as the mean ± SEM (**P* < 0.0001 versus week 0).

B: Human primary hepatocytes obtained in the HepatoPac platform were washed in serum-free application media and pre-incubated in application media in the absence of insulin. Following aspiration, cells were incubated with application media in the absence or presence of 1 nM of insulin. ANGPTL3/8 and ANGPTL4/8 levels in the media were measured using sandwich immunoassays, with the results shown as the mean ± SEM (n = 8).

2.2.8 Insulin stimulated release of ANGPTL4/8 from adipocytes*

The above observations indicated that insulin did not increase ANGPTL4/8 release from the liver and caused us to hypothesize that insulin-stimulated secretion of ANGPTL4/8 might occur from the fat. We considered previous reports describing that while ANGPTL8 mRNA was highly insulin-responsive in human adipocytes, levels of the secreted protein did not increase upon insulin treatment (214, 215). We hypothesized that there might be two reasons for this. The first could be that a further confounding factor might prevent the ability of adipocytes to release the ANGPTL4/8 complex *in vitro*. The second could be that another signal in addition to insulin might be required

for maximal ANGPTL4/8 secretion from adipocytes. In this latter scenario, in order for postprandial increases in ANGPTL4/8 to occur, increased insulin levels alone might not be sufficient, but rather an additional stimulus might be required. If a second signal beyond insulin was indeed required for optimal ANGPTL4/8 secretion from adipose tissue, we believed a likely candidate would be glucose-dependent insulinotropic peptide (GIP), an incretin secreted by K-cells in the gut in response to fat and carbohydrate intake, as the GIP receptor is highly expressed in adipocytes (216). Further influencing our thinking was the fact that we had shown in a previous study that postprandial increases in GIP manifested a pattern very similar to those observed for the postprandial ANGPTL4/8 increases observed in our current study (216).

We therefore turned our attention to measuring insulin-stimulated secretion of ANGPTL4/8 from adipocytes. As shown in Figure 2.8A, we confirmed that exposure of human adipocytes to insulin increased levels of ANGPTL8 mRNA. In contrast, ANGPTL4 mRNA levels did not change with insulin treatment (Figure 2.8B). We also observed that ANGPTL3 mRNA levels were undetectable, consistent with previous reports that adipocytes do not express ANGPTL3 (217). To understand why previous researchers were unable to measure insulin stimulated ANGPTL8 release from adipocytes, we considered that ANGPTL8 might be secreted as part of an ANGPTL4/8 complex that could remain tightly bound to plasma membranes via interaction with heparin sulfate proteoglycans, thereby preventing release into the media. To understand if this might be the case, we first expressed ANGPTL8 and ANGPTL4 in HEK293 cells in the absence or presence of 0.1 mg/ml dextran sulfate (a heparin-like compound). Interestingly, the addition of dextran sulfate, greatly increased the release of ANGPTL4 and ANGPTL8 (Figure 2.8C), causing us to conduct subsequent experiments in adipocytes in the presence of heparin.

We thus treated adipocytes in heparin-containing media with insulin in the absence or presence of GIP and measured release of ANGPTL4/8. Under these conditions, insulin dose-dependently increased the secretion of ANGPTL4/8, and this dose-dependent increase was greatly augmented by the addition of GIP (Figure 2.8D). In the absence of GIP, 1, 10, and 100 nM insulin increased adipocyte ANGPTL4/8 secretion by 2.1, 6.5 and 7.7-fold respectively compared to control, whereas in the presence of GIP, 1, 10, and 100 nM insulin increased adipocyte ANGPTL4/8 secretion by 14.4, 22.7, and 27.4-fold respectively.

FIGURE 2.8

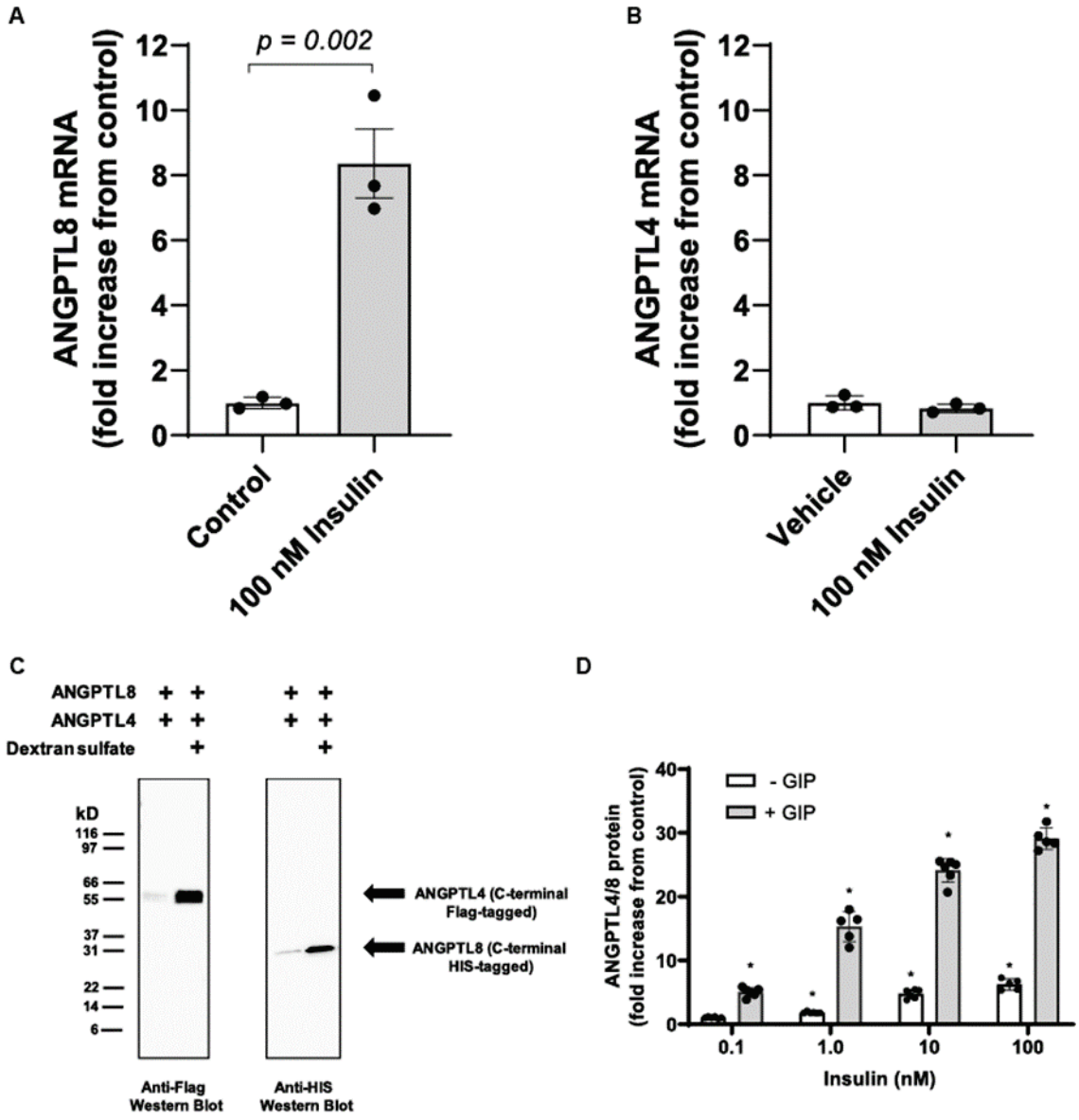

Figure 2.8 Insulin stimulates ANGPTL4/8 secretion from human adipocytes.

A: Human adipocytes were incubated in the absence or presence of insulin, and 1 µg of total RNA was reverse transcribed. ANGPTL8 transcript levels were quantitated. Insulin treatment resulted in an approximate 8-fold increase in ANGPTL8 mRNA levels. Results are shown as the mean ± SEM (n = 3).

B: ANGPTL4 transcript levels were quantitated in the human adipocytes in A. Results are shown as the mean ± SEM (n = 3).

C: Flag-tagged ANGPTL4 and HIS-tagged ANGPTL8 constructs were transfected into HEK293 cells. Afterward, dextran sulfate was added, media were harvested, and equal volumes from each condition were immunoblotted with anti-Flag or anti-HIS antibody.

D: Human adipocytes were treated in heparin-containing media supplemented with 0–100 nM insulin in the absence and presence of 10 nM GIP. Media were collected and analyzed for ANGPTL4/8. Results are shown as the mean ± SEM (n = 6, *p < 0.0001 versus control)

In contrast, no ANGPTL4/8 was measurable in the absence of heparin, indicating that ANGPTL4/8 secreted by adipocytes may remain mostly localized in the adipose tissue *in vivo*. This suggests that ANGPTL4/8 present in the circulation likely reflects adipose tissue ANGPTL4/8 concentrations, with ANGPTL4/8 entering the circulation from blood flow through the adipose capillary beds. Of note, we also attempted to measure ANGPTL3/8 secreted from the adipocytes stimulated with insulin but were unable to detect any ANGPTL3/8 in the media, consistent with undetectable adipocyte ANGPTL3 mRNA levels.

Together, these results indicated that by staying mainly localized in the adipose tissue, increased postprandial ANGPTL4/8 may prevent the increased postprandial circulating ANGPTL3/8 (as well as localized ANGPTL4) from inhibiting LPL in the fat. This suggests a mechanism for the elevated circulating ANGPTL3/8 that occurs after feeding to act mainly in the skeletal muscle and not the adipose tissue, thereby ensuring that conflicting LPL inhibitory signals are not sent to both tissues simultaneously.

2.3 Discussion

In this study, we show that ANGPTL8 is an insulin-responsive mediator of FA uptake that directs the storage of calories from food into the fat for future energy needs. ANGPTL8 does this by forming ANGPTL3/8 and ANGPTL4/8 complexes with respective protein ratios of 3:1 and 1:1. By forming an ANGPTL3/8 complex, ANGPTL8 markedly increases ANGPTL3 inhibition of LPL to decrease skeletal muscle LPL activity and thus decrease skeletal muscle FA uptake. Through forming an ANGPTL4/8 complex, ANGPTL8 markedly decreases ANGPTL4 inhibition of LPL to increase LPL activity in the fat to facilitate adipose tissue FA uptake. Through its tight binding to adipocyte-associated LPL, ANGPTL4/8 may also block the ability of circulating ANGPTL3/8 (and localized ANGPTL4) to inhibit LPL in adipose tissue. These properties of ANGPTL8 allow for the postprandial increase of LPL-inhibitory activity of ANGPTL3/8 to occur mainly in the skeletal muscle so that FA are taken up mostly into the fat after feeding.

This system provides a mechanism to ensure that LPL in adipose tissue is active after feeding while LPL in muscle is inhibited, thus allowing for proper storage of dietary lipids and preventing ectopic fat deposition. ANGPTL4/8 present in the circulation probably comes from localized ANGPTL4/8 in the fat that becomes detached as a result of the capillary flow across luminal surfaces of the adipose endothelium. In our experiments in HEK293 cells and adipocytes,

ANGPTL4/8 was only released *in vitro* in the presence of dextran sulfate or heparin. These *in vitro* models, however, are unable to mimic the dynamic capillary flow that may cause some localized ANGPTL4/8 to enter the circulation. In addition, we cannot rule out the possibility, that some ANGPTL4/8 (as well as some ANGPTL4) that we detected in the circulation might come from skeletal muscle where ANGPTL4 has also been shown to be expressed. (218)

In our study, ANGPTL3/8 demonstrated more than a 100-fold increased potency of LPL inhibitory activity compared to ANGPTL3, while ANGPTL4/8 showed at least a 100-fold decreased potency of LPL inhibitory activity compared to ANGPTL4. The changes in potency suggest that these proteins and their complexes exist in a symmetrically modifiable system. ANGPTL4 is a much more potent inhibitor of LPL than ANGPTL3. Formation of the ANGPTL4/8 complex greatly diminishes ANGPTL4's LPL inhibitory activity to the point that it becomes similar to that of ANGPTL3. In contrast, formation of the ANGPTL3/8 complex greatly increases ANGPTL3's LPL inhibitory activity, resulting in an LPL inhibition profile comparable to that of ANGPTL4. An important caveat, however, is that our *in vitro* functional experiments were performed in conditions bearing little resemblance to capillary endothelial surfaces, where LPL acts *in vivo*. This is potentially important because several proteins (including APOC2, APOC3, and GPIHBP1) can affect LPL activity and stability, and may modulate the effects of ANGPTL proteins and complexes (22, 187-190). Nevertheless, our data showing that circulating levels of active (N-terminally intact) ANGPTL4 are negligible compared to ANGPTL3/8 are consistent with our *in vitro* functional observations. Because active ANGPTL4 inhibits LPL as potently as ANGPTL3/8, it would be difficult for the system to operate properly if both active ANGPTL4 and ANGPTL3/8 reached the skeletal muscle at comparable levels.

Our study is the first to examine in detail the circulating levels of ANGPTL3/8 and ANGPTL4/8 complexes in man. Our data are consistent with the idea that most, if not all, ANGPTL8 released from hepatocytes is secreted as part of the ANGPTL3/8 complex. In contrast, our data also indicate that while some ANGPTL3 is secreted by the liver as part of an ANGPTL3/8 complex, most ANGPTL3 is secreted as free ANGPTL3 not complexed with ANGPTL8. Interestingly, ANGPTL3/8 and ANGPTL4/8 circulate at similar levels (roughly 20 ng/mL). For ANGPTL3/8, these levels are close to the IC_{50} we observed for the ANGPTL3/8 complex on LPL activity, consistent with the idea that circulating ANGPTL3/8 works in an endocrine manner. In the case of ANGPTL4/8, however, these levels are well below those required for a direct effect on

LPL activity or for blocking the LPL-inhibitory effects of ANGPTL4 and ANGPTL3/8, further supporting the idea that the ANGPTL4/8 complex acts mainly in an autocrine/paracrine manner.

In our competition experiments, pre-incubation of LPL with ANGPTL4/8 blocked the inhibition of LPL by ANGPTL3/8, indicating that localized ANGPTL4/8 may prevent circulating ANGPTL3/8 from inhibiting LPL in the fat. These results suggest a mechanism by which ANGPTL4/8 localized in adipose tissue could block circulating ANGPTL3/8 from inhibiting LPL in the fat, thus ensuring that increased ANGPTL3/8 after feeding inhibits LPL mainly in skeletal muscle. We also contemplated examining the effect of active ANGPTL4 on ANGPTL3/8 mediated LPL inhibition, however because active ANGPTL4 and ANGPTL3/8 inhibit LPL to almost the same extent, it would have been extremely difficult to sort out ANGPTL4-mediated inhibition of LPL versus that caused by ANGPTL3/8.

In our *in vitro* binding experiments, ANGPTL4 and ANGPTL3/8 had similar, relatively high off rates with regard to their LPL binding. In contrast, ANGPTL4/8 demonstrated a very low off rate. In spite of this, ANGPTL4/8 showed much less inhibition of LPL than did ANGPTL4, causing us to reflect on how ANGPTL4/8 could bind to LPL with comparable or higher affinity compared to ANGPTL4 but without inhibiting it to the same degree. It is possible that ANGPTL4 and ANGPTL4/8 might bind to different domains of LPL, with ANGPTL4 binding causing marked LPL inhibition while ANGPTL4/8 binds to a somewhat different domain, resulting in much less inhibitory effect. This concept is consistent with the idea that binding alone, even high affinity binding, does not necessarily guarantee inhibition. Understanding exactly why ANGPTL4/8 can bind LPL with comparable or higher affinity than ANGPTL4 binds LPL, but without inhibiting it to the same extent, will be an important area of future study.

Additional novel findings in our study are the inverse correlations of ANGPTL3/8 and ANGPTL4/8 with HDL, and the direct correlations of both complexes with all other metabolic syndrome markers. For ANGPTL3/8, the positive correlation with TG and other markers of metabolic syndrome was not surprising. In the case of ANGPTL4/8, however, it was less obvious why despite relieving ANGPTL4-mediated LPL inhibition, ANGPTL 4/8 was also positively correlated with serum TG. One possibility might be that by blocking ANGPTL3/8 inhibition of LPL in the fat, ANGPTL4/8 shifts more ANGPTL3/8 to the skeletal muscle, where it inhibits LPL activity and thus decreases FA uptake into skeletal muscle, resulting in increased circulating TG. Further experiments will be needed to test this idea. Interestingly, we noted that ANGPTL3/8 was

directly correlated with LDL-C, while ANGPTL4/8 was not. This could be related to LPL-facilitated uptake of cholesterol-containing lipoprotein particles into the liver via VLDL and related receptors (55, 219-223). Our data demonstrating that ANGPTL3/8 inhibited LPL-facilitated hepatocyte VLDL-C uptake might provide a possible explanation for the positive correlation of ANGPTL3/8 with LDL-C, but further mechanistic investigations along these lines will be needed.

Our observations build upon those of Zhang (who proposed an ANGPTL3-4-8 model), Kovrov and colleagues (who incubated N-terminal ANGPTL3 and ANGPTL4 fragments with ANGPTL8 and showed approximate 4-fold activation of ANGPTL3 and 4-fold inhibition of ANGPTL4), and Chi and colleagues (who showed that ANGPTL8 complexed with ANGPTL3 and enhanced its ability to bind and inhibit LPL) (4, 91, 117). Importantly, the study by Chi and colleagues also showed that ANGPTL8 required complex formation in order to be efficiently secreted. This helps explains why, in our present study, almost all serum ANGPTL8 was observed in complexes with ANGPTL3 or ANGPTL4.

Our observations in this study are also consistent with the observed ANGPTL knockout phenotypes (84, 205, 224). Humans with ANGPTL3 knockout mutations have decreased TG and LDL-C and decreased cardiovascular risk (199). These mutations might reduce circulating ANGPTL3/8, resulting in increased LPL activity and uptake of FA into skeletal muscle, thus lowering TG levels. Decreased circulating ANGPTL3/8 complex might also result in less inhibition of LPL-mediated cholesterol uptake by the liver, thereby lowering LDL-C levels. In contemplating why an ANGPTL4 knockout or E40K mutation would be beneficial, one possibility might be that reduction of ANGPTL4 in the fat causes increased adipose LPL activity, directly lowering TG. Another possibility could be that less ANGPTL4/8 in the adipose tissue is available to block ANGPTL3/8-mediated inhibition of adipose LPL. This might shift FA uptake more toward skeletal muscle for oxidation, thereby decreasing TG. It is hard to know which, if either, of these mechanisms is correct, and further study will be required to address these possibilities.

In the case of the human ANGPTL8 knockout (121X) mutation, decreased circulating ANGPTL3/8 complex should result in decreased TG, which has been reported (141). The ANGPTL8 121X mutation should provide cardiovascular protection, as ANGPTL8 knockout mice have decreased TG and decreased fat mass (138). The mutation in humans, however, is so rare that even the extensive genetic study probing this question was underpowered (141). In retrospect, this

is not surprising, as the ANGPTL8 121X mutation would have been extremely disadvantageous in a world of caloric insufficiency.

Taken together, our data explain how ANGPTL8 responds to caloric intake to steer FA away from skeletal muscle and toward adipose tissue for storage as TG, as shown by the possible model in Figure 2.9. Under fasting conditions (Figure 2.9A), ANGPTL8 levels are low, and low levels of ANGPTL3/8 and ANGPTL4/8 complexes are made. As a result, LPL is inhibited locally in the fat by ANGPTL4, leading to minimal adipose tissue FA uptake, with most FA uptake occurring in skeletal muscle. Feeding dramatically changes this dynamic by stimulating release of ANGPTL8 in two different complexes to shift FA away from skeletal muscle and toward adipose tissue (Figure 2.9B). Postprandial increases in insulin stimulate hepatic secretion of ANGPTL3/8, which potently inhibits LPL activity. The circulating ANGPTL3/8 complex reaches the skeletal muscle to inhibit LPL and prevent FA uptake. At the same time, postprandial increases in both insulin and GIP stimulate ANGPTL4/8 secretion from adipocytes. When ANGPTL8 is present in this localized complex with ANGPTL4, it drastically decreases the potency of ANGPTL4's LPL inhibitory activity. The increased, localized ANGPTL4/8 in the adipose tissue not only preserves LPL activity but also blocks the ability of circulating ANGPTL3/8 and localized ANGPTL4 to inhibit LPL, with the net result of these actions being increased FA uptake into the adipose tissue for storage as TG.

When viewed holistically, it becomes apparent that the major metabolic problem in our developed world is that, unlike our ancestors, we hardly ever go through any periods of prolonged fasting. Instead, our constant feeding chronically increases our ANGPTL3/8 and ANGPTL4/8 levels. Increased levels of these complexes lead to elevated circulating TG and excessive FA storage in our adipose tissue, which in turn lead to obesity, hypertension, insulin resistance, and ultimately type 2 diabetes. Ironically, in a world of caloric abundance, the same ANGPTL8 protein that likely protected our ancestors from starvation now predisposes us to metabolic syndrome.

FIGURE 2.9

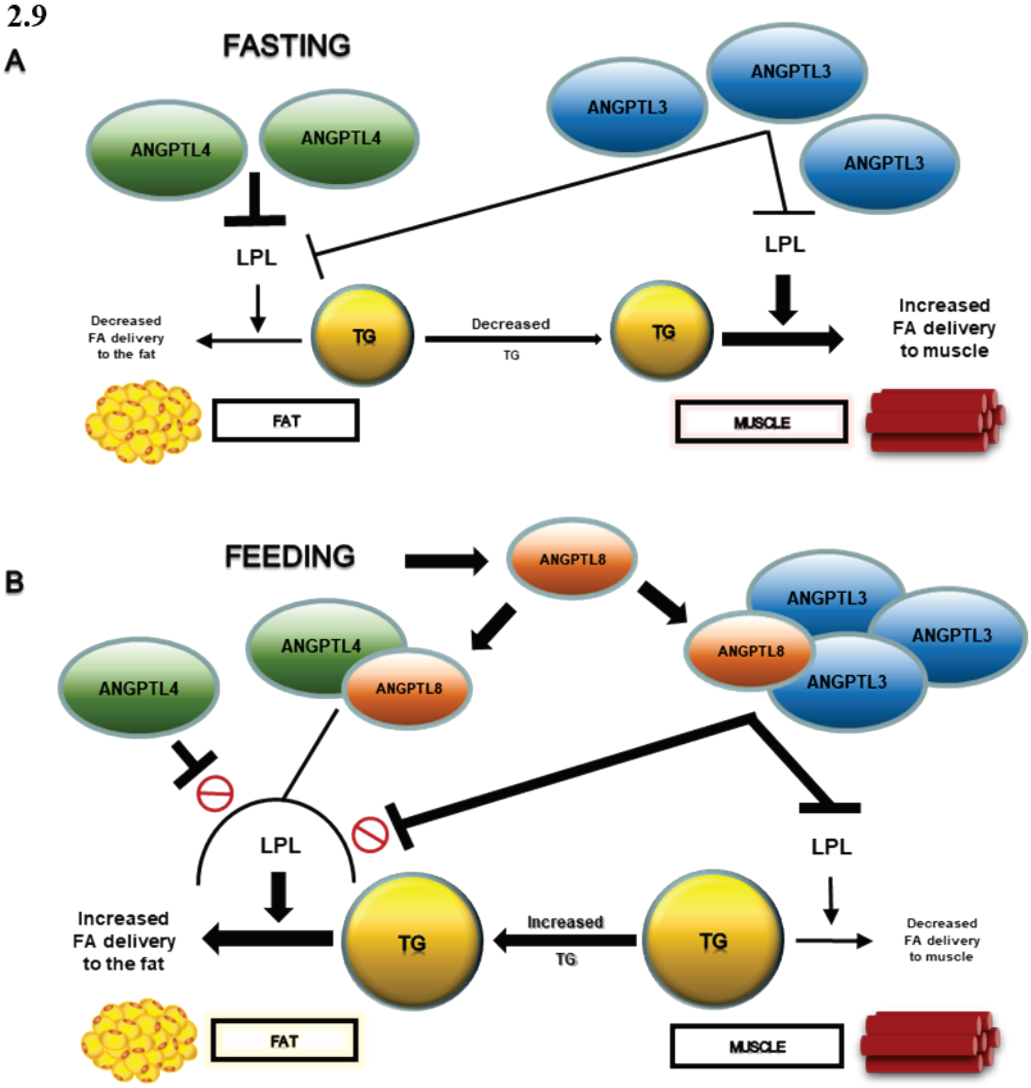

Figure 2.9 A possible model for how ANGPTL8 shifts FA toward adipose tissue after feeding.

A: While fasting, ANGPTL8 levels are low. Localized ANGPTL4 inhibits adipose tissue LPL to minimize FA uptake into the fat for storage, and FAs are mainly taken up into skeletal muscle for use as energy.

B: During feeding, ANGPTL8 forms a circulating complex with ANGPTL3 that increases its ability to inhibit LPL, thus minimizing FA uptake into skeletal muscle. ANGPTL8 also forms a mostly localized complex with ANGPTL4 in adipose tissue that decreases the ability of ANGPTL4 to inhibit LPL. The ANGPTL4/8 complex also protects LPL in the fat from inhibition by circulating ANGPTL3/8 and localized ANGPTL4, thereby preserving adipose tissue LPL activity to promote FA uptake into the fat for storage as TG.

2.4 Data availability

All study data are contained within the manuscript and the Supplementary Data File. All primary mass spectrometry data have been deposited at PeptideAtlas (Server name: ftp.peptideatlas.org) as follows: full URL, ftp://PASS01578:NM8576fr@ftp.peptideatlas.org/; data identifier, PASS01578; dataset type, SRM; dataset tag, ANGPTL; dataset title, SRM quantification of ANGPTL3/4/8 proteins.

2.5 Acknowledgements

This study was funded by Eli Lilly and Company. The authors thank Melissa Bellinger and Robert Schmidt for their expert technical assistance with LPL cell lines and initial characterization of ANGPTL proteins. The authors also thank Rick Conway and George Rodgers for their expert technical assistance in performing immunoassays.

CHAPTER 3. THE MECHANISM OF ACTION OF APOLIPOPROTEIN A5 - SUPPRESSION OF ANGPTL3/8 COMPLEX-MEDIATED INHIBITION OF LPL ACTIVITY

A modified version of this chapter has been submitted for publication approval in the Journal of Lipid Research.

3.1 Introduction

Control of triglyceride (TG) metabolism to enable delivery of fatty acids (FA) to target tissues such as muscle and fat involves a number of different proteins and is incompletely understood. We have recently shown that the angiopoietin-like protein 3/4/8 (ANGPTL3/4/8) family of proteins is critical in regulating circulating TG levels through modulation of lipoprotein lipase (LPL) activity in adipose tissue and skeletal muscle (225). In particular, we demonstrated that ANGPTL8 serves as the critical insulin-responsive protein in this system by forming complexes with ANGPTL3 and ANGPTL4 to increase and decrease markedly their respective LPL-inhibitory activities. ANGPTL8 forms a circulating ANGPTL3/8 complex that dramatically increases ANGPTL3 inhibition of LPL in the skeletal muscle, resulting in increased circulating TG that can be routed to the fat, where LPL inhibition is simultaneously decreased through formation of a localized ANGPTL4/8 complex. The localized ANGPTL4/8 complex also protects LPL in the adipose tissue from circulating ANGPTL3/8 to ensure that adipose tissue LPL is active after feeding. Together, these properties of ANGPTL8 result in increased LPL-inhibition in the skeletal muscle and decreased LPL inhibition in the adipose tissue so that FA are taken up into the fat postprandially and not deposited ectopically (146, 225). As elegant as this remarkable system of proteins is, the above observations cannot fully explain the control of TG metabolism, as several other proteins are known to influence TG concentrations. These include apolipoprotein C2 (ApoC2) (which is thought to activate LPL), ApoC3 (which is thought to inhibit LPL), and the atypical apolipoprotein, ApoA5 (226-232).

Interestingly, while there is clear agreement that ApoA5 potently decreases TG levels, its mechanism of action has remained obscure despite the fact that it was discovered in 2001. The gene for ApoA5 was identified through experiments searching for open reading frames in the ApoA1-ApoC3-ApoA4 gene cluster located on human chromosome 11q23 (228-232). The new

gene that emerged from this search coded for a novel apolipoprotein with greatest homology to ApoA4, and the corresponding apolipoprotein was appropriately named ApoA5. It soon became clear that ApoA5 was crucial in controlling circulating TG levels. When human ApoA5 was overexpressed in mice, it decreased TG concentrations by 50–75%, and when the mouse ApoA5 gene was knocked out, TG concentrations increased approximately 4-fold (228-232). In addition, a number of ApoA5 mutations were reported in humans that correlated with circulating TG (233-236). It was also shown that mRNA expression of ApoA5 was regulated by peroxisome proliferator-activated receptor-α (PPAR-α) agonists, and that administration of a PPAR-α agonist increased circulating ApoA5 levels, suggesting that this class of compounds may reduce serum TG by increasing ApoA5 (237-239). Together, these initial observations clearly established APOA5 as a critical player in TG metabolism.

Despite these compelling early data, however, no clear consensus has emerged for how ApoA5 actually acts at the molecular level to decrease TG. Current hypotheses include suggestions that it may directly stimulate LPL activity, facilitate TG-containing lipoprotein particle uptake by the liver, or intracellularly regulate the secretion of hepatic TG (240-242). One potential clue that the mechanism of action might be unusual came when we measured human serum levels of ApoA5 and found that it circulated as a 39 kD monomer at levels of 24-406 ng/mL, which are much lower than those of other apolipoproteins (243, 244). To put this in perspective, the molar concentration of ApoA5 is approximately 4-6 nM, compared with approximately 40 μM for ApoA1 and 2 μM for ApoB. Yet when transgenic mice had both ApoA5 and ApoC3 either knocked-out or overexpressed, the result was essentially normal TG concentrations, even though ApoC3 levels during overexpression were approximately 500-fold higher than those of over-expressed ApoA5, thus confirming the potent ability of ApoA5 to reduce serum TG (232).

In light of these observations regarding ApoA5 as well as our own and other groups' recent studies on the ANGPTL3/4/8 system of proteins (4, 117, 146, 225), we sought to understand better the possible connections between these two important regulators of TG metabolism. In our present study, we demonstrate that ApoA5 associates with ANGPTL3/8 in human serum and present evidence that ApoA5 works through selective suppression of the LPL-inhibitory activity of the ANGPTL3/8 complex. Using functional LPL assays, we show that ApoA5 has no direct effect on LPL activity, and that it does not affect the LPL-inhibitory activities of ANGPTL3, ANGPTL4, or the ANGPTL4/8 complex. Importantly, we also demonstrate that the suppression of ANGPTL3/8-

mediated LPL-inhibition occurs at a molar ratio that is consistent with that of the molar concentrations of ApoA5 and ANGPTL3/8 in human serum. Upon obtaining these data, we also considered reports of liver X-receptor (LXR) agonists decreasing ApoA5 expression and causing increases in TG (245, 246). We observed that the prototypical LXR agonist T0901317 actually caused modest increases in hepatocyte ApoA5 secretion, but markedly stimulated ANGPTL3/8 secretion. We also observed that the addition of insulin to T0901317 attenuated ApoA5 secretion while further increasing T0901317-stimulated ANGPTL3/8 secretion. Taken together, our results shed light on a novel intersection of ApoA5 and the ANGPTL3/4/8 family of proteins in the regulation of TG metabolism and also provide a possible explanation for LXR agonist-induced hypertriglyceridemia.

3.2 Results

*Result sections denoted with * after the subsection heading were addressed through my personal contributions.*

3.2.1 Association of ApoA5 with ANGPTL3/8 complex in human serum*

To determine which circulating proteins associate with ANGPTL3/8, we incubated immobilized ANGPTL3/8 with human serum. After washing, bound proteins were eluted, reduced, and alkylated prior to trypsin digestion. Tryptic peptides were separated chromatographically, and the MS/MS spectra of each peptide was searched against a human database. Seventeen peptide ions were positively identified from ApoA5, and these 17 ions contained 12 unique peptide sequences covering 52% of the protein sequence. The mean AUCs for these 17 peptide ions from ANGPTL3/8-coated wells and control wells are shown in Figure 3.1A. Database search results and mean AUC for the ApoA5 peptide ions are listed in Supplemental Table B1, and extracted ion chromatograms are shown in Supplemental Figures A1-A17. Of the 17 ApoA5 ions, 3 ions present at a much lower level also registered positive AUC values in the control samples when extracting with a 2 ppm mass tolerance window. Detailed analyses, however, revealed that these were interference ions with a different isotope pattern compared to the corresponding ApoA5 ions.

Statistical analysis revealed that ApoA5 was the only protein enriched greater than 5-fold ($p < 0.001$) compared to control. Under these conditions, no other proteins were enriched greater than

5-fold, indicating that the main protein associated with ANGPTL3/8 in human serum was ApoA5. To verify this observation, we coupled anti-ANGPTL3/8, anti-ApoA5, and irrelevant control antibodies to beads, incubated the beads with human serum, separated bound proteins via electrophoresis, transferred the proteins to PVDF, and performed Western blotting with anti-ApoA5 antibody. As Figure 3.1B shows, ApoA5 co-immunoprecipitated with ANGPTL3/8, confirming the association observed via mass spectrometry.

FIGURE 3.1

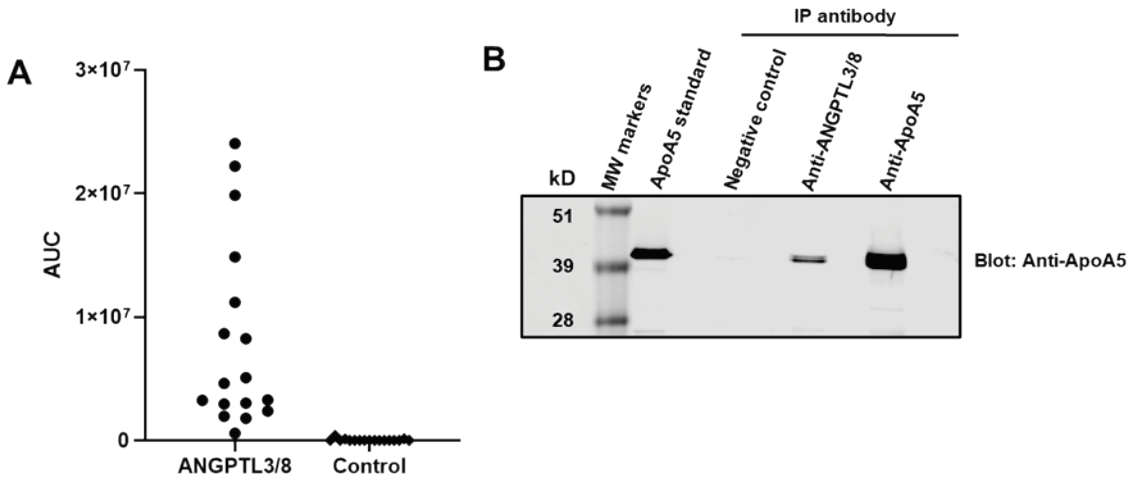

Figure 3.1 ApoA5 associates with ANGPTL3/8 in human serum.

(A) ANGPTL3/8 complex was coupled to beads incubated with human serum. Bound proteins were reduced, alkylated, and digested with trypsin. The means (from triplicate samples) of the areas under the curve (AUC) for peptide ions significantly different from control ($p < 0.05$ and fold change > 5) were plotted in a scatter dot plot. Only ApoA5 peptide ions met these criteria. The AUC was extracted for each ion with a mass tolerance of 2 ppm. Results shown are representative of 3 independent experiments.

(B) An irrelevant control antibody, an anti-ANGPTL3/8 antibody, and an anti-ApoA5 antibody were covalently coupled to beads, with heavy and light chains further cross-linked, and were used to immunoprecipitate human serum. Proteins were separated on a 12% Bis-Tris gel and transferred to PVDF membrane. The blot was stained with anti-ApoA5 antibody. Results are representative of 2 independent experiments.

3.2.2 Generation of recombinant ApoA5 protein

Initial attempts to express human ApoA5 (residues 24-366) were unsuccessful, with the recombinant protein proving to be unstable. We therefore took a new approach and expressed ApoA5 coupled to HIS tag-mature human serum albumin (HSA) at either the N-terminus (HSA-ApoA5) or the C-terminus (ApoA5-HSA) of ApoA5. The ApoA5 could then be used either as an intact ApoA5 fusion protein or could undergo PreScission cleavage to generate HSA and ApoA5

immediately prior to use in LPL assays. Figure 3.2 shows a Coomassie-stained gel, with ApoA5-HSA, HSA-ApoA5, and HSA alone evaluated either without or with PreScission cleavage. As the figure demonstrates, this approach provided large quantities of very pure ApoA5 suitable for subsequent experiments.

FIGURE 3.2

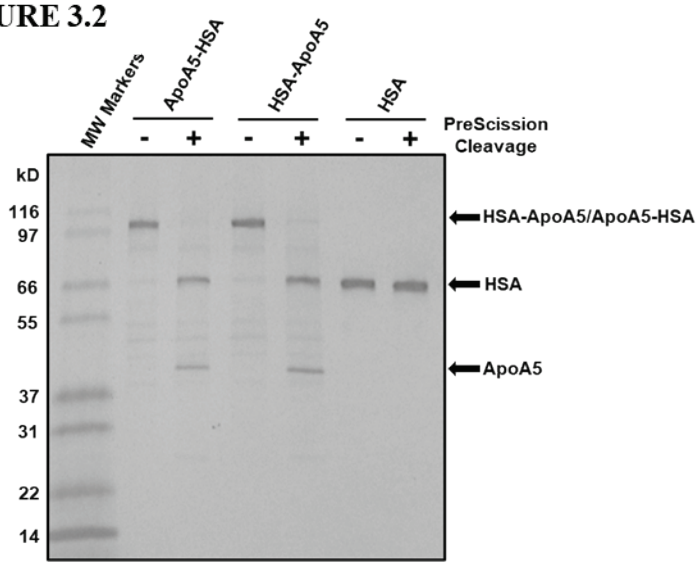

Figure 3.2 Expression and purification of recombinant ApoA5 proteins.

Recombinant human ApoA5-HSA, HSA-ApoA5, and control HSA protein (0.5 µg of each) were analyzed either without or with PreScission cleavage of the HSA tag. Proteins were separated via gradient gel electrophoresis using a 4-20% Tris-glycine gel and stained with Coomassie Blue.

3.2.3 ApoA5 suppression of ANGPTL3/8-mediated LPL-inhibitory activity.

Upon observing the association of ApoA5 with ANGPTL3/8 in human serum, we sought to determine if ApoA5 altered the ability of ANGPTL3/8 to inhibit LPL activity. To do this, we assessed the ability of increasing concentrations of ANGPTL3/8 to inhibit LPL activity in the presence of 0-300 nM ApoA5. Figure 3.3A shows the results of these experiments, in which HSA-ApoA5 dose-dependently decreased the ability of ANGPTL3/8 to inhibit LPL activity. In contrast, when similar experiments were performed with ANGPTL4 (which inhibits LPL activity to roughly the same degree as ANGPTL3/8), there was no decrease observed in the ability of ANGPTL4 to inhibit LPL in the presence of increasing concentrations of ApoA5 (Figure 3.3B). Similarly, when the same experiments were performed with ANGPTL3 and ANGPTL4/8 (which are both relatively weak inhibitors of LPL), there was no ApoA5-mediated decrease in their ability to inhibit LPL (Figures 3.3C and 3.3D, respectively).

Comparable results to those in Figure 3.3 were also obtained when using ApoA5-HSA, PreScission-cleaved HSA-ApoA5, or PreScission-cleaved ApoA5-HSA. As Figure 3.4A shows, HSA-ApoA5 and ApoA5-HSA demonstrated similar suppression of ANGPTL3/8-mediated LPL-inhibitory activity. Likewise, as shown in Figure 3.4B, PreScission-cleaved HSA-ApoA5 and PreScission-cleaved ApoA5-HSA also demonstrated comparable suppression of ANGPTL3/8-mediated LPL-inhibitory activity. In addition, HSA itself had no effect on ANGPTL3/8-mediated LPL-inhibitory activity. Together, these data confirmed the results in Figure 3.3 and led us to conduct future LPL activity assays with HSA-ApoA5.

FIGURE 3.3

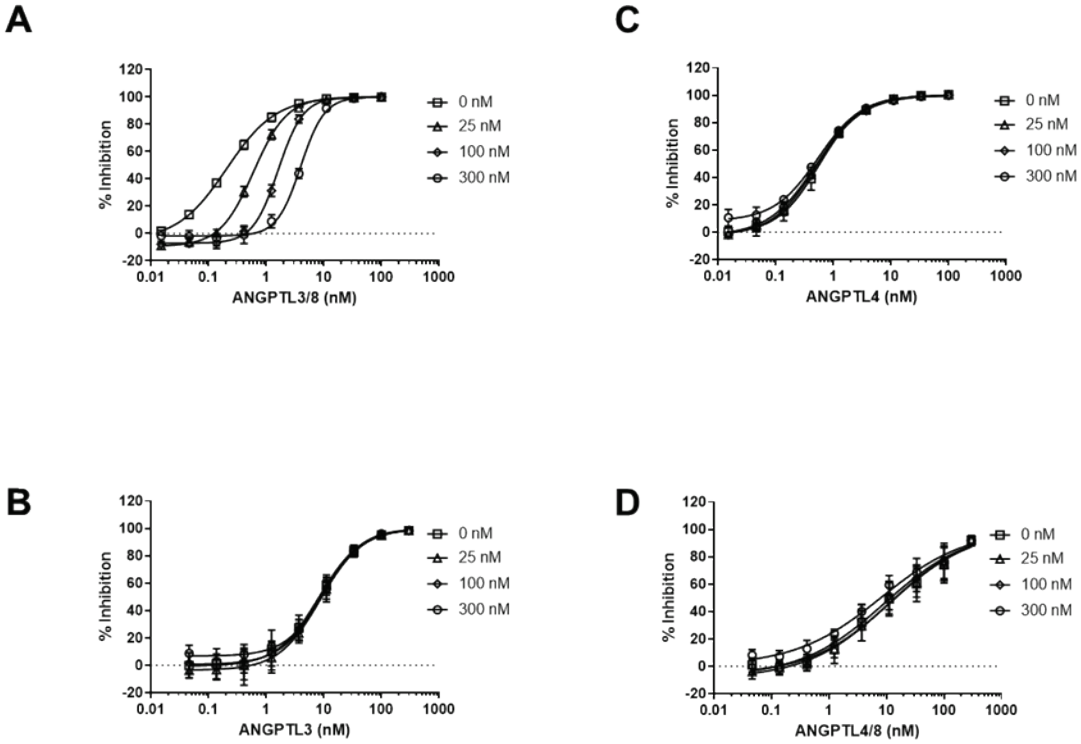

Figure 3.3 ApoA5 selectively blocks the ability of ANGPTL3/8 to inhibit LPL activity.

The ability of ANGPTL3/8, ANGPTL3, ANGPTL4, and ANGPTL4/8 to inhibit LPL activity in the presence of 0 nM (squares), 25 nM (triangles), 100 nM (diamonds) and 300 nM (circles) of ApoA5 (HSA-ApoA5) was assessed using LPL-stable expression cells. All results are shown as the mean ± SD (n = 3 from 3 independent experiments).

(A) ANGPTL3/8 was pre-incubated with ApoA5 prior to the addition of lipase substrate.

(B) ANGPTL3 was pre-incubated with ApoA5 prior to the addition of lipase substrate.

(C) ANGPTL4 was pre-incubated with ApoA5 prior to the addition of lipase substrate.

(D) ANGPTL4/8 was pre-incubated with ApoA5 prior to the addition of lipase substrate.

FIGURE 3.4

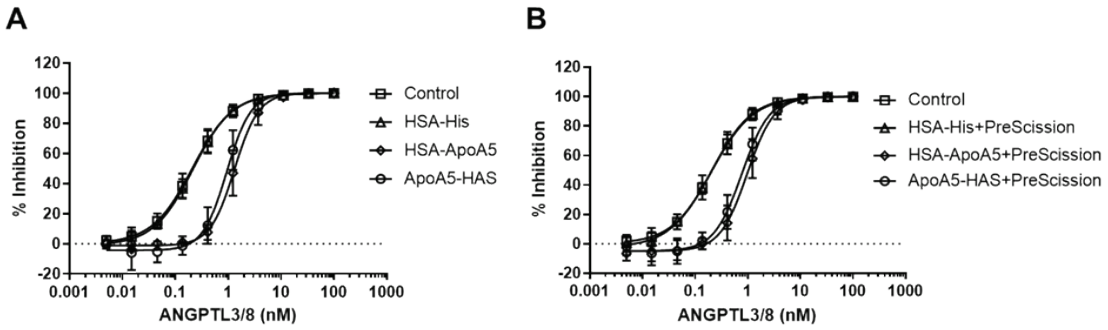

Figure 3.4 HSA-ApoA5 and ApoA5-HSA block ANGPTL3/8-mediated LPL inhibitory activity in a similar manner to PreScission-cleaved HSA-ApoA5 and ApoA5-HSA.

(A) The ability of 100 nM HSA-ApoA5 (diamonds) and 100 nM ApoA5-HSA (circles) to inhibit LPL activity in the presence of increasing concentrations of ANGPTL3/8 was assessed using LPL-stable expression cells. Control (squares) and HSA-His alone (triangles) conditions are also shown. Results are shown as the mean ± SD (n = 3 from 3 independent experiments).

(B) The ability of 100 nM PreScission-cleaved HSA-ApoA5 (diamonds) and 100 nM PreScission-cleaved ApoA5-HSA (circles) to inhibit LPL activity in the presence of increasing concentrations of ANGPTL3/8 was assessed using LPL-stable expression cells. Control (squares) and HSA-His alone plus PreScission cleavage (triangles) are also shown. Results are shown as the mean ± SD (n = 3 from 3 independent experiments).

To confirm further the specific effect of ApoA5 on ANGPTL3/8 versus other ANGPTL proteins and complexes, we performed kinetic analyses of the LPL-inhibitory activity of 1.2 nM of ANGPTL3/8 complex in the presence of increasing concentrations of ApoA5. As Figure 3.5A shows, at a concentration of 25 nM ApoA5, a decrease in the ability of ANGPTL3/8 to inhibit LPL activity was clearly evident. At 100 nM of ApoA5, the ability of ANGPTL3/8 to inhibit LPL activity was more than cut in half. At 300 nM of ApoA5, the ability of ANGPTL3/8 to inhibit LPL activity was almost completely blocked. The effect of ApoA5 was thus more than half-maximal at concentrations of 100 nM ApoA5 and 1.2 nM of ANGPTL3/8, where the molar ratio was 83:1. This ratio is consistent with the approximate 60:1 molar ratio for the reported circulating concentrations of ApoA5 (6 nM) and ANGPTL3/8 (0.1 nM) (225, 243).

To probe this concept further, we directly assessed the effect of increasing concentrations of ApoA5 on the ability of 0.3 nM ANGPTL3/8 (the approximately IC_{60} for ANGPTL3/8) to inhibit LPL. In these experiments, 0.3 nM of ANGPTL3/8 was first pre-incubated with increasing concentrations of ApoA5 prior to its evaluation in the LPL assay. As Figure 3.5B demonstrates, the EC_{50} for ApoA5 to block 0.3 nM ANGPTL3/8-mediated inhibition of LPL activity was 21 nM,

for a molar ratio of ApoA5:ANGPTL3/8 of 70:1. This ratio was very close to the 83:1 ratio estimated from the kinetic analyses, as well as the 60:1 ratio for the respective circulating molar concentrations of ApoA5 and ANGPTL3/8.

FIGURE 3.5

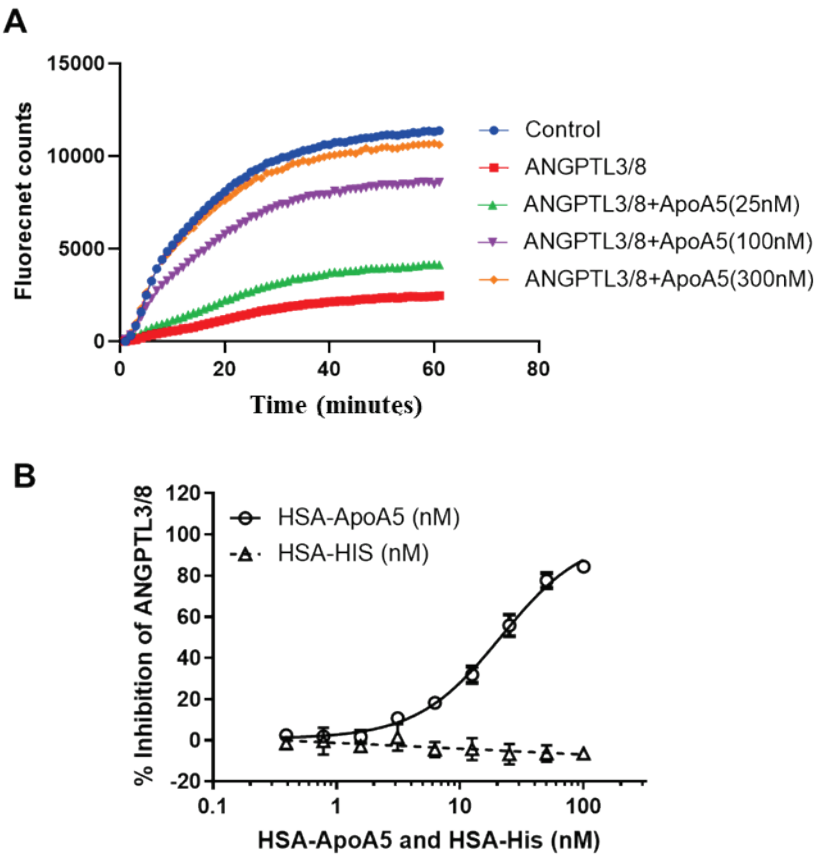

Figure 3.5 Analyses of ApoA5 effect on ANGPTL3/8-mediated LPL inhibition.

(A) The ability of 1.2 nM of ANGPTL3/8 to inhibit LPL activity in the presence of HSA-ApoA5 was assessed via kinetic analyses using LPL-stable expression cells. ANGPTL3/8 was pre-incubated with 0 nM (red squares), 25 nM (green tringles), 100 nM (purple triangles) or 300 nM (orange diamonds) of HSA-ApoA5 prior to the addition of lipase substrate. The control condition (blue circles) indicates the absence of ANGPTL3/8. Results are representative of 3 independent experiments.

(B) The effect of increasing concentrations of HSA-ApoA5 (circles) on the ability of 0.3 nM of ANGPTL3/8 (the IC_{60} of ANGPTL3/8) to inhibit LPL activity was assessed using LPL-stable expression cells. ANGPTL3/8 was pre-incubated with increasing concentrations of HSA-ApoA5 prior to the addition of lipase substrate. The effect of HSA alone (triangles) was also evaluated. Results are shown as the mean ± SD (n = 4 from 2 independent experiments).

In order to confirm that the observed effect of ApoA5 to suppress the LPL-inhibitory activity of ANGPTL3/8 was specific for ANGPTL3/8, we performed additional kinetic analyses of the

LPL-inhibitory activity of 1.2 nM of ANGPTL4, ANGPTL3, and ANGPTL4/8 in the presence of increasing concentrations of ApoA5. As Figures 3.6A-C demonstrate, ApoA5 did not suppress the ability of ANGPTL4, ANGPTL3, or ANGPTL4/8 to inhibit LPL activity (in the case of ANGPTL4/8 there was a very slight trend toward increasing the LPL-inhibitory activity). These experiments thus verified that the ability of ApoA5 to suppress the LPL-inhibitory activity of ANGPTL3/8 was specific for the ANGPTL3/8 complex and that this property was not shared with regard to any of the other ANGPTL proteins or complexes tested. Importantly, as Figure 3.6D shows, there was no ability of ApoA5 alone to stimulate LPL activity, indicating that ApoA5 on its own was not capable of directly increasing LPL activity, but rather could only act to increase LPL activity by decreasing the ability of ANGPTL3/8 to inhibit LPL.

FIGURE 3.6

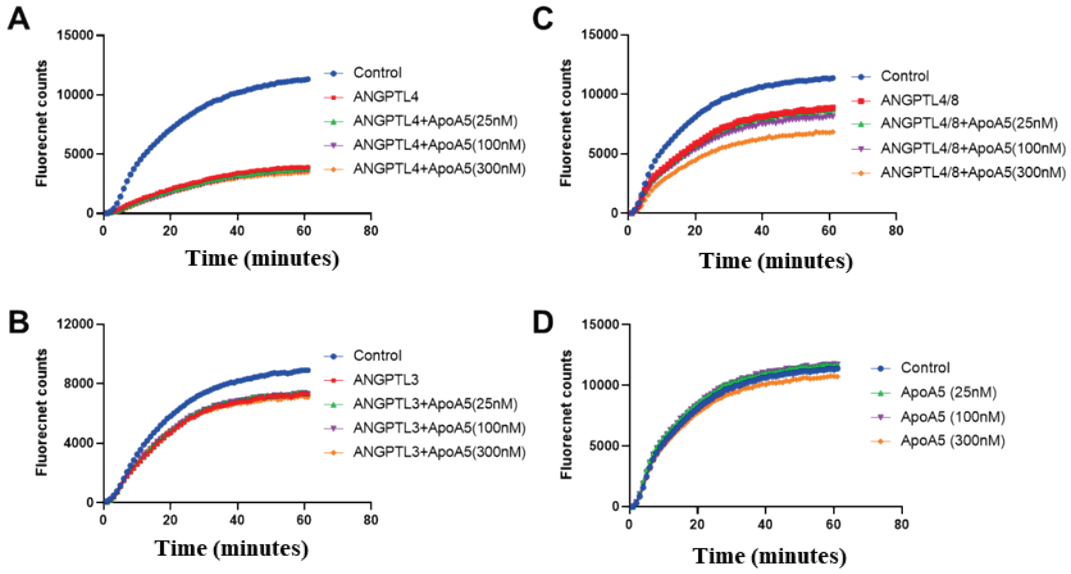

Figure 3.6 Kinetic analyses of the ApoA5 effect on LPL-inhibitory activities of ANGPTL4, ANGPTL3, and ANGPTL4/8.

The ability of ANGPTL4, ANGPTL3, or ANGPTL4/8 (each at 1.2 nM) to inhibit LPL activity in the presence of different concentrations of ApoA5 at 0 nM (red squares), 25 nM (green triangles), 100nM (purple triangles), and 300 nM (orange diamonds) was assessed using LPL-stable expression cells. The control condition (blue circles) indicates the absence of each respective ANGPTL protein or complex. All results are representative of 3 independent experiments

(A) ANGPTL4 was pre-incubated with ApoA5 prior to the addition of lipase substrate.

(B) ANGPTL3 was pre-incubated with ApoA5 prior to the addition of lipase substrate.

(C) ANGPTL4/8 was pre-incubated with ApoA5 prior to the addition of lipase substrate.

(D) The effect of ApoA5 alone at 0 nM (blue circles), 25 nM (green triangles), 100 nM (purple triangles), and 300 nM (orange diamonds) on LPL activity was assessed.

3.2.4 Insulin & LXR agonist-stimulated secretion of ANGPTL3/8 and ApoA5 from hepatocytes*

In light of the above results showing that ApoA5 selectively suppressed the LPL-inhibitory activity of ANGPTL3/8, we considered previous reports showing that LXR agonists cause hypertriglyceridemia and decrease expression of ApoA5 (245, 246). We hypothesized that the reported increases in TG levels following administration of LXR agonists might be due more to increased hepatic secretion of ANGPTL3/8 than to decreased ApoA5 secretion. We also considered that LXR agonist-induced increases in hepatic ANGPTL3/8 secretion might be further augmented by insulin since we previously demonstrated that insulin stimulated the secretion of ANGPTL3/8 from hepatocytes (225).

To test these hypotheses, we first performed an insulin-response dose curve in primary human hepatocytes and measured secreted ANGPTL3/8 and ApoA5. Figure 3.7A shows the results from these experiments, in which insulin dose-dependently increased hepatocyte secretion of ANGPTL3/8 while dose-dependently decreasing the secretion of ApoA5. We next performed similar experiments with the LXR agonist T0901317. In these experiments shown in Figure 3.7B, T0901317 actually caused a modest dose-dependent increase in ApoA5 secretion, but stimulated a marked, dose-dependent increase in ANGPTL3/8 secretion that was far greater in magnitude than the effect observed for ApoA5.

After obtaining these results, we next investigated the combined effects of T0901317 and insulin on hepatocyte secretion of ANGPTL3/8 and ApoA5. As Figure 3.8A shows, the combination of T0901317 and insulin stimulated ANGPTL3/8 secretion to a greater extent than was seen with either insulin or the LXR-agonist alone. When ApoA5 secretion was measured in the same experiments, however, a very different pattern emerged. As shown in Figure 3.8B, increasing amounts of insulin blocked the ability of T0901317 to stimulate hepatocyte ApoA5 secretion, so much so that at 1 nM insulin, ApoA5 secretion was actually less than that of the control, even in the presence of the maximal concentration of T0901317 tested. Together, these results demonstrated that while T0901317-stimulated hepatocyte ANGPTL3/8 secretion was enhanced by insulin, T0901317-stimulated ApoA5 secretion from hepatocytes was simultaneously attenuated by insulin.

FIGURE 3.7

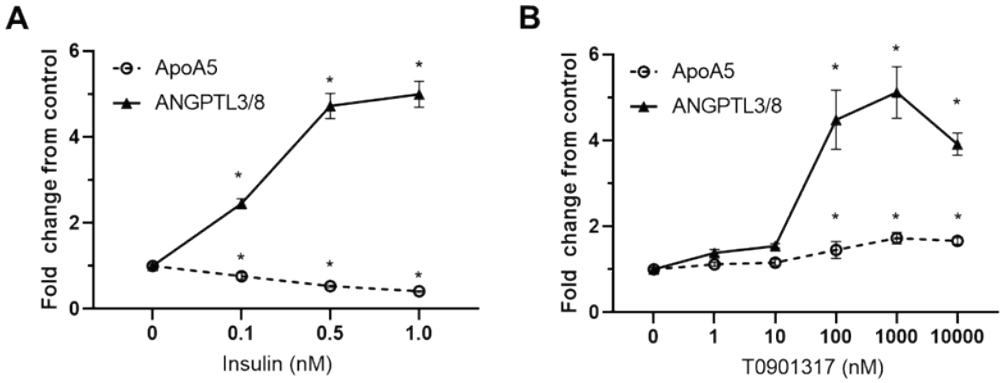

Figure 3.7 Effect of insulin or LXR agonist TO901317 on hepatocyte secretion of ANGPTL3/8 and ApoA5

(A) Human primary hepatocytes were pre-incubated in application media in the absence of insulin. Following aspiration, cells were incubated with application media in the presence of 0-1 nM insulin. ANGPTL3/8 (filled circles) and ApoA5 (open circles) levels in the media were measured using immunoassays, with results shown as the mean ± SEM (n = 8 from 2 independent experiments, *$p <$ 0.01).

(B) Human primary hepatocytes were pre-incubated in application media in the absence of insulin. Following aspiration, cells were incubated with application media in the presence of 0-10,000 nM TO901317. ANGPTL3/8 (filled circles) and ApoA5 (open circles) in the media were measured using sandwich immunoassays, with results shown as the mean ± SEM (n = 8 from 2 independent experiments, *$p < 0.01$).

FIGURE 3.8

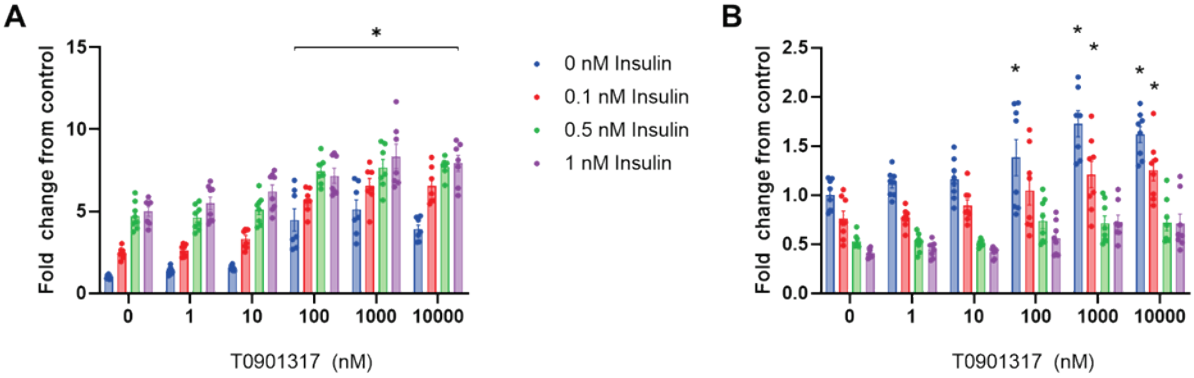

Figure 3.8 Effect of the combination of insulin and the LXR agonist TO901317 on hepatocyte secretion of ANGPTL3/8 and ApoA5

(A) Human primary hepatocytes were pre-incubated in application media in the absence of insulin. Following aspiration, cells were incubated with application media in the presence of 0-1 nM insulin and 0-10,000 nM TO901317. ANGPTL3/8 levels in the media were measured using an immunoassay, with results shown as the mean ± SEM (n = 8 from 2 independent experiments, *$p < 0.001$).

(B) ApoA5 levels from the exact same media samples collected in Figure 3.8A were measured using an immunoassay, with results shown as the mean ± SEM (n = 8 from 2 independent experiments, *$p < 0.01$).

3.3 Discussion

The data in our study reveal a novel intersection of ApoA5 and ANGPTL3/4/8 protein family in the regulation of TG metabolism. Our results indicate that the likely mechanism through which ApoA5 lowers TG is through suppression of ANGPTL3/8-mediated LPL inhibition. Remarkably ApoA5 selectively suppressed the LPL-inhibitory activity of the ANGPTL3/8 complex while not decreasing the LPL-inhibitory activity of ANGPTL4, ANGPTL3, or ANGPTL4/8. Importantly, half-maximal ApoA5 suppression of ANGPTL3/8-mediated LPL-inhibitory activity occurred at an ApoA5:ANGPTL3/8 molar ratio consistent with the molar ratio observed in human serum (243). This supports the concept that the suppression of ANGPTL3/8 LPL-inhibitory activity by ApoA5 observed in our *in vitro* functional assays occurs under conditions consistent with the normal physiological regulation of TG metabolism.

Importantly, our data also reveal an additional mechanism by which insulin may direct the uptake of FA into adipose tissue. We previously demonstrated that insulin acts through ANGPTL8 to direct the postprandial storage of FA from food into the fat for future energy needs (225). By increasing ANGPTL8, insulin stimulates the formation of a circulating ANGPTL3/8 complex that inhibits LPL in skeletal muscle and a localized ANGPTL4/8 complex in the fat that both reduces ANGPTL4-mediated inhibition of LPL and serves to block ANGPTL3/8 inhibition of LPL in the adipose tissue. In so doing, insulin thus directs the postprandial increase of LPL-inhibitory activity to occur mainly in the skeletal muscle while ensuring that adipose tissue LPL is active so that FA are taken up mostly into the fat after feeding. By decreasing hepatocyte secretion of ApoA5, insulin further accentuates this effect since ApoA5 blocks the LPL-inhibitory activity of the ANGPTL3/8 complex. Thus, under postprandial conditions when insulin levels are high, both the absolute amount of ANGPTL3/8 and the relative extent of the LPL-inhibitory activity of ANGPTL3/8 are increased since insulin increases ANGPTL3/8 secretion from the liver and decreases hepatic secretion of ApoA5, thus causing less suppression of the LPL-inhibitory activity of the secreted ANGPTL3/8 complex.

A caveat with regard to our findings is that our *in vitro* functional experiments were performed under conditions in which it is impossible to replicate completely the environment of capillary endothelial surfaces where LPL acts *in vivo* to hydrolyze TG into FA. This is potentially important because several different proteins (including ApoC2, ApoC3, and GPIHBP1) are thought to affect LPL activity and stability, and may possibly modulate the effect of ANGPTL3/8

on LPL activity (190, 226, 227, 247). In adipose tissue, LPL is transported from the underlying adipocytes across the capillary endothelial cells by GPIHPB1 and remains bound to GPIHBP1 in the capillary lumens, where GPIHBP1 appears to be important in shielding LPL and preserving its activity (190, 247). In addition, LPL activity *in vivo* is modulated by apolipoproteins including ApoC2, which is believed to be an important stimulator of LPL activity, and ApoC3, which is thought to be an inhibitor of LPL activity (226, 227). The binding of each of these proteins to LPL therefore may affect the stability and activity of LPL as well as its interactions with the ANGPTL3/8 complex, and these interactions cannot be replicated in the *in vitro* functional assays used to characterize LPL activity.

Nevertheless, our data strongly suggest that the long-sought mechanism through which ApoA5 works to lower serum TG is by selectively suppressing the LPL-inhibitory activity of the ANGPTL3/8 complex. The unusual nature of this mechanism helps explain why despite being discovered almost 20 years ago and being recognized almost immediately as a key player in TG metabolism, the exact manner in which ApoA5 acts to decrease TG has remained stubbornly elusive. In retrospect, some hints did emerge relatively early on suggesting that the mechanism of ApoA5-mediated TG lowering was atypical. One of the first clues came with the discovery that circulating concentrations of ApoA5 were in the ng/mL range compared to other apolipoproteins such as ApoA1 which are present in the μg/mL range (243). Early suggestions that ApoA5 might act by inhibiting VLDL-TG production or directly stimulating LPL-mediated VLDL-TG hydrolysis proved difficult to reconcile with the idea that only a very small minority of VLDL particles would actually contain a molecule of ApoA5 (243).

In addition to providing the mechanism through which ApoA5 lowers TG, our data also shed light on another long-standing area of investigation in the area of TG metabolism – the increases in serum TG that occur following administration of LXR agonists. For many years, LXR agonists have been studied in preclinical models of atherosclerosis. In these models, improvements in atherosclerotic lesion formation were seen, however, so too were undesired increases in circulating TG (248-251). The increases in TG were initially thought to be the result of increases in hepatic fatty acid synthesis and VLDL secretion and potentially surmountable, and the LXR agonist BMS-852927 was even advanced into clinical testing (245). In a multiple ascending dose (MAD) study, however, TG elevations occurred in a dose-dependent manner with increases of up to 198%

observed at day 14, suggesting that LXR agonism could cause hypertriglyceridemia in humans (245).

After considering these reports, and in light of our previous finding that insulin can stimulate secretion of ANGPTL3/8 from hepatocytes (225), we hypothesized that LXR agonists might cause hypertriglyceridemia by stimulating hepatic secretion of ANGPTL3/8. Supporting this hypothesis, LXR activation has been shown to increase ANGPTL3 and ANGPTL8 mRNA levels via sterol regulatory element-binding protein 1c (SREBP-1c), while insulin activation of SREBP-1c in hepatocytes can be blocked by LXR antagonists (95, 134, 252). With regard to ApoA5, LXR activation has been shown to down-regulate ApoA5 mRNA levels through SREBP-1c, and insulin has been demonstrated to decrease the expression of ApoA5 via the phosphatidylinositol 3-kinase pathway (246, 253). When viewed together, these observations suggested that LXR agonists might possibly stimulate hepatocyte ANGPTL3/8 secretion while potentially decreasing ApoA5 secretion.

Using primary human hepatocytes, we were able to demonstrate that the prototypical LXR agonist T0901317 caused an almost 6-fold increase in ANGPTL3/8 secretion in the absence of insulin and that this became an almost 8-fold increase in the presence of insulin. Somewhat surprisingly, we also found that T0901317 caused a modest, yet significant, increase in hepatocyte ApoA5 secretion in the absence of insulin. This potentially beneficial increase in ApoA5 secretion, however, was largely negated by the addition of insulin. Thus, it seems likely that the hypertriglyceridemia observed with LXR agonists is at least in part due to LXR agonist-induced hepatic secretion of ANGPTL3/8.

In summary, our data shed important light on TG metabolism by showing that two key players known to be extremely important in the control of TG levels – the ANGPTL3/4/8 family of proteins and the apolipoprotein ApoA5 - are actually interconnected. Their unique intersection occurs through the ability of ApoA5 to selectively suppress the LPL-inhibitory activity of the ANGPTL3/8 complex. In uncovering this mode of action of ApoA5, we were able to determine that an additional mechanism through which insulin stimulates FA uptake into adipose tissue may be by decreasing hepatocyte secretion of ApoA5. Because ApoA5 is an inhibitor of ANGPTL3/8, the increased ANGPTL3/8 secreted by hepatocytes in response to insulin would be expected to have even greater LPL-inhibitory activity if ApoA5 secretion is also reduced. Similarly, we were also able to ascertain that a likely mechanism by which LXR agonists cause hypertriglyceridemia

is through stimulation of hepatic ANGPTL3/8 secretion. Together, these findings provide further novel insight into the regulation of TG metabolism while at the same time suggesting that additional investigation will be required to understand more fully the molecular basis for the suppression of ANGPTL3/8-mediated LPL-inhibitory activity by ApoA5.

3.4 Data availability

All data presented as part of this study are contained within the manuscript itself and the accompanying Supplemental Data File.

3.5 Acknowledgements

This study was funded by Eli Lilly and Company. The authors thank Melissa Bellinger for her assistance with LPL cell lines.

CHAPTER 4. DISCUSSION

4.1 Updates to the ANGPTL3-4-8 model of triglyceride partitioning

The data contained within this thesis describe how excessive caloric intake and minimal periods of fasting alter TG partitioning through modulation of the ANGPTL3-4-8 system. Frequent elevations in insulin either due to dietary patterns or as seen in the development of MetS result in increased circulating TG and may potentiate unwanted gains in adiposity. In turn, a dietary imbalance can further MetS progression and increase the likelihood for subsequent comorbidities.

In this model (shown in Figure 4.1 and Figure 4.2), elevated insulin concentrations result in increased hepatic ANGPTL3/8 secretion (Figure 4.2 [1]) that works as an endocrine molecule to inhibit skeletal muscle LPL from hydrolyzing circulating TG (Figure 4.2 [4]). Simultaneously, insulin results in increased ANGPTL4/8 in the adipose (Figure 4.2 [2]) where it works in a paracrine mechanism to attach to LPL on the endothelial vasculature adjacent to adipose tissue to alleviate ANGPTL4-mediated LPL inhibition (Figure 4.2 [3]). This results in increasing TG hydrolysis and FA are shunted into adipocytes for longer term storage. Under conditions of sustained elevations in insulin, adipocytes expand as they incorporate more FA for storage resulting in increased BMI and visceral adiposity.

Additional factors such as ApoA5, LXR agonism via oxysterols, and GIP exacerbate the impact of insulin driven changes to this system. When fasting, lowered insulin levels allow for increased secretion of ApoA5 from the liver – an effect which is enhanced by LXR activation. As a result, ApoA5 binds to the already decreased, secreted ANGPTL3/8 reducing its capacity to inhibit LPL. In relation to ANGPTL4/8 secretion, circulating GIP concentrations increase postprandially. GIP in the presence of insulin greatly stimulates the secretion of ANGPTL4/8 from adipocytes. This secretion heavily alters the balance of systemic LPL activity towards adipocytes ensuring that TG from the diet are stored in the fat and not deposited ectopically.

During periods of fasting, lower insulin concentrations result in decreased production of ANGPTL8 from both the liver (Figure 4.1 [1]) and fat (Figure 4.1 [2]), while allowing for the simultaneous secretion of ApoA5 (Figure 4.1 [1]) ApoA5 binds to the small concentration of ANGPTL3/8 hepatically produced and decreases its LPL inhibitory potential (Figure 4.1 [4]). As a result, LPL around skeletal muscle can hydrolyze TG for energy utilization (Figure 4.1 [4]). The

diminished production of ANGPTL8 from adipocytes allows for ANGPTL4 to act on local LPL, prevent TG hydrolysis, and consequently, reduce FA uptake by adipocytes for storage (Figure 4.1 [3]).

Feeding, however, induces insulin and GIP secretion. Insulin causes ANGPTL3/8 to be released from the liver while suppressing the secretion of ApoA5 (Figure 4.2 [1]). Thus, fully active ANGPTL3/8 circulates, binds LPL adjacent to skeletal muscles, and reduces the amount of TG utilized for immediate energy needs (Figure 4.2 [4]). GIP acts in conjunction with insulin in the adipocytes to greatly enhance the amount of ANGPTL4/8 which is secreted. ANGPTL4/8 binds to LPL and prevents circulating ANGPTL3/8 from inhibiting the enzyme (Figure 4.2 [3]). Thus, LPL around adipocytes is fully active allowing for TG hydrolysis and subsequent energy storage within the fat. The regulated secretion of these complexes heavily alters the balance of systemic LPL activity towards adipocytes ensuring that TG from the diet are stored in adipose tissue and not deposited ectopically.

FIGURE 4.1

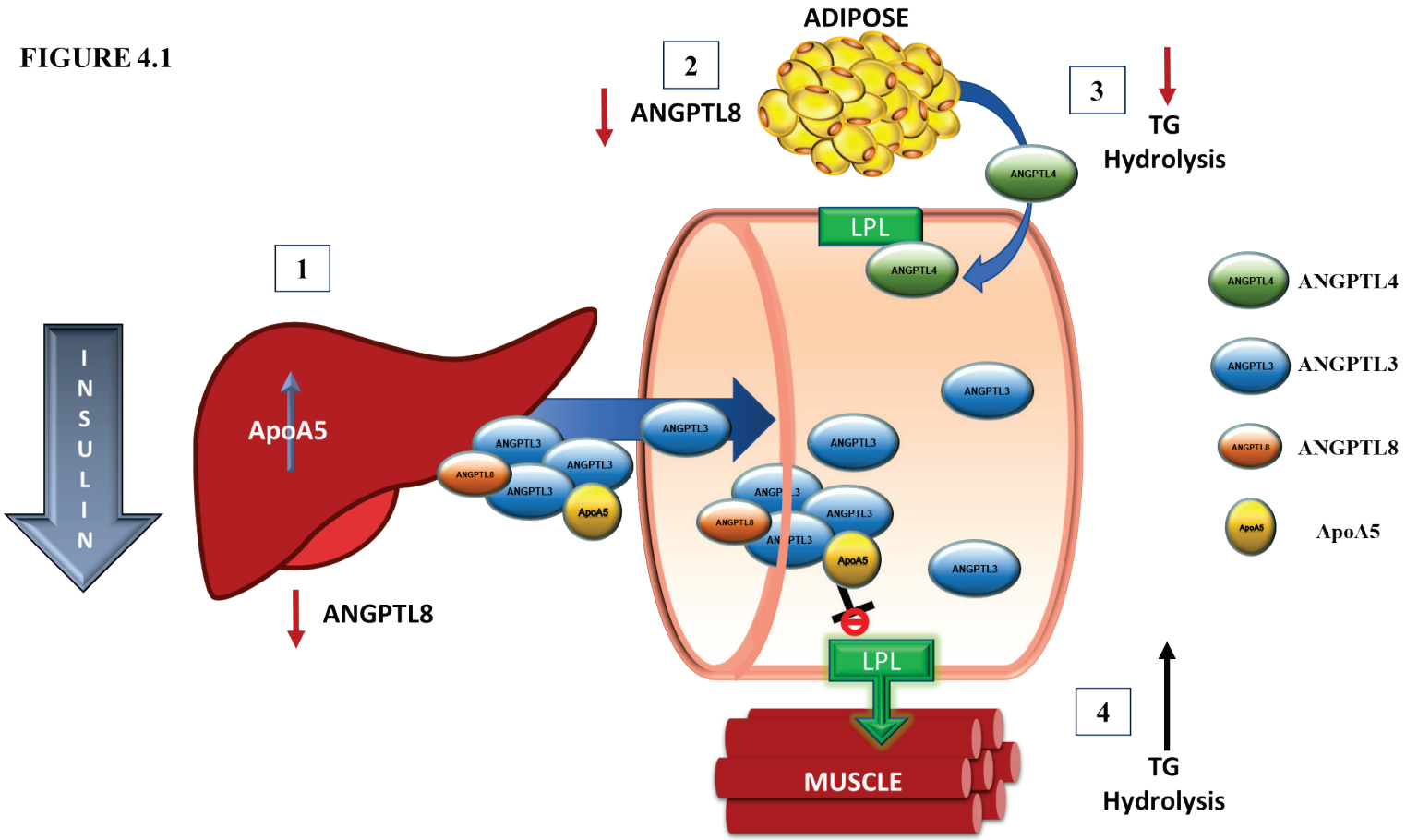

Figure 4.1 Triglyceride partitioning under fasting conditions.

1) Without elevated concentrations of insulin, the liver produces minimal amounts of ANGPTL8 and increased amounts of ApoA5. The liver however continues to produce similar amounts of ANGPTL3 regardless of insulin concentration. Thus, ANGPTL3 is continually secreted while ANGPTL3/8 is now secreted at low levels but in combination with ApoA5. (2) Adipose tissue without the stimulation from insulin predominantly releases ANGPTL4. The paracrine ANGPTL4 blunts the ability of LPL to hydrolyze circulating TG containing molecules thereby denying FA to adipocytes for energy storage. (4) Circulating ANGPTL3/8 with ApoA5 still binds LPL, however; the ability of ANGPTL3/8 to inhibit LPL is negated. Thus, capillary LPL adjacent to skeletal muscle continues to hydrolyze TG. Thus, energy contained within TG is partitioned towards expenditure in muscle and away from storage.

FIGURE 4.2

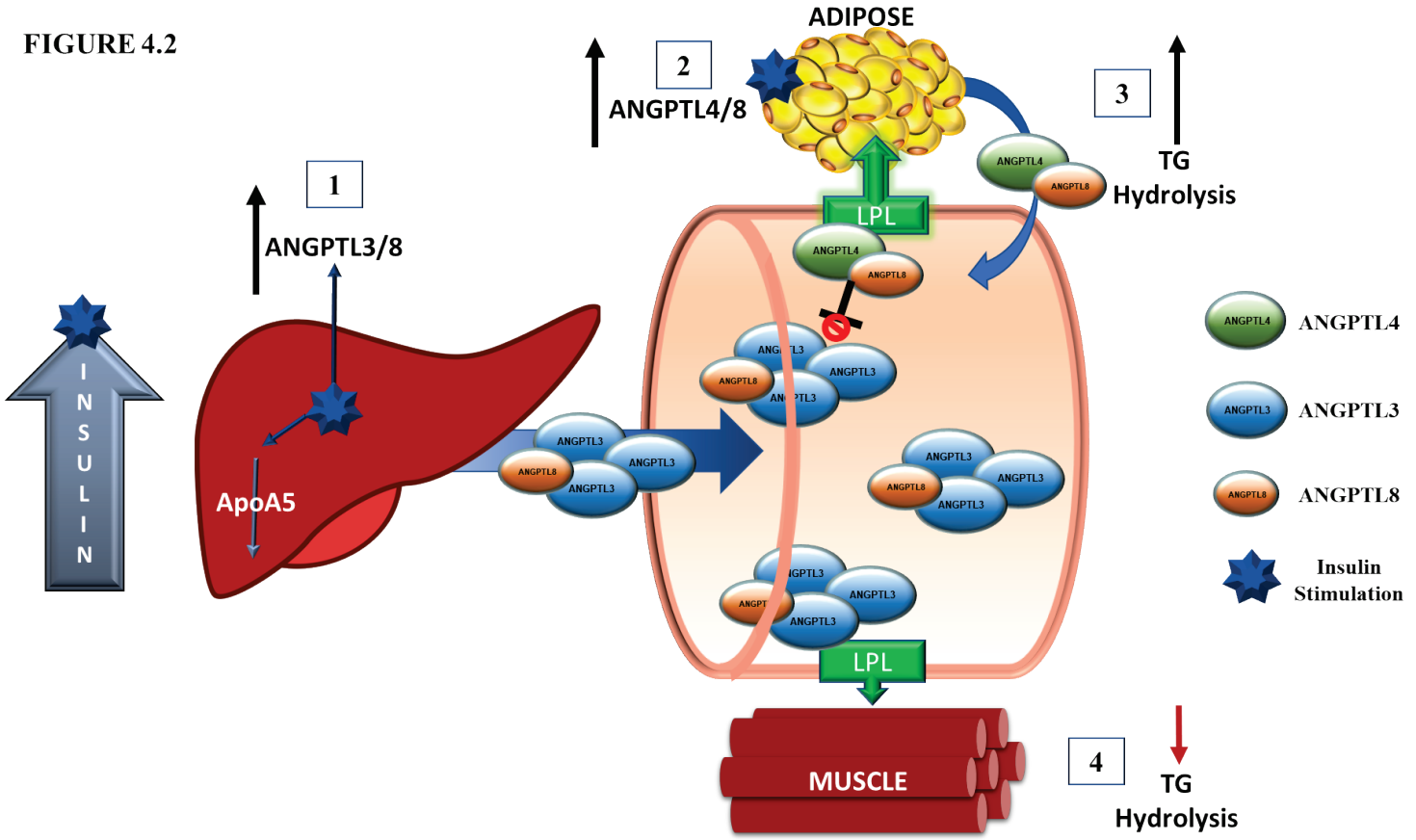

Figure 4.2 Triglyceride partitioning postprandially.

(1) The liver when exposed to elevated insulin concentrations down regulates ApoA5 and increases the production of ANGPTL3/8. ANGPTL3/8 is then secreted from hepatocytes into circulation. (2) Insulin also stimulates the production of ANGPTL4/8 from adipocytes. It is important to note that postprandially, GIP stimulation greatly enhances insulin driven secretion of ANGPTL4/8 from adipocytes. (3) This secreted ANGPTL4/8 acts to preserve LPL activity on the capillary endothelial lumen by blocking circulating ANGPTL3/8. Thus, LPL adjacent to adipocytes continues to hydrolyze TG, release FA for uptake, and enable adipocytes to store this released energy. (4) The endocrine ANGPTL3/8 attaches to LPL localized at skeletal muscle capillaries and blunts LPL hydrolysis of TG. Thus, energy contained within TG partitioned towards storage and away from expenditure

4.2 Supportive Experiments

Within this thesis, the mechanisms for this model are explained using data derived from human samples, recombinant proteins, and in vitro assays. Kovrov et al. first demonstrated that fragments of ANGPTL3 and ANGPTL8 form a complex when refolded together after expression. ANGPTL4 and ANGPTL8 fragments similarly combine during refolding (117). Moreover, the data suggested that the fragment ANGPTL3/8 enhanced LPL inhibition by ANGPTL3 and that ANGPTL4/8 did not inhibit LPL activity (117). Other groups had previously suggested that ANGPTL3 and ANGPTL8 had the potential to combine and be secreted as a complex (91, 129, 144). Thus, our first experiments required verification of these complexes within human samples. Using non-cross-reactive antibodies which individually target ANGPTL3, ANGPTL4, and ANGPTL8, we demonstrated that ANGPTL8 is pulled down with ANGPTL3 and ANGPTL4 immunoprecipitations. Furthermore, we demonstrated that ANGPTL3 and ANGPTL4 are immunoprecipitated using an ANGPTL8 antibody. This data was corroborated by both western blotting and mass spectrometry analyses. Mass spectrometry analysis further identified that ANGPTL3/8 exists in a 3:1 protein ratio (ANGPTL3:ANGPTL8) while ANGPTL4/8 exists in a 1:1 protein ratio.

After establishing the existence of circulating ANGPTL8 complexes, immunoassays were developed to measure the ANGPTL3/8 and ANGPTL4/8 moieties from human samples. First, recombinant ANGPTL complexes were created using mammalian cell lines and dual tag purifications. These complexes would allow for quantification of measured complexes in the immunoassays. The measurements helped identify positive correlations for both ANGPTL3/8 and ANGPTL4/8 with TG, BMI, and insulin. It is important to note that prior to these ANGPTL8 complex assays, published data had been discrepant on the correlations between individual ANGPTL proteins and TG. These highly specific and appropriately sensitive assays enabled us to conduct correlations which are accurate and reliable.

LPL functional assays were subsequently utilized to ascertain how these complexes alter hydrolysis activity. Using both cell based and recombinant systems, we found the addition of ANGPTL8 to ANGPTL3 increased the latter's inhibitory capacity to be equivalent to that generated by ANGPTL4. Moreover, we found that by combining ANGPTL8 with ANGPTL4, the inhibitory capacity of ANGPTL4 was reduced. However, a question remained – if both proteins circulate, how does each control LPL at the sites of TG hydrolysis?

To understand this better, affinity and cell-based competition experiments were conducted. These experiments identified that when complexed to ANGPTL8, ANGPTL4 has a negligible off-rate from LPL. Similarly, ANGPTL8 increases the affinity of ANGPTL3 to bind to LPL. Moreover, when LPL was pre-incubated with ANGPTL4/8, LPL inhibition mediated by ANGPTL3/8 or ANGPTL4 was able to be suppressed. In these competition experiments, a 10-fold excess of ANGPTL4/8 was able to prevent ANGPTL3/8- or ANGPTL4-mediated LPL inhibition.

This data suggested that ANGPTL4/8 acts in a localized environment where concentrations can be higher than those seen in circulation. This notion of localized ANGPTL4/8 protection of LPL was supported through the generation of recombinant proteins as well as through work utilizing adipocytes. Only through the addition of dextran sulfate, to negate ANGPTL4/8's ability to bind to heparin proteoglycans on cellular membranes, did we see measurable amounts of ANGPTL4/8 released into the media.

Lastly, secretion of ANGPTL3/8 and ANGPTL4/8 was demonstrated. Several publications have referenced the ability of ANGPTL8 mRNA to be increased by insulin in adipocytes and hepatocytes (127, 134). However, none of these publications have demonstrated secretion of the protein complex. Thus, our experiments used primary human adipocytes and primary human hepatocytes to evaluate how insulin regulates these complexes.

For ANGPTL4/8, exposure to insulin stimulates the release of the complex from adipocytes. Due to a lack of ANGPTL3 expression in adipocytes, no ANGPTL3/8 is present upon insulin stimulation. To further understand TG trafficking postprandially, GIP was utilized in conjunction with insulin to stimulate the ANGPTL4/8 secretion. Without GIP, a 7.7-fold increase in ANGPTL4/8 secretion was seen using 100 nM of insulin. However, GIP and 100 nM of insulin worked in conjunction to produce a 27.4-fold increase in ANGPTL4/8 secretion. Thus, after a meal, GIP and insulin work in conjunction to greatly upregulate ANGPTL4/8. This secreted complex remains localized on the cellular surface due to heparin proteoglycans and acts a paracrine molecule protecting LPL from inhibition by both ANGPTL4 and ANGPTL3/8.

For ANGPTL3/8, exposure to insulin stimulates hepatocyte derived secretion in a dose dependent manner. Near maximal stimulation around 1 nM insulin results in roughly a 4- to 6-fold increase in ANGPTL3/8 secretion. It is important to note that this concentration is much lower than the respective increase in ANGPTL4/8 secretion seen from adipocytes using 1 nM of insulin (approximately 15- to 20-fold increase). This comparative increase helps support the notion of

elevated localized ANGPTL4/8 concentrations blocking ANGPTL3/8-mediated inhibition of LPL. Hepatic expression of ANGPTL4/8 did not change upon exposure to insulin.

Further support of hepatic ANGPTL3/8 secretion came from analysis of subjects exposed to basal insulin peglispro (a hepato-preferential insulin) over the course of a year. After 52 weeks, ANGPTL3/8 increased ~1.3 fold from pre-exposure. This increase was highly statistically significant. ANGPTL4/8, however, did not increase during this period of treatment.

The 4- to 6-fold increase in ANGPTL3/8 secretion produced using 1 nM of insulin can be further enhanced by the addition of an LXR agonist at concentrations as low as 100 nM. At maximal stimulation (1 nM insulin in conjunction with 1000 nM LXR agonist) an 8-fold increase in ANGPTL3/8 is produced. It is important to re-emphasize that oxysterols which can be absorbed via the diet or produced endogenously during the oxidation of cholesterol accumulate in response to increased insulin concentrations. Thus, in the development of MetS, increases in insulin and the associated accumulation of LXR agonists may result in greatly enhanced ANGPTL3/8 expression.

Lastly using immunoprecipitation followed by western blotting and mass spectrometry analysis, ApoA5 was found to be associated with ANGPTL3/8. Assessed via LPL functional assays, ApoA5 reduces ANGPTL3/8 mediated LPL inhibition. However, ANGPTL3, ANGPTL4, and ANGPTL4/8 mediated alterations in LPL activity are not influenced by ApoA5 co-incubation. While LXR agonists alone can increase hepatic ApoA5 expression ~1.8-fold insulin, even at concentrations as low as 0.1 nM, can significantly decrease ApoA5 secretion. Moreover, whereas LXR and insulin act as additive stimuli to increase hepatic ANGPTL3/8 secretion, maximal stimulation by LXR and insulin together decrease ApoA5 release from hepatocytes. In this situation, ANGPTL3/8 is increased and more capable of inhibiting skeletal LPL as the ANGPTL3/8 suppressor, ApoA5, is decreased.

4.3 Caveats and Potential Future Directions

While we have attempted to minimize research caveats by using either primary human cells or by using human sera for analysis, our proposed mechanisms are based on *in vitro* data. To this extent, further innovative research is required to corroborate our findings. It is important to note, however, that many of the conclusions in this work have been validated using orthogonal *in vivo* methods by the Hobbs group (146).

LPL affinity experiments, while conducted with LPL co-expressed with GPIHBP1, were performed without other LPL activity modifying cofactors present. Similarly, LPL functional assays assessed how the ANGPTL proteins and complexes inhibited LPL in the absence of other molecules such as other apolipoproteins aside from ApoA5. For instance, how do LPL activation factors such as ApoC2 influence the affinities or LPL-inhibitory activities of the ANGPTL complexes?

To assess the functionality of ANGPTL4 and ANGPTL4/8, LPL was expressed on the surface of the cells and then exposed to these activity modifying factors by media exchange. However, LPL is normally an active participant in TG metabolism in the capillaries adjacent to the adipose tissue that are responsible for the release of these paracrine inhibitors. While LPL can be secreted from adipocytes, postprandially there is no increase in LPL expression but rather there is an increase in its localization (41-43). Thus, ANGPTL4 and ANGPTL4/8 must be released from adipocytes and, as paracrine molecules, must diffuse through interstitial space and translocate to the luminal surface of the capillary endothelium where functional LPL is sequestered. This complex process is not yet understood.

The recycling of LPL after binding to any of these ANGPTL complexes has not yet been addressed. While LPL dimerization has an inherent dissociation rate, it remains unclear as to how the LPL head-to-tail dimer associated with ANGPTL4/8, a molecule with no appreciable dissociation rate, becomes recycled. Without adequate regulation of this uninhibited LPL-ANGPTL4/8 moiety on the capillary lumen, adipose tissue should be able to continuously take up FA from TG-containing molecules. Understanding this aspect of LPL's lifecycle is important to further clarify how TG metabolism is balanced between fat and aerobic tissue.

The same questions raised about LPL recycling can also be asked of ANGPTL3/8. As an endocrine molecule, ANGPTL3/8 must be eliminated from circulation after its desired action is completed. In other words, ANGPTL3/8 which has increased secretion postprandially must be eliminated prior to periods of fasting to minimize LPL inhibition at skeletal and cardiac muscles. It would also be advantageous to clarify if circulating ANGPTL3/8 predominantly influences LPL located around skeletal muscle or affects all LPL around aerobic tissues. If ANGPTL3/8 inhibits LPL around all aerobic tissues, what mechanism compensates for the decreased availability of FA for cardiac tissue postprandially?

The effect of glucose on this insulin-sensitive, TG-partitioning system must also be explored. Specifically, how do both high glucose and high insulin concentrations work in conjunction to alter the downstream effects of LXR activation? Insulin is known to downregulate hepatic gluconeogenesis and promote lipogenesis via the LXR pathway (254). Our research has helped to understand how hepatic insulin receptor knockouts demonstrate reduced plasma TG (254-260). However, LXR activation has been shown to regulate lipogenesis, to respond to excess intracellular glucose, and to cause the efflux of excess cholesterol (254, 260-263).

The role of glucose in relation to LXR agonism has not reached a consensus within the literature (264-266). However, numerous studies have indicated that glucose can activate SREBP-1c possibly through direct LXR activation (267-271). For example, using human HepG2 cells, glucose at physiological concentrations can induce a 50-fold activation of LXR when cells are grown in glucose free media (271). Glucose caused LXR coactivator recruitment – a necessity to form the LXR-RXR heterocomplex required for downstream gene transcription (271-279). Further evidence was provided when insulin production was abolished through treatment of streptozotocin. In this animal model system, hyperglycemia was able to induce SREBP-1c mRNA (a downstream target of LXR), repress gluconeogenesis genes, and upregulate lipogenesis (270, 271, 280-284).

Glucose may also indirectly modify LXR (e.g. O-GlcNAcylation during refeeding) to respond differently to other LXR agonists (280). LXR has been shown to target the carbohydrate response element-binding protein (ChREBP) gene (263). ChREBP is a transcription factor that is glucose sensitive and promotes the creation of lipids via conversion from excess glucose (285-287). However, questions remain as to how excess glucose alters the production of ANGPTL3/8 from hepatocytes.

As we have shown in our research, some claims about LXR agonism are contrary to our findings from primary human hepatocytes. For example, LXR agonism was thought to down regulate ApoA5 production; however, this is only true in the presence of insulin (246). Without insulin, hepatic LXR agonism induces ApoA5 expression and secretion. In the presence of low levels of insulin, this is no longer true as insulin antagonizes the effect of LXR activation and reduces the amount of ApoA5 produced. Thus, an investigation of how elevated insulin concentrations in the presence of high glucose modulate hepatic secretion of ANGPTL3/8 and ApoA5 is warranted.

Insulin alone can dose-dependently increase ANGPTL8 mRNA expression (288). Furthermore, insulin in the presence of elevated glucose concentrations further stimulates expression of ANGPTL8 from adipocytes but not hepatocytes (288). As we have shown, this increased ANGPTL8 mRNA expression results in elevated hepatic ANGPTL3/8 secretion. Given our contradictory findings in hepatocytes regarding LXR-stimulated secretion of ApoA5, it is of interest to understand how high glucose and elevated insulin concentrations may have a combinatorial effect on the secretion of hepatic ANGPTL3/8 and of adipocyte derived ANGPTL4/8.

Similar to assessing the effects of elevated glucose on this ANGPTL system, the consequences of other endocrine and paracrine molecules should be explored. For example, leptins may indirectly alter the sensitivity of adipocytes to insulin (289). Based on the presented data, this may further enhance ANGPTL4/8 production. Relevant to ANGPTL3/8 secretion, decreased thyroid hormone concentrations alter liver physiology to result in increased circulating TG (290). Many more hormones affect the liver and adipose tissue. As such, investigations into how these hormones, individually and in combination, alter the expression of the ANGPTL complexes should be enacted.

Lastly, an investigation into the risk ratios for CVD events must be undertaken. Now that the levels of ANGPTL3/8 and ANGPTL4/8 can be ascertained accurately, understanding the relationship of these complexes with CVD outcomes is possible. In analyzing longitudinal fasting samples, such research could guide therapeutic interventions.

4.4 Implications

The model described above, in which insulin drives the secretion of hepatic ANGPTL3/8 and adipocyte-derived ANGPTL4/8, emphasizes the necessity to maintain low to normal insulin levels. Consistently elevated insulin levels are detrimental to the partitioning of triglycerides and may increase the risk of future cardiac events. This, to an extent, holds with the idea of both the "thrifty" and the "drifty" genotype theories in which genes/physiological systems designed to promote energy storage in periods of nutritional excess have become disadvantageous in today's current environment of excess caloric intake and decreased selective pressure (149, 291).

Regardless of theory, the data outlined in this thesis provide a cohesive model for how excess circulating insulin levels lead to HTG and demonstrate the necessity to focus MetS treatments

toward decreasing the amount of circulating fasting insulin. Investigations into different diets such as intermittent fasting or low glycemic index foods may help derive the optimal non-therapeutic approach to MetS. However, if lifestyle alterations are not feasible or insufficient, therapeutic approaches must be created.

Based on the data in this thesis, pharmacological interventions aimed at decreasing the expression of ANGPTL8 should be strongly advocated. By doing so, obesity should decrease as ANGPTL4/8 can no longer drive TG into adipose tissue and skeletal muscle should be able to continuously burn FA derived from TG-containing lipoproteins. However, if only one complex can be therapeutically targeted, ANGPTL3/8 should be the focus. Whereas ANGPTL4/8 is active locally, ANGPTL3/8 circulates. Oldoni et al. further corroborates this finding as adipocyte specific ANGPTL8 KO mice demonstrated no reductions in circulating ANGPTL8 and increased postprandial systemic TG. Conversely, liver specific KO demonstrated not only abolishment of circulating ANGPTL8 (ANGPTL3/8) but decreased postprandial TG likely due to elevated LPL activity around skeletal muscles (146). As a result, liver-specific therapies targeting ANGPTL3/8 via small molecule inhibitors or small interfering RNA (siRNA) would enable a systemic decrease in LPL inhibition while preventing the undesirable TG increase which arises when ANGPTL8 is knocked out in adipocytes.

An antibody against ANGPTL3/8 may be the most effective solution. Therapeutic targeting of ANGPTL3 has been shown to be effective during clinical trials. During a Phase 1 trial in normal healthy individuals and in patients with homozygous familial hypercholesterolemia, 350 mg weekly subcutaneous administration of an ANGPTL3 antibody reduced triglycerides by 51.9%, whereas an 88.2% TG reduction was achieved with 20 mg/kg intravenous dosing (197). For a Phase 3 trial, Evinacumab, when administered at 15 mg/kg intravenously every four weeks, decreased LDL-C by roughly 45% TG by 55% (198, 292). As our work demonstrated, such large therapeutic dosing is required as a consequence of the high circulating concentrations of ANGPTL3 (198, 225). The cost to produce sufficient antibody for weekly intervention may make ANGPTL3 targeted therapies financially infeasible for patients.

Antisense oligonucleotides have been attempted against ANGPTL3 mRNA. In a Phase 1 study, 20 mg subcutaneous administration of antisense oligonucleotides led to a 63% reduction in TG compared to the placebo group (293). However, long term effects of inhibiting ANGPTL3

protein expression were unable to be assessed over this six-week study. Individually, ANGPTL3 and ANGPTL8 may have other necessary physiological effects which are currently unknown.

In contrast to the individual ANGPTL proteins, ANGPTL3/8 is now well characterized. An antibody which specifically targets this complex may be beneficial. First, ANGPTL3/8 does not circulate at the same high concentrations seen with ANGPTL3. Hence, the amount of therapeutic required for treatment is less. Moreover, because of our understanding of the mechanism of action of ANGPTL3/8, we can be more assured that a blockade of ANGPTL3/8 will result in fewer unintentional side effects. A targeted therapeutic to ANGPTL3/8 is likely to create meaningful and lasting change for patients who struggle with lifestyle changes to reverse MetS.

4.5 Conclusions

This thesis presents a novel, unified model of TG trafficking which has only been hinted at within the literature. In our model, insulin drives hepatic ANGPTL3/8 secretion to inhibit skeletal muscle LPL while simultaneously inducing ANGPTL4/8 secretion from adipocytes to enhance FA storage in the fat. The systemic effects of ANGPTL3/8 and the paracrine action of ANGPTL4/8 on LPL activity alter the balance of TG hydrolysis from skeletal muscle towards adipose tissue. As a result, energy is stored rather than utilized. When unbalanced, this system can predispose individuals to MetS. Progression to MetS can then lead into the development of T2DM and its subsequent comorbidities. This research will enable subsequent therapies for patients who struggle to treat MetS with lifestyle modifications.

CHAPTER 5. METHODS

5.1 From Chapter 2: Angiopoietin-like protein 8 differentially regulates ANGPTL3 & ANGPTL4 during postprandial partitioning of fatty acids

5.1.1 Normal human serum samples and SCARF control samples

Sera were obtained (with consent) from healthy volunteers from the Eli Lilly Research Blood Donor Program. To study fasting and postprandial conditions, sera were obtained from 10 healthy volunteers after overnight fasting and 1 and 2 hours following a mixed-meal breakfast consisting of approximately 400 carbohydrate calories, 400 fat calories, and 100 protein calories. All samples were stored at −80°C. SCARF is a case-control study from northern Stockholm comprising consecutive, unselected MI survivors below age 60 and controls matched for age, sex, and area of residence (208-210). The study was approved by the Ethics Committee of the Karolinska University Hospital and conducted in agreement with the Declaration of Helsinki. All subjects gave informed consent to participate. Control subjects were interviewed regarding lifestyle characteristics, medical history, and medication, and a physical examination was performed. Samples were collected under fasting conditions and stored at -80ºC. The Clinical Chemistry Laboratory of the Karolinska University performed standard serum analyses (208).

5.1.2 Recombinant ANGPTL protein and complex generation

Human sequences were as follows: ANGPTL8: NP_061157.3; ANGPTL3: NP_055310.1; ANGPTL4: NP_647475.1. Mature ANGPTL8 (residues 22-198) was produced in *E. coli* as inclusion bodies and refolded *in vitro*. C-terminal HIS-tagged ANGPTL4 and ANGPTL3 were produced stably in CHO cells and transiently in HEK293 cells, respectively. Both were purified through nickel-nitrilotriacetic acid (Ni-NTA) affinity, followed by size exclusion chromatography (SEC). ANGPTL3/8 complex was produced in HEK293 cells through transient co-transfection. Nucleotide sequences encoding mouse IgG kappa signal peptide-HIS tag-mature human serum albumin (HSA)-PreScission cleavage site-mature ANGPTL8 were inserted into a mammalian expression vector containing a cytomegalovirus (CMV) promoter, as were the nucleotide sequences encoding C-terminal Flag-tagged ANGPTL3. Protein expression was performed through transient co-transfection of both expression constructs in HEK293 cells cultured in serum-

free media. Culture media were harvested 5 days post transfection and stored at 4ºC for subsequent protein purification at 4ºC. Four liters of culture media were supplemented with 1 M Tris-HCl (pH 8.0) and 5 M NaCl to final concentrations of 25 mM and 150 mM, respectively. The media were incubated with 150 ml of Ni-NTA resin (Qiagen) overnight. The resin was then packed into a column and washed with buffer A (50 mM Tris-HCl, pH 8.0, 0.3 M NaCl). Elution was performed with a 0-300 mM imidazole gradient in buffer A. Fractions containing HIS-HSA-ANGPTL3/8 complex were pooled, concentrated, loaded onto a HiLoad Superdex 200 column (GE Healthcare), and eluted with buffer A. Fractions containing HIS-HSA-ANGPTL3/8 were again pooled, concentrated, and digested with PreScission protease to remove HSA from the HIS-HSA-ANGPTL8 fusion protein. The PreScission digested protein sample was loaded onto another HiLoad Superdex 200 column and eluted with storage buffer (20 mM HEPES pH 8.0, 150 mM NaCl). Fractions containing ANGPTL3/8 complex were pooled and concentrated. Protein concentrations were determined using a bicinchoninic acid (BCA) protein assay.

During the ANGPTL3/8 purification process, it was important for the ANGPTL3/8 complex not to contain free proteins. To ensure purity, the initial Ni-NTA affinity purification first removed all free ANGPTL3. After SEC, purified HIS-HSA-ANGPLT3/8 complex and free HIS-HSA-ANGPLT8 were obtained. PreScission digestion (which cleaved between HSA and ANGPTL8) resulted in ANGPTL3/8 complex, HIS-HSA, and free ANGPTL8. Free ANGPTL8 was precipitated out, leaving only ANGPTL3/8 complex and HIS-HSA. ANGPTL3/8 complex and HIS-HSA were separated with a second SEC step, resulting in highly purified ANGPTL3/8 complex without any HIS-HSA contamination (as shown in Figure 2.2A). This strategy ensured that very pure ANGPTL3/8 complex was produced. The same approach was used for expression and purification of the ANGPTL4/8 complex. All proteins and complexes were maintained at a <0.01 EU/ug of endotoxin. One μg of each recombinant ANGPTL protein or complex was characterized using gradient gel electrophoresis with Bio-Rad 4-20% Mini-Protean Tris-glycine gels, followed by Coomassie Blue staining to verify the purity of the respective proteins and complexes, which were all stored at -80ºC. For purposes of molar conversions, a molecular weight of 179 kD was used for ANGPTL3/8 (3:1 ratio), while a molecular weight of 64 kD was used for ANGPTL4/8 (1:1 ratio).

5.1.3 ANGPTL antibodies

Anti-human ANGPTL8 antibodies (residues 22-198) were generated using hybridoma techniques by Precision Antibody Sciences. Anti-human ANGPTL4 antibodies were generated by immunization with recombinant ANGPTL4 (residues 26-161), or purchased commercially (R&D Systems, AF3485). Anti-human ANGPTL3 antibodies were generated after immunization with mammalian produced recombinant ANGPTL3 (residues 17-220) or purchased commercially (R&D AF3829). Clones of interest were screened for non-overlapping epitopes, and antigen-specific variable heavy (VH) and light (VL) gene sequences were determined from extracted RNA using a mouse Ig primer set (EMD Millipore). Variable domains were transferred into separate murine constant region expression vectors for antibody production, transfected into CHO cells, and purified using protein A chromatography. Antibodies were biotinylated using a Pierce kit and ruthenium-labeled using a MesoScale Discovery (MSD) kit, with MALDI-TOF performed to verify appropriate labeling. Antibodies were diluted in 50% glycerol and stored at -20ºC.

5.1.4 Immunoprecipitation/Western blotting

Anti-ANGPTL and control antibodies were covalently coupled to tosyl-activated beads (Thermo), with heavy and light chains further cross-linked using dimethyl pimelimidate (DMP). Fifty µL of beads containing 20 µg of antibody were added to 4 mL of pooled donor serum diluted 1:2 with PBS and incubated at 4°C overnight. Beads were washed with PBS and boiled in sample buffer. Proteins were separated on a Novex 12% Bis-Tris gel and transferred to PVDF using an iBlot system (Thermo). Membranes were probed with biotinylated anti-ANGPTL antibodies. Visualization was performed with Alexa Fluro 680-conjugated streptavidin. Images were recorded using an Odyssey CLx image system (LI-COR Biosciences).

5.1.5 Immunoprecipitation-mass spectrometry

Proteins were immunoprecipitated from normal human serum using anti-ANGPTL8, ANGPTL4, or ANGPLT3 antibodies. The anti-ANGPTL4 antibody utilized was an N-terminal antibody. Irrelevant IgG was used as a negative control. Biotinylated antibodies (10 µg) were added to 1 ml of human serum diluted with 1 ml of PBS, and samples were incubated at 4°C overnight. The next day, 30 µL of streptavidin magnetic beads (Thermo) were added, and tubes

were incubated at 4°C for 2 hours. Beads were washed using PBS, and bound proteins were reduced with DTT and alkylated with iodoacetamide. Proteins were digested using 1 µg of Trypsin/Lys-C (Promega) at 37°C for 4 hours. Digests were acidified using 5 µl of 10% trifluoroacetic acid (TFA). Stable-isotope-labeled (SIL) peptides (0.2 pmole) were spiked into each sample before analysis with a TSQ Quantiva (Thermo) using liquid chromatography–multiple reaction monitoring (LC–MRM). Peptides were separated using a Hypersil Gold C18 HPLC column (50 x 2.1 mm) with a Dionex Ultimate 3000 system at a flow rate of 250 µL/min. Solvent A consisted of 0.1% formic acid in water, and solvent B consisted of 0.1% formic acid in acetonitrile. For protein quantification, SIL peptides for each ANGPTL protein were synthesized with selected lysine or arginine residues labeled with ^{13}C and ^{15}N, and peptide content of SIL peptides was determined through amino acid analysis. Peak area ratios between the endogenous and corresponding SIL peptides were used to estimate protein concentrations after averaging results from two peptides for each protein analyzed. The specific SIL peptides used for quantitation are listed in Supplemental Figures A18-A24.

5.1.6 Mass spectrometry assessment of ANGPTL complexes

ANGPTL3/8 and ANGPTL4/8 were digested at 37°C for 4 hours using a mixture of Trypsin/Lys-C, after reduction with DTT and alkylation with iodoacetamide. Two peptides from each protein were used for quantitation as described in Supplemental Figures A18-A24 and Tables S2-5. For LC-MRM quantification, an identical molar amount of each SIL peptide was added to the protein digest, and samples were analyzed using a TSQ Quantiva triple quadrupole mass spectrometer. Xcalibur software (version 4.2.47, Thermo) was used to determine peak area ratios between the digested peptide and its corresponding SIL peptide. Detailed peak integration parameters used for the analysis are included in the Supplemental Figures A18-A24. Individual protein ratios in ANGPTL3/8 and ANGPTL4/8 were calculated using the average ratio from two SIL peptides for each protein in each complex. To assess the protein ratios of endogenous complexes, ANGPTL3/8 and ANGPTL4/8 were immunoprecipitated from human serum. Molar ratios for ANGPTL3:ANGPTL8 and ANGPTL4:ANGPTL8 were then calculated using spiked-in SIL peptide standards utilizing the methods described above for the recombinant complexes.

5.1.7 Mass spectrometry experimental design and rationale

Peptides with robust ionization after tryptic digest analysis of ANGPTL proteins were selected for MRM experiments. Blast searches against the NCBI human database confirmed that these peptides were unique to the corresponding protein, with no known post-translational modifications (PTM). At least two transitions were selected for each peptide for MRM monitoring. The amino acid sequences of these peptides and specific transitions are listed in Supplemental Tables B2-B5. The transitions selected, the collision energy, and RF lens values were optimized by infusing the synthesized SIL peptides. No significant interference was detected at the corresponding retention time for each peptide in the negative controls.

5.1.8 ANGPTL immunoassays

We used dedicated immunoassays to measure each protein or complex of interest. For the ANGPTL8 assay, monoclonal antibodies directed against independent ANGPTL8 epitopes were used for capture and detection. Based on our mass spectrometry and immunoassay-based quantitation of human serum ANGPTL8, ANGPTL3/8 complex, and ANGPTL4/8 complex, ANGPTL8 measured by this assay was mainly present in either ANGPTL3/8 or ANGPTL4/8 complexes, however, we could not rule out the possibility that a small amount of free ANGPTL8 might also circulate. For ANGPTL3, a monoclonal antibody was used for capture and a polyclonal anti-ANGPTL3 antibody (R&D AF3829) was utilized for detection. The total level of ANGPTL3 was found to be much greater than that of the ANGPTL3/8, suggesting that the vast majority of ANGPTL3 detected by this assay was free ANGPTL3. An assay employing two different monoclonal antibodies recognizing independent N-terminal epitopes of ANGPTL4 was used to measure active ANGPTL4 (defined as full-length ANGPTL4 or the N-terminal fragment of ANGPTL4). For measurement of C-terminal domain-containing (CTDC) ANGPTL4 (defined as full-length ANGPTL4 or the inactive C-terminal fragment of ANGPTL4), an R&D kit (Catalog # DY3485) was utilized. For the ANGPTL3/8 assay, the capture antibody recognized ANGPTL8, and the detection antibody recognized ANGPTL3. For the ANGPTL4/8 assay, the capture antibody recognized ANGPTL4, and the detection antibody recognized ANGPTL8. The ANGPTL4/8 complex assay could not distinguish between N-terminal ANGPTL4 fragment or full-length ANGPTL4 present in the ANGPTL4/8 complex.

For each assay, MesoScale Discovery (MSD) streptavidin plates were washed three times with TBST (Tris buffered saline containing 10 mmol/L Tris pH 7.40, 150 mmol/L NaCl, and 1 mL/L Tween 20). Plates were blocked with TBS plus 1% bovine serum albumin (BSA) for 1 hour at room temperature (RT). After aspiration and washing, wells were incubated with biotinylated capture antibody for 1 hour. Following aspiration and washing, 50 µL of recombinant protein or complex (serially diluted to form a standard curve), were added to the wells in assay buffer (50 mmol/L HEPES, pH 7.40, 150 mmol/L NaCl, 10 mL/L Triton X-100, 5 mmol/L EDTA, and 5 mmol/L EGTA). Serum samples were diluted in assay buffer and added to their respective wells for a 2-hour incubation at RT. After aspiration, wells were washed three times, and 50 µL of ruthenium-labeled detection antibody were added for a 1-hour incubation at RT. Following aspiration, wells were washed three times, and 150 µL of MSD read buffer were added. Electrochemiluminescence from electrical excitation of ruthenium in the wells was detected using an MSD plate reader. Specificity of each novel assay was tested using the other proteins/complexes, and each had cross-reactivity of less than 1%.

5.1.9 Very low-density lipoprotein-cholesterol (VLDL-C) uptake assay

We adopted the method of Neher and colleagues (55). In this assay, VLDL particles are labeled with a fluorescent phospholipid probe, which is inserted into the outer phospholipid layer of the VLDL particle, and the assay measures the adherence of the fluorescence probe to Huh7 cells. For labeling of VLDL (Lee Solutions) with 1,2-dioleoyl-sn-glycero-3-phosphoethanolamine-N-carboxyfluorescein (18:1 PECF, Avanti), 100 µL PECF (1 mg/ml in chloroform) was dried under argon. Next, 400 µL of VLDL (10 mg/ml TG, in PBS) was added to the vial, vortexed, and sonicated for 6 minutes to yield final concentrations of 10 mg/ml TG VLDL and 0.25 mg/ml PECF. Huh7 cells were plated at a density of 40,000 cells/well in a poly-D-lysine 96-well plate in medium consisting of DMEM/F-12 3:1 (Gibco), 10% FBS (Gibco), 1% penicillin-streptomycin (Gibco), and 20 mM HEPES (Gibco). Cells were grown overnight before medium was replaced with 150 µL of PBS for 2.5 hours. LPL (Sigma) was mixed with ANGPTL3/8 or ANGPTL4/8 and incubated at RT for 1 hour with gentle shaking. Mixtures were combined with equal volumes of VLDL-PECF (final concentrations of 11 U/mL LPL, 50 nM ANGPTL3/8 or ANGPTL4/8, 100 µg/ml VLDL-PECF), and 50 µL of the mixtures replaced the PBS. Cells were incubated at 37ºC for 30 minutes. Media were then replaced with 150 µL/well of fixative. Cells

were fixed for 20 minutes, washed twice with 200 µL PBS and covered with 50 µL/well of PBS. Fluorescence at 495 nm/525 nm was measured using a SpectraMax3 plate reader, with VLDL uptake calculated as relative fluorescent units at 525 nm.

5.1.10 Binding assessments

ANGPTL interactions with LPL were assessed with bio-layer interferometry using Octet RED96e® (Molecular Devices). Avidin-tagged LPL was immobilized on streptavidin biosensors. Immobilized LPL (Sigma) was incubated with 50 nM of ANGPTL3, ANGPTL3/8, ANGPTL4, or ANGPTL4/8 and transferred into buffer-only wells to monitor dissociation.

5.1.11 LPL stable expression cell line and activity assays

The nucleotide sequence for human LPL (NP_000228.1) was inserted into pLenti6.3 vector (Invitrogen) to generate lentivirus, which was used to create a stable expression cell line confirmed by qPCR and enzymatic activities. The cell line was maintained in DMEM/F12 (3:1) (Invitrogen), 10% FBS (Hyclone), and 5 µg/ml blasticidin (Invitrogen). The wild-type human LPL-stable expression cells were seeded at a density of 50,000 cells/well in a tissue culture-treated 96-well plates (Costar) in growth medium (3:1 DMEM/F12, 10% FBS, and 5 µg/ml blasticidin). After overnight incubation, medium was replaced with 80 µL of medium containing serially diluted ANGPTL proteins. Cells were incubated for 1 h before 20 µL of 5X working solution, freshly prepared with 0.05% Zwittergent detergent 3-(N,N-dimethyl-octadecylammonio)-propanesulfonate (Sigma) and containing EnzChek lipase substrate BODIPY-dabcyl-labeled TG analog (Invitrogen), were added to achieve a final concentration of 1 µM (294). Fluorescence was monitored at 1 and 30 min with a Synergy Neo2 plate reader with an excitation wavelength of 485 nm and emission wavelength of 516 nm to correct for background. To study the ability of ANGPTL4/8 to protect LPL from ANGPTL3/8 and ANGPTL4 inhibition, ANGPTL4/8 was first serially diluted in growth medium, and 60 µL of the medium containing ANGPTL4/8 were added to the cells for a 1 h incubation with gentle shaking. Afterward, 20 µL of 5 nM ANGPTL3/8 or ANGPTL4 working solution (5X) prepared in growth medium were added for a further 1 h incubation. Finally, 20 µL of EnzChek lipase substrate was added to start the reaction.

Fluorescence was monitored at 1 and 30 min with a Synergy Neo2 plate reader with an excitation wavelength of 485 nm and emission wavelength of 516 nm to correct for background.

5.1.12 LPL activity assay with very low-density lipoprotein (VLDL) as substrate

The assay was similar to those described above, except that Enzchek lipase substrate was replaced with 20 μL/well of (Lee Solutions) VLDL (2 mM TG, final 0.4 mM TG in the well), and non-esterified fatty acids (NEFA) released by LPL were measured using an NEFA-HR kit (Wako). Human LPL-stable expression cells were seeded at 50,000 cells/well in a poly-D-lysine coated 96-well plate. Cells were grown overnight, and medium was replaced with 80 μL of medium containing serially diluted ANGPTL4 or ANGPTL4/8 complex. Cells were incubated for 1 hour with gentle shaking. Twenty μL of VLDL (2 mM TG) were added to each well, and the plate was incubated for 30 minutes, after which 5 μL of medium were used for NEFA measurement.

5.1.13 Samples from patients treated with hepato-preferential insulin

Basal insulin peglispro (BIL) is a pegylated version of insulin lispro with a large dynamic radius that restricts it from the periphery but allows it to pass through hepatic sinusoids, thus making it hepato-preferential (212). Clinical trial samples were obtained from a previously described study in which insulin-naïve patients were administered BIL for 52 weeks (213). These samples were from 279 patients at baseline and during 52 weeks of BIL treatment (all drawn under morning fasting conditions). Ideally, we would have analyzed samples from early time points, however, the only post-baseline sera available were those collected after 12, 26, and 52 weeks of treatment. Samples were stored at −80°C prior to analyses.

5.1.14 Secretion of ANGPTL complexes from hepatocytes

Human primary hepatocytes were obtained from BioIVT in the HepatoPac platform. Cells were incubated for 2 days in BioIVT maintenance media. Following aspiration, cells were washed in serum-free BioIVT application media. Afterward, cells were pre-incubated for one day in application media in the absence of insulin, then incubated overnight with application media in the absence or presence of 1 nM insulin. Media were collected and stored at -80ºC prior to analyses.

5.1.15 Effect of dextran sulfate on ANGPTL protein release

C-terminal Flag-tagged ANGPTL4 and C-terminal HIS-tagged ANGPTL8 mammalian expression constructs were transfected into HEK293 cells. At 24 hours post-transfection, 0 or 0.1 mg/mL of dextran sulfate was added to the media. The media were harvested 5 days post-transfection, and equal volumes from each treatment condition were used for immunoblotting with either anti-Flag or anti-HIS antibody.

5.1.16 Adipocyte experiments

Human adipose-derived stem cells were obtained from Zen-Bio and seeded in 96-well plates (160,000 cells/cm^2 in 100 µL of EGM2-MV media, Zen-Bio). After 24 hours, media was replaced by PM1 (Zenbio) followed by replacement with DM2 (Zen-Bio) media. Fresh DM2 was added on the third day followed by replacement with AM1 (Zen-Bio) every 3-days until the cells were used. Differentiated adipocytes were utilized between days 12 and 14. For adipocyte mRNA analyses, differentiated cells were treated for 8 hours in PM1 in the absence or presence of 100 nM insulin (Sigma) in DMEM/F12(3:1) (Gibco) containing 0.2% fatty acid free BSA (Thermo). RNA was extracted using a miRNeasy mini kit (Qiagen). One ug of total RNA was reverse transcribed using a high capacity cDNA kit (Applied Biosystems). The cDNA was diluted 1:10, and ANGPTL4 (Applied Biosystems, taqman mix Hs01101127_m1) and ANGPTL8 (Applied Biosystems, taqman mix Hs00218820_m1) transcript levels were quantitated. For insulin-stimulated release of ANGPTL4/8 complex, adipocytes were cultured in DMEM (Gibco) containing 0.2% fatty acid free BSA (Thermo). Cells were treated overnight in media containing 20 units/mL heparin (Sigma) with 0-100 nM insulin in the absence and presence of 10 nM glucose-dependent insulinotropic peptide (GIP). Media were collected and stored at -80^{o}C prior to analyses.

5.1.17 Statistics

For SCARF samples, variables that presented skewed distribution were logarithmically transformed, and associations between ANGPTL complexes and selected phenotypes were assessed using Spearman rank correlation coefficients. A four-parameter logistic non-linear regression model was used to fit curves for LPL activity assays, while MSD software was used for immunoassay calibration curves. Significance for the feeding effect on ANGPTL complexes was

assessed using a paired t-test. Significance for the effect of complexes on VLDL-C uptake and the effect of insulin on adipocyte ANGPTL4/8 secretion was assessed using an unpaired t-test. A Dunnett's test was used for insulin stimulation of ANGPTL mRNA expression. Significance of insulin-stimulated ANGPTL3/8 and ANGPTL4/8 secretion from hepatocytes was calculated using a two-tailed parametric paired t-test. Significance for BIL effects on circulating ANGPTL3/8 and ANGPTL4/8 complex levels was assessed using a two-way ANOVA with Dunnett's multiple comparisons test.

5.2 From Chapter 3: The mechanism of action of apolipoprotein A5 - suppression of ANGPTL3/8 complex-mediated inhibition of LPL activity

5.2.1 Generation of recombinant ANGPTL proteins and complexes and ApoA5 protein

ANGPTL3, ANGPTL4, ANGPTL3/8, and ANGPTL4/8 were expressed as previously described (225). For ApoA5, the nucleotide sequences encoding 1) human ApoA5 (NP_443200.2)-PreScission cleavage site-mature human serum albumin (HSA)-HIS tag, 2) mouse IgG kappa signal peptide-HIS tag-mature human serum albumin (HSA)-PreScission cleavage site-mature human ApoA5 (residues 24-366), and 3) mouse IgG kappa signal peptide-mature human serum albumin (HSA)-HIS tag were each inserted into a mammalian expression vector containing a cytomegalovirus (CMV) promoter. Protein expression was performed through transient transfection in HEK293 cells cultured in serum-free media. Culture media were harvested 5 days post transfection and stored at 4ºC for subsequent protein purification at 4ºC. Two liters of culture media were supplemented with 1 M Tris-HCl (pH 8.0) and 5 M NaCl to final concentrations of 25 mM and 150 mM, respectively. The media were then incubated with 20 ml of HisPur Ni-NTA resin (Thermo) overnight. The resin was packed into a column and washed with buffer A (50 mM Tris-HCl, 0.3 M NaCl, pH 8.0), and elution was performed with a 0-300 mM imidazole gradient in buffer A. Fractions containing the protein of interest were pooled, concentrated, and loaded onto a HiLoad Superdex 200 column (GE Healthcare), and eluted with PBS. Fractions of interest were pooled, and protein concentrations were determined using a bicinchoninic acid (BCA) protein assay. All proteins were maintained at a <0.01 EU/ug of endotoxin. Each protein (0.5 µg) was characterized with or without PreScission cleavage using gradient gel electrophoresis with Bio-Rad 4-20% Mini-Protean Tris-glycine gels, followed by Coomassie Blue staining to verify purity. All proteins were stored at -20ºC .

5.2.2 ApoA5 antibodies and ANGPTL3/8 complex-specific antibodies

ApoA5 antibodies were generated as previously described (243). Briefly, peptides corresponding to N-terminal and the C-terminal regions of human ApoA5 were synthesized (Anaspec). Terminal cysteine residues were added for conjugation to carrier proteins and chromatography beads, and peptides were conjugated to activated carriers. Rabbits were immunized every 21 days with 100 μg of peptide carrier conjugates in Freund's adjuvant and bled 10 days after booster injections beginning after the third injection. Polyclonal anti-C-terminal antisera were pooled, and polyclonal anti-N-terminal antisera were pooled. Afterward, the antibodies were affinity-purified against their respective peptides, concentrated with an Amicon stir cell concentrator, diluted in 50% glycerol, and stored at -20ºC .

Anti-human ANGPTL3/8 complex specific antibodies were generated by immunizing mice with recombinant ANGPTL3/8 complex using hybridoma techniques. Clones of interest were screened for non-overlapping epitopes, and antigen-specific variable heavy (VH) and light (VL) gene sequences were determined from extracted RNA. Variable domains were transferred into separate constant region expression vectors for antibody production, transfected into CHO cells, and purified using protein A chromatography. Antibodies were tested for specificity to ensure that they bound only ANGPTL3/8 complex and not ANGPTL3 or ANGPTL8. Antibodies were diluted in 50% glycerol and stored at -20ºC.

5.2.3 Identification of ANGPTL3/8 associated proteins by mass spectrometry

Biotinylated anti-FLAG antibody in PBS was first captured on streptavidin-coated 96-well plates (Thermo). After washing way unbound antibody with PBS, ANGPTL3/8 complex containing a FLAG-tag sequence at the C-terminus of ANGPTL3 was added to selected wells. For control samples, no ANGPTL3/8 was added. Triplicate samples were incubated at room temperature (RT) for 2 hours with gentle shaking. Afterward, wells were washed with PBS, and 200 μl of pooled human serum (diluted 1:2 in PBS) were added to each well. The plate was incubated at 4ºC overnight with gentle shaking. The next day, the plate was washed 10 times using ice-cold PBS, and bound proteins were eluted using 100 μl of 1% acetic acid. The eluate was dried under nitrogen to remove acetic acid, and proteins were digested overnight at 37ºC using trypsin,

after reduction and alkylation using triethylphosphine and iodoethanol, respectively (295). Digested peptides were desalted using micro Ziptips.

Samples were analyzed with a Thermo Q Exactive HF-X mass spectrometer using a Thermo Easy 1200 nLC-HPLC system. Peptide separation was carried out with a 75 µm x 15 cm Easy-Spray PepMap C18 column (Thermo) coupled to a Thermo Easy-Spray source. Solvents A was 0.1% formic acid in water (Thermo Fisher Scientific, Optima™ LC/MS Grade), and Solvent B was 80% acetonitrile with 0.1% formic acid (Thermo, Optima™ LC/MS Grade). The gradient was 35 minutes using a flow rate of 250 nL/min, starting with a 32 min 5-45% B ramp, followed by a 1 min 45-95% B ramp, and a 2 min hold at 100% B. The HF-X was run with the following settings: spray voltage: 1.9 kV; capillary temperature: 275 ºC; full scan at 120,000 resolution with AGC target at 3e6, max IT of 50 ms; dd-MS2 at 30,000 resolution with AGC target of 1e5, max IT of 100 ms, loop count of 20, CE of 25, isolation window of 2.0 m/z. Peptide sequences were identified by searching MS/MS spectra against the NCBI human database (296).

5.2.4 Immunoprecipitation and Western blotting

An anti-ANGPTL3/8 antibody, an anti-ApoA5 C-terminal antibody, and an irrelevant control antibody were each covalently coupled to Tosyl-activated M-280 Dynabeads (Thermo), with heavy and light chains further cross-linked using dimethyl pimelimidate (DMP). Fifty µL of beads containing 20 µg of antibody were added to 2 mL of pooled donor serum (diluted 1:2 in PBS) and incubated at 4°C overnight. The following day, beads were washed with PBS and boiled in sample buffer. Proteins were separated on a Novex 4-12% Bis-Tris gel and transferred to PVDF using an iBlot system (Thermo). The membrane was fixed by incubation with cold acetone for 30 min, incubated at 50°C for 30 min, and then probed with biotinylated anti-ApoA5 C-terminal antibody. Bands were visualized with Alexa Fluro 680-conjugated streptavidin using an Odyssey CLx image system (LI-COR Biosciences). PreScission-cleaved recombinant HSA-ApoA5 served as the positive control.

5.2.5 ANGPTL3/8 and ApoA5 immunoassays

ANGPTL3/8 was measured as previously described (225). ApoA5 was also measured as previously described but with some modifications, including the use of human recombinant HSA-

ApoA5 for the calibration curve (243). For performing the ApoA5 assay, MesoScale Discovery (MSD) streptavidin plates were washed three times with TBST (Tris buffered saline containing 10 mmol/L Tris pH 7.40, 150 mmol/L NaCl, and 1 mL/L Tween 20) and blocked with TBS plus 1% bovine serum albumin (BSA) for 1 hour at RT. After aspiration and washing, wells were incubated with biotinylated anti-N-terminal ApoA5 capture antibody for 1 hour. Following aspiration and washing, 50 µL of recombinant HSA-ApoA5 (serially diluted as a standard curve) were added to the wells in assay buffer (50 mmol/L HEPES, pH 7.40, 150 mmol/L NaCl, 10 mL/L Triton X-100, 5 mmol/L EDTA, and 5 mmol/L EGTA). Samples were diluted in assay buffer and added to their respective wells for a 2-hour RT incubation. After aspiration, wells were washed three times, and 50 µL of ruthenium-labeled anti-C-terminal ApoA5 detection antibody were added for a 1-hour RT incubation. Following aspiration, wells were washed three times, and 150 µL of MSD read buffer were added. Electrochemiluminescence of ruthenium was detected using a MSD plate reader.

5.2.6 LPL activity assays

LPL activity assays were performed as previously described with minor modifications to characterize LPL-inhibitory activities of ANGPTL proteins and complexes in the presence or absence of ApoA5 (225). After wild-type human LPL-stable expression cells were incubated overnight in growth medium, the medium was replaced with 80 µL of medium containing serially diluted ANGPTL proteins or complexes (that were previously pre-incubated in the absence or presence of ApoA5). Cells were incubated for 1 hour at 37ºC before 20 µL of 5X working solution containing lipase substrate were added to achieve a final concentration of 1 µM of substrate. The incubation was then continued at 37ºC for 60 minutes, and fluorescence was monitored at 1 and 30 min with a Synergy Neo2 plate reader with an excitation wavelength of 485 nm and emission wavelength of 516 nm to correct for background.

Kinetic analyses of LPL activity were performed with modifications to allow for continuous characterization of LPL-inhibitory activities of ANGPTL proteins and complexes in the absence or presence of ApoA5. After overnight incubation of LPL-stable expression cells in growth medium, the medium was replaced with 80 µL of medium containing ANGPTL proteins or complexes (previously pre-incubated in the absence or presence of ApoA5). Cells were incubated for 1 h at 37ºC before 20 µL of 5X working solution were added to achieve a final concentration

of 1 μM substrate. The incubation was continued at 37ºC for 60 minutes, and fluorescence was monitored every minute.

5.2.7 Secretion of ANGPTL3/8 and ApoA5 from hepatocytes

Human primary hepatocytes were obtained from BioIVT in the HepatoPac platform and were incubated for two days in BioIVT maintenance media (225). Following aspiration, cells were washed in serum-free BioIVT application media. Afterward, cells were pre-incubated for one day in application media in the absence of insulin, then incubated overnight with application media in the absence or presence of 0-1 nM insulin and/or 0-10,000 nM of the LXR agonist T0901317. Media were collected and stored at -80ºC prior to subsequent analyses of secreted ApoA5 and ANGPTL3/8 via their respective immunoassays.

5.2.8 Statistics

A four-parameter logistic non-linear regression model was used to fit curves for LPL activity assays. For kinetic analyses of LPL activity assays, fluorescence was recorded every minute, and counts were plotted versus time to show the degree of LPL inhibition. For ANGPTL3/8 and ApoA5 assays, MSD software was used for fitting of the immunoassay calibration curves using a 5-parameter fit with $1/y^2$ weighting. For mass spectrometry data, a Student's t-test was used to compare the $\log_2$ mean AUC of the three replicates from control and ANGPTL3/8 samples. For those ions with an extract AUC below 1024, the $\log_2$ AUC was adjusted to the $\log_2$ of 10 prior to statistical analysis. Peptide ions in ANGPTL3/8 samples differing from the control samples with a $p < 0.05$ and a fold-change > 5 were considered to be significant. Significance for the effect of insulin and T0901307 on ANGPTL3/8 and ApoA5 secretion from hepatocytes was calculated using a one-way ANOVA. Significance for the combined effect of insulin and T0901307 on ANGPTL3/8 and ApoA5 secretion from hepatocytes was calculated using a two-way ANOVA.

APPENDIX A. SUPPLEMENTAL FIGURES

Supplemental Figures A1- A17: Chromatograms for ApoA5 peptide ions from ANGPTL3/8 and control samples.

The peptide ion sequence and parent m/z value are listed on top of the corresponding figures. Oxidized methionine residues were denoted with [15.9949] at the sequences. The peaks were extracted using Freestyle software with a minimum S/N threshold of 2.0 and a mass tolerance window of 2 ppm. For each ion, the ion intensity was globally normalized to the highest one in the group. For control samples, the peak areas were extracted within a window of ± 0.4 min of the mean retention times of the corresponding peaks detected in ANGPTL3/8 samples, as illustrated by the dashed lines. The ± 0.4 min window was selected based on evaluating the maximum retention time shift of landmark ions in the samples.

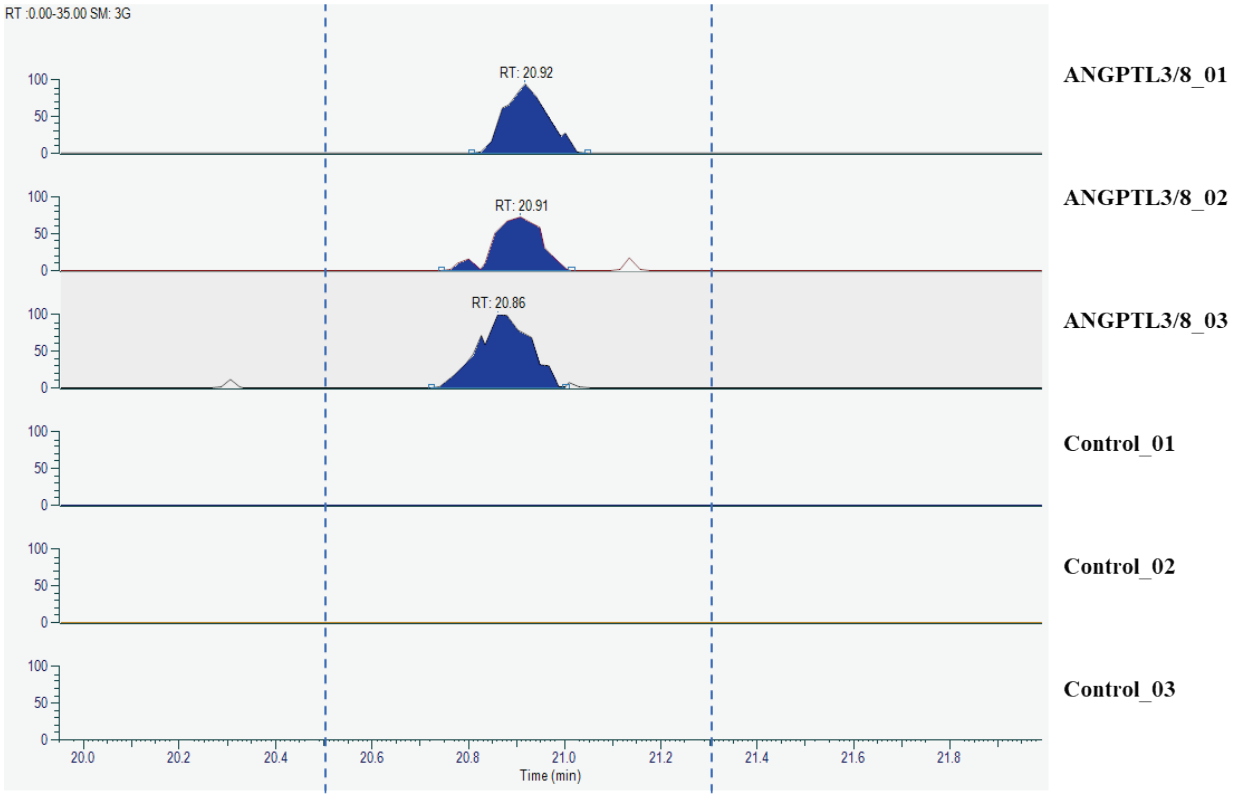

Figure A1: KGFWDYFSQTSGDK; Parent m/z: 555.9234

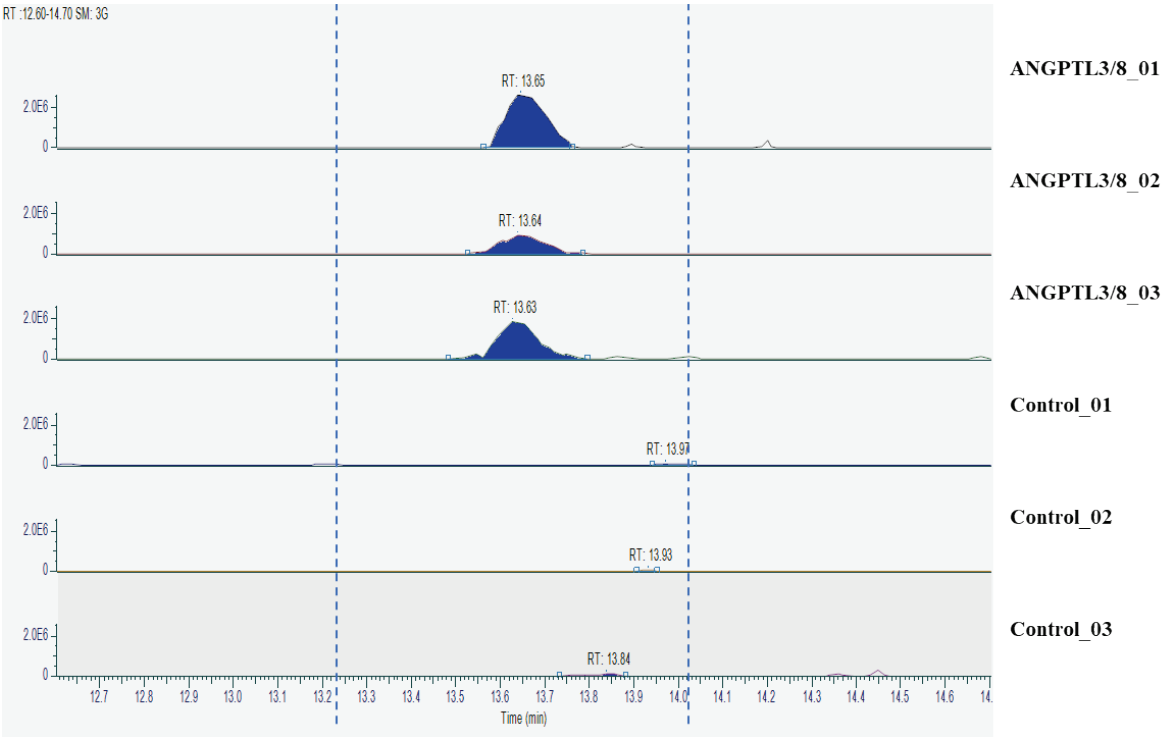

Figure A2: DSLEQDLNNM[15.9949]NK, Parent m/z: 718.8205

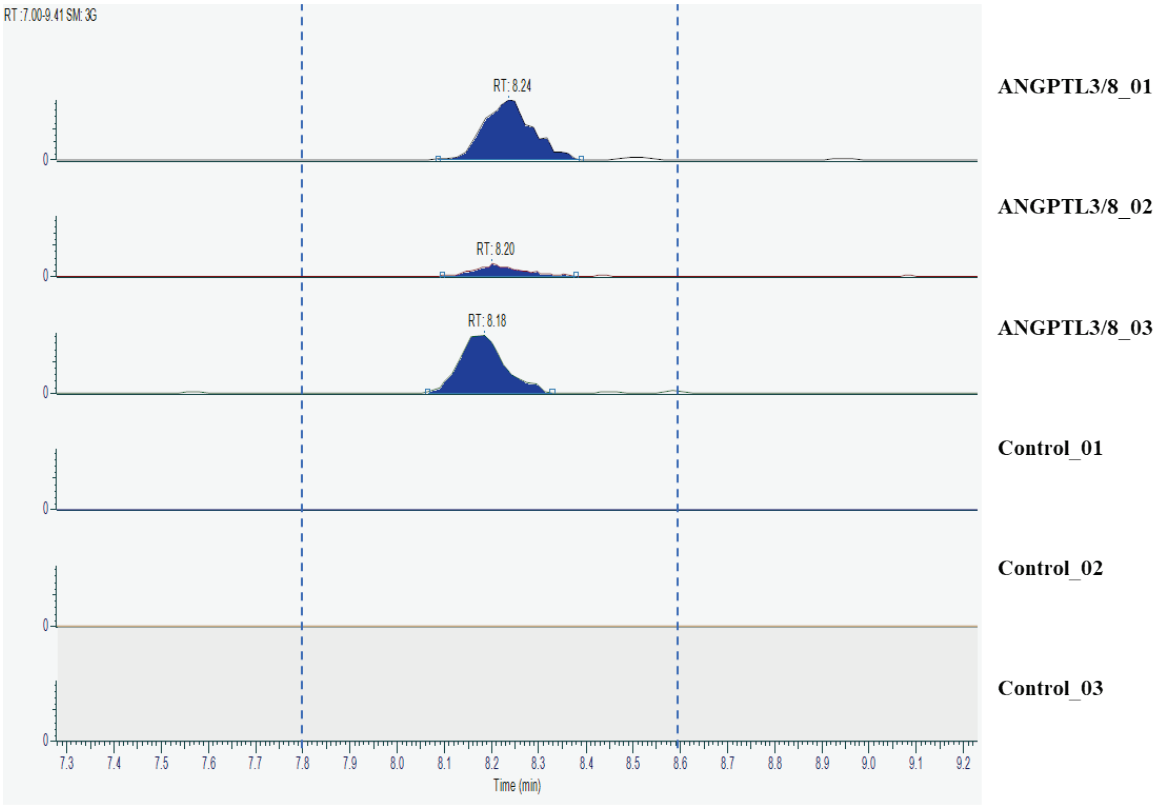

Figure A3: LRPLSGSEAPR, Parent m/z: 394.8911

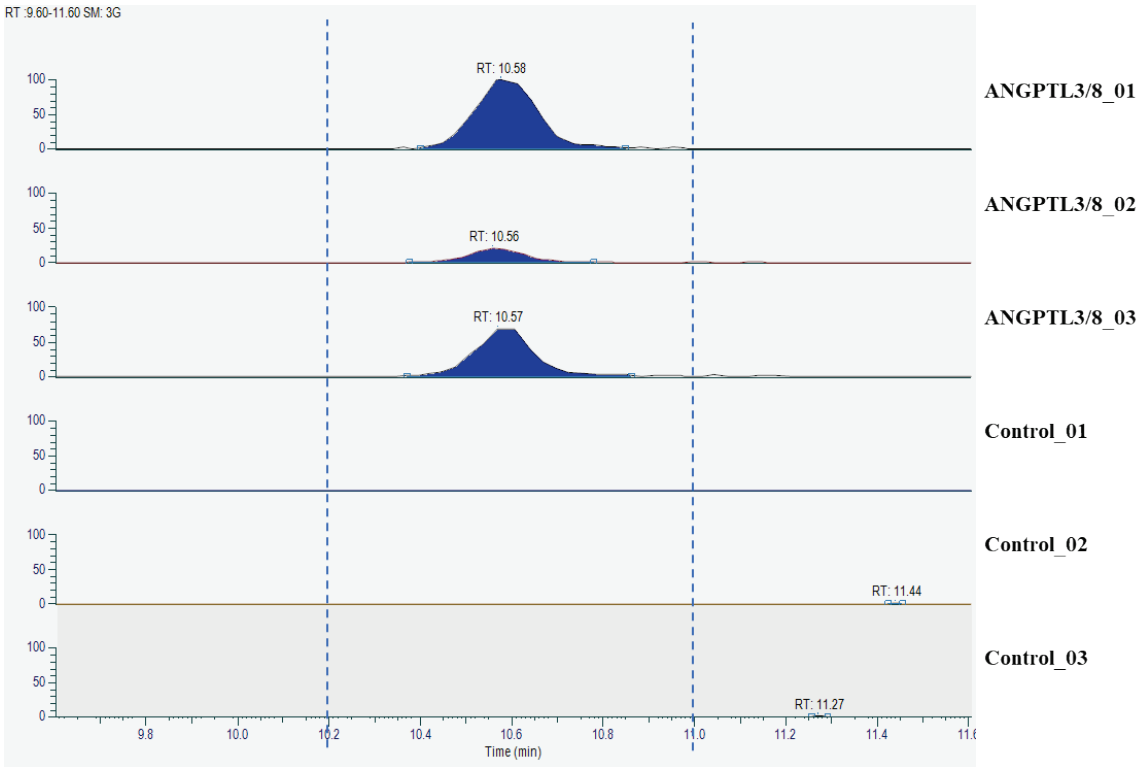

Figure A4: LPQDPVGM[15.9949]R, Parent m/z: 514.7640

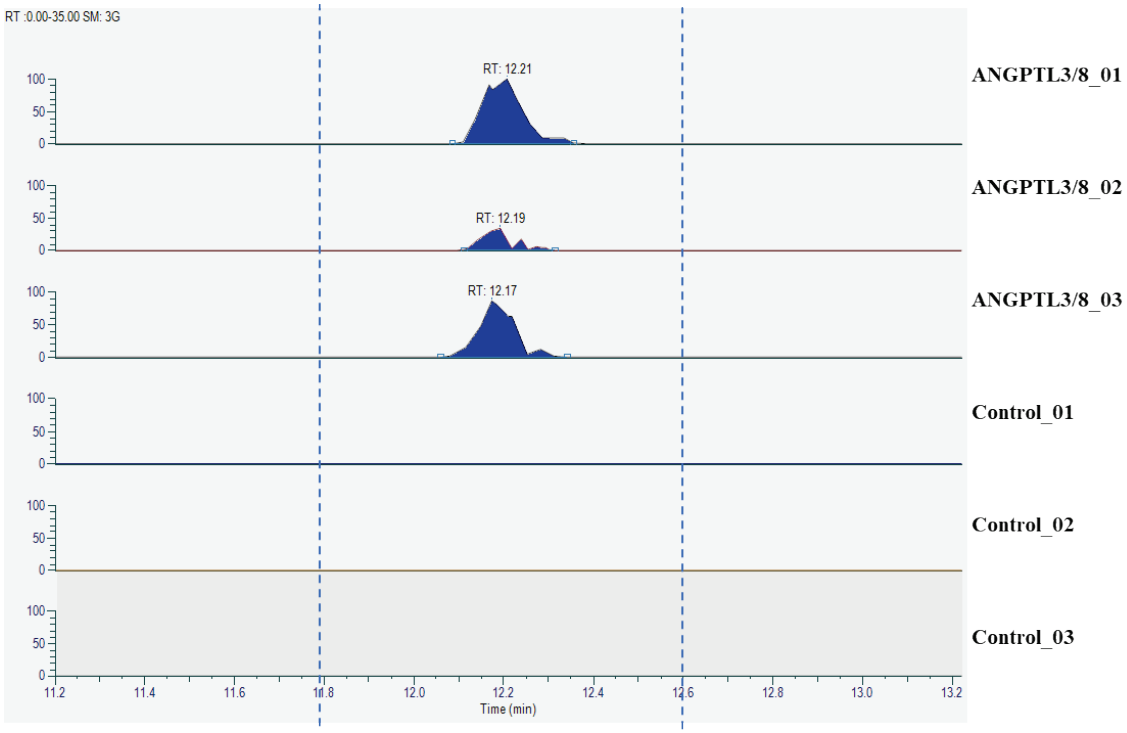

Figure A5: RQLQEELEEVK, Parent m/z: 700.8737

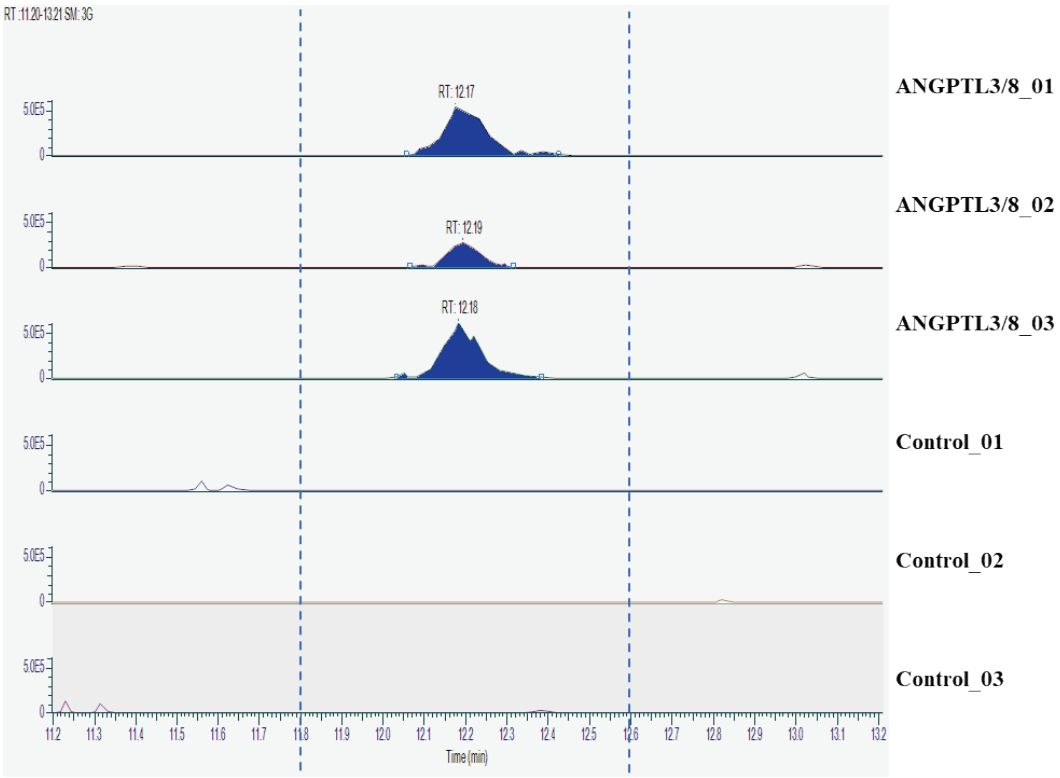

Figure A6: RQLQEELEEVK, Parent m/z: 467.5844

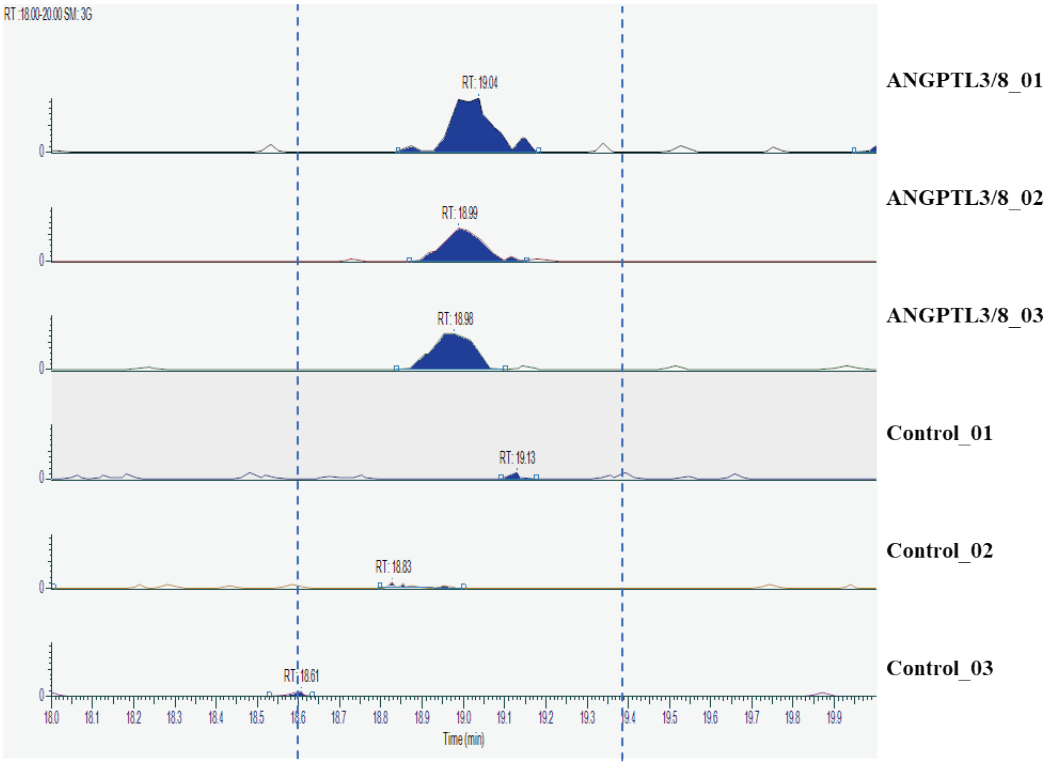

Figure A7: M[15.9949]AEAHELVGWNLEGLR, Parent m/z: 614.3059

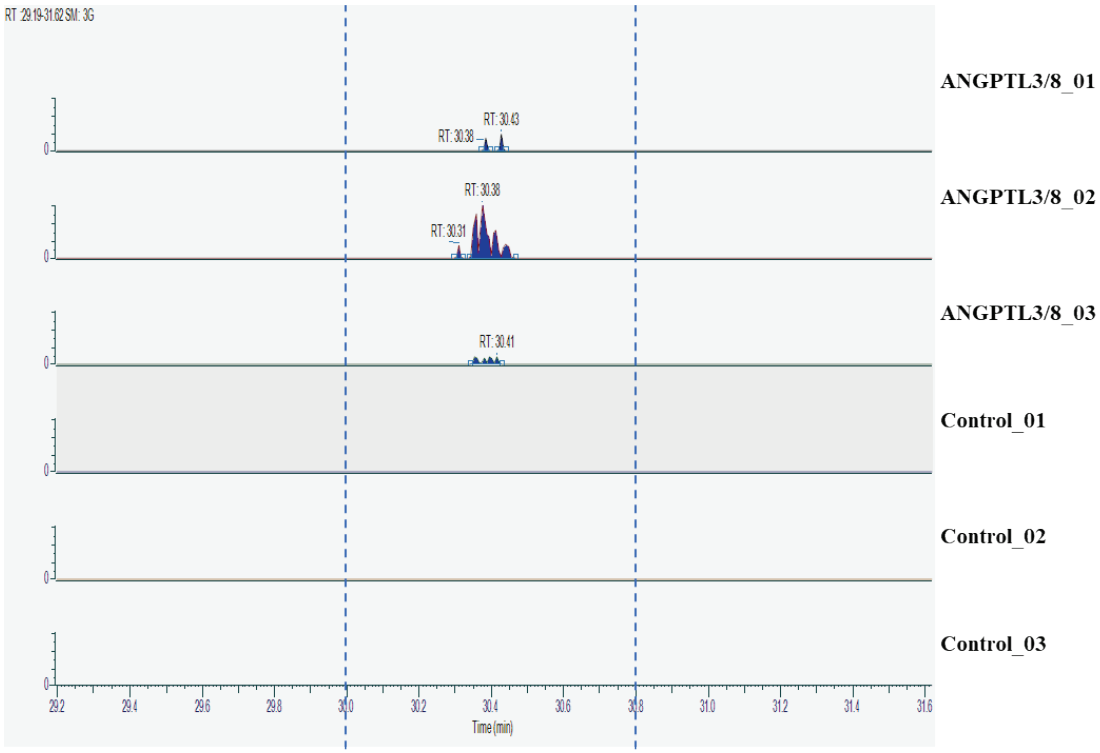

Figure A8 AQLLGGVDEAWALLQGLQSR, Parent m/z

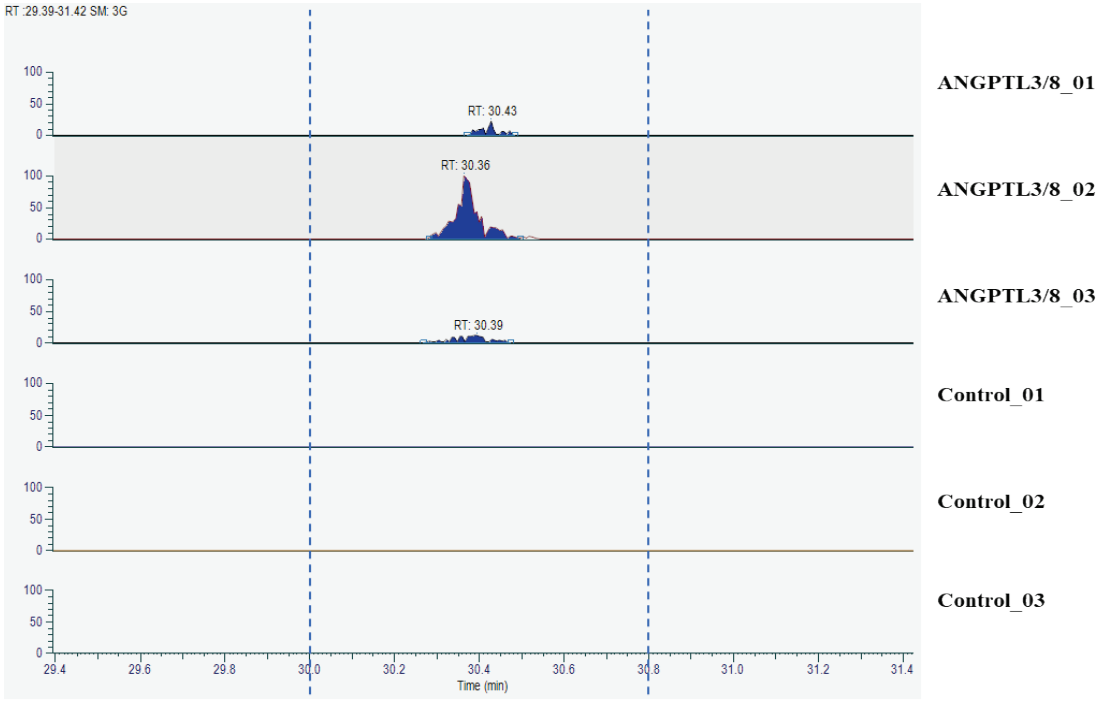

Figure A9 AQLLGGVDEAWALLQGLQSR, Parent m/z: 709.0530

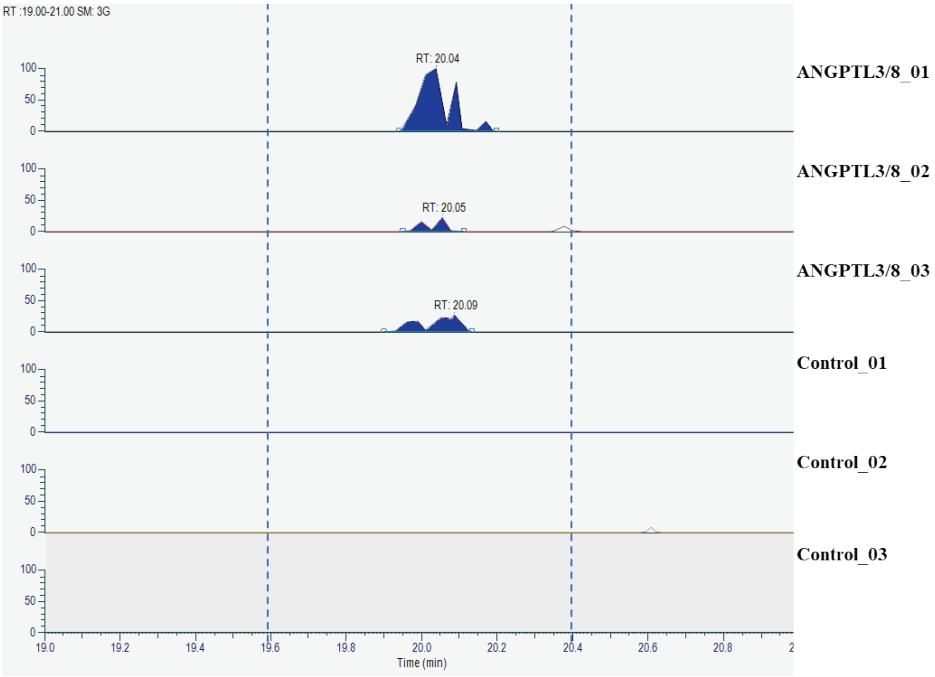

Figure A10 ELFHPYAESLVSGIGR, Parent m/z: 887.9617

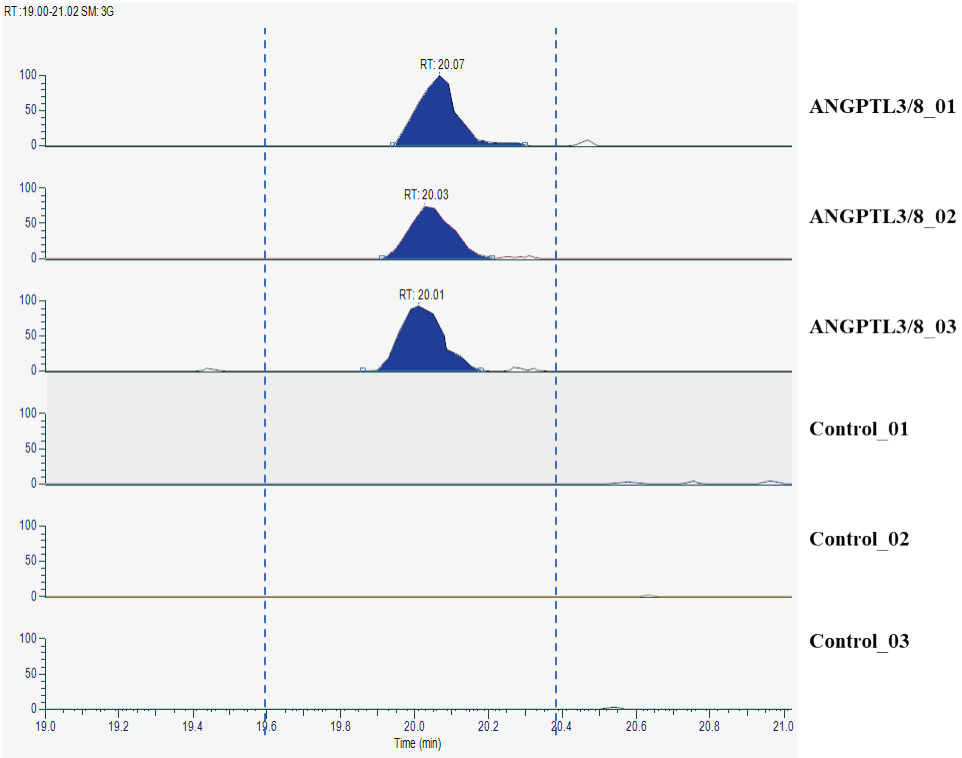

Figure A11 ELFHPYAESLVSGIGR, Parent m/z: 592.3093

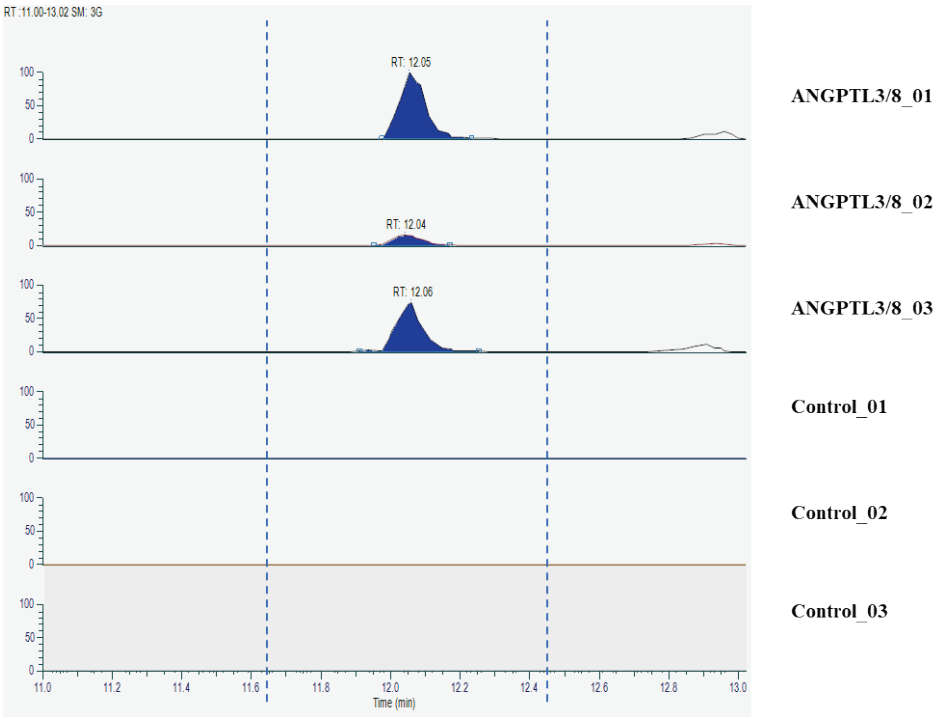

Figure A12 IQQNLDQLR, Parent m/z

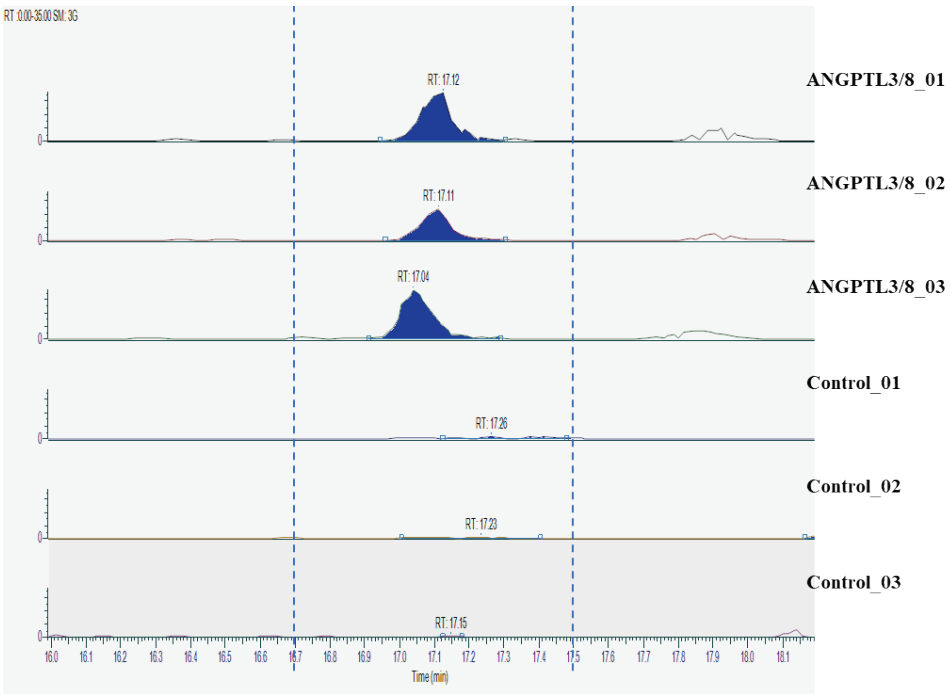

Figure A13 IQQNLDQLREELSR, Parent m/z: 581.3115

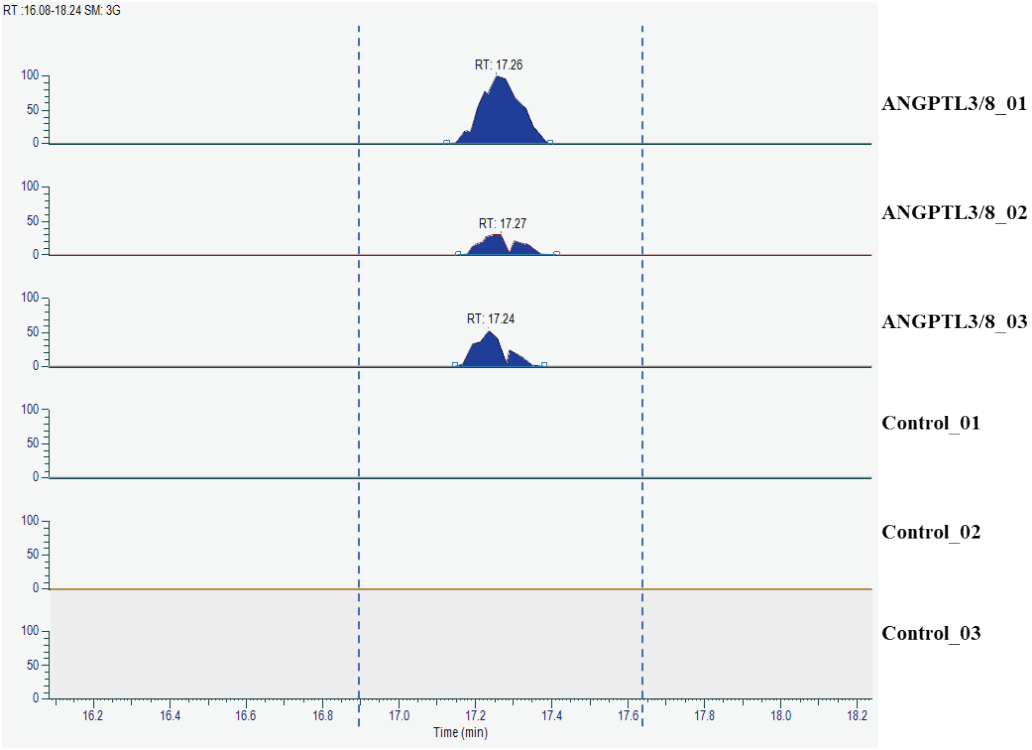

Figure A14 AFAGTGTEEGAGPDPQM [15.9949] LSEEVR, Parent m/z: 1183.0353

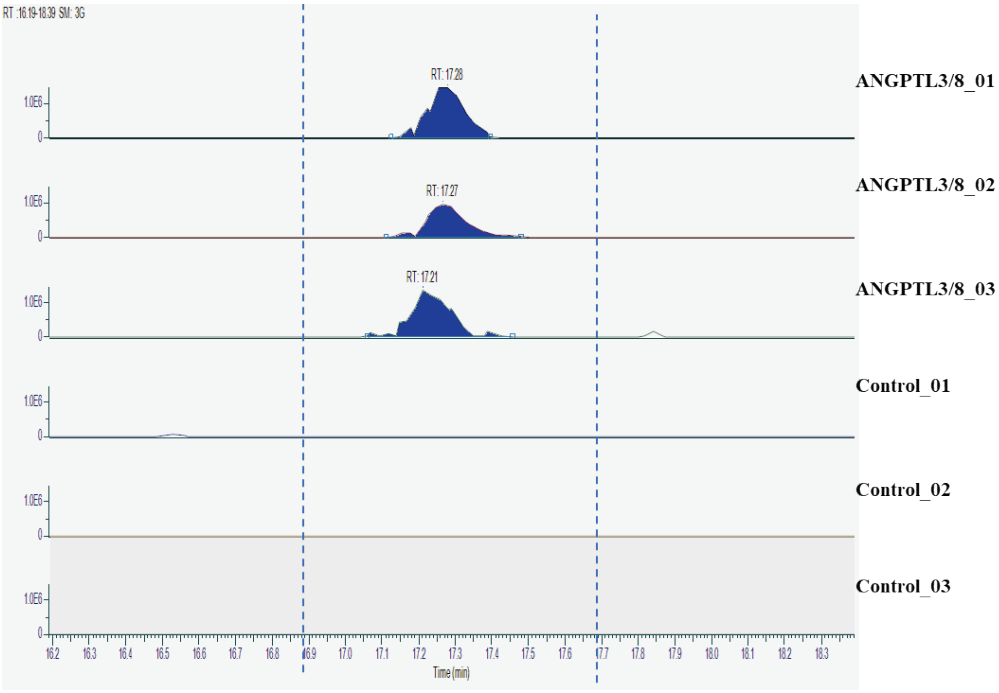

Figure A15 AFAGTGTEEGAGPDPQM[15.9949]LSEEVR, Parent m/z: 789.0278

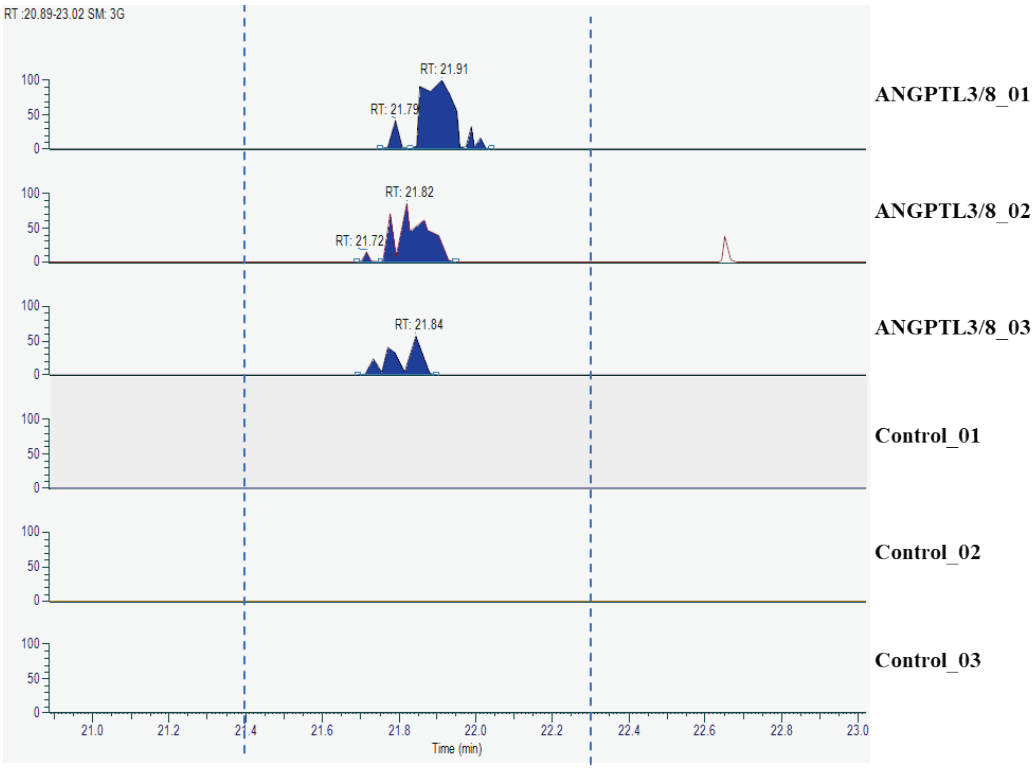

Figure A16 LDDLWEDITHSLHDQGHSHLGDP, Parent m/z: 879.7406

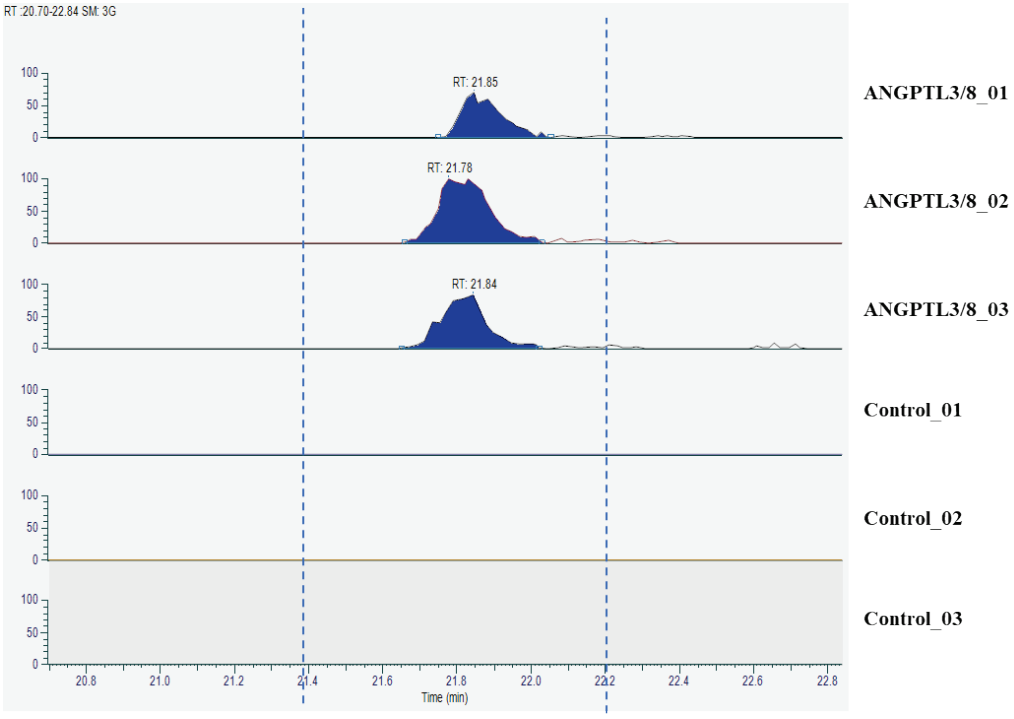

Figure A17 LDDLWEDITHSLHDQGHSHLGDP, Parent m/z: 660.0556

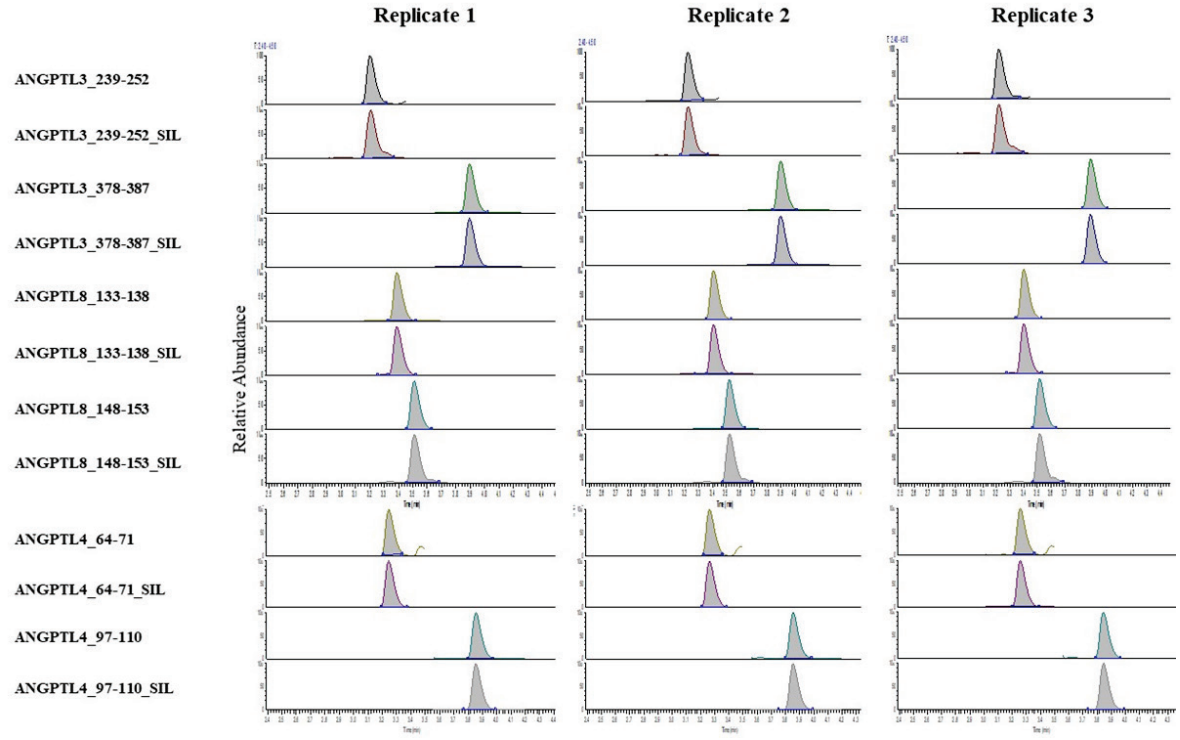

Figure A18 Chromatograms of protein ions detected in ANGPTL8 immunoprecipitation experiments.

MRM data were quantified using Thermo Xcalibur (version 4.2.47) with ICIS peak detection algorithm. The following parameters were used for peak integration: Smoothing points: 7; Baseline window: 20; Area noise factor: 5; Peak noise factor: 10. Two peptides per protein were monitored. SIL peptides (0.2 pmole) were spiked into each replicate after digestion. The ratio between endogenous peptide and the corresponding SIL peptide was calculated and the amount of protein detected was determined using the molecular weight. All analyses were performed in triplicate. The SIL peptides used for quantitation of ANGPTL8 were: 133-138 and 148-153, those used for ANGPTL4 were 64-71 and 97-110, and those used for ANGPTL3 were 239-252 and 378-387. The Y-axis shows relative abundance, and the X-axis shows retention time in minutes, with grey shading indicating the integrated area. The integrated AUC values for each peptide ion and calculated protein concentrations are listed in Supplemental Table B2

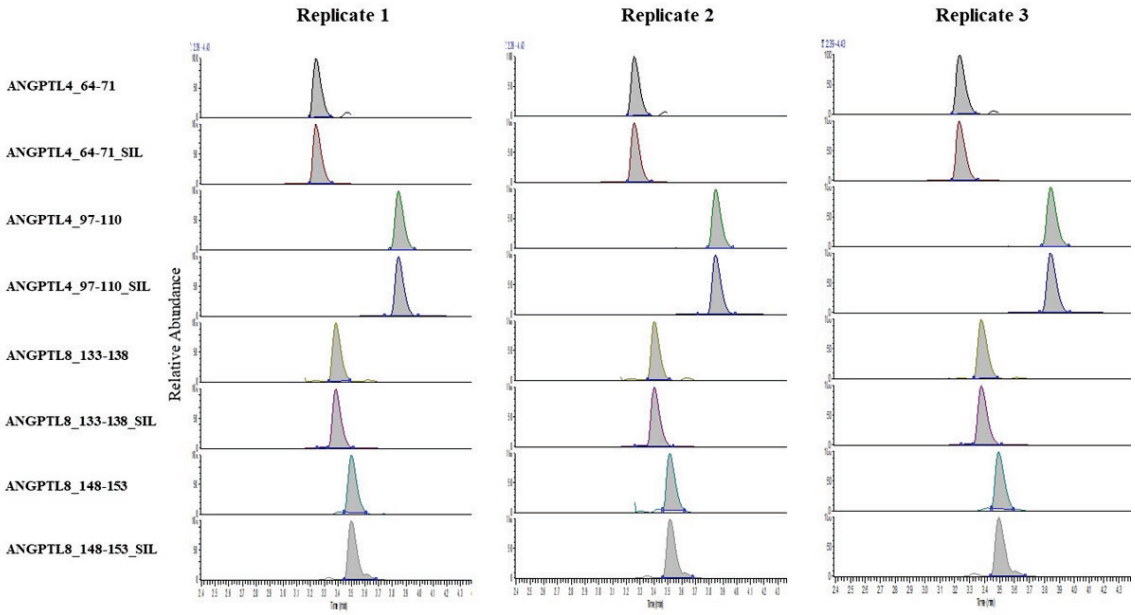

Figure A19 Chromatograms of protein ions detected in ANGPTL4 immunoprecipitation experiments.

MRM data were quantified using Thermo Xcalibur (version 4.2.47) with ICIS peak detection algorithm. The following parameters were used for peak integration: Smoothing points: 7; Baseline window: 20; Area noise factor: 5; Peak noise factor: 10. Two peptides per protein were monitored. SIL peptides (0.2 pmole) were spiked into each replicate after digestion. The ratio between endogenous peptide and the corresponding SIL peptide was calculated and the amount of protein detected was determined using the molecular weight. All analyses were performed in triplicate. The SIL peptides used for quantitation of ANGPTL4 were: 64-71 and 97-110, and those used for ANGPTL8 were 133-138 and 148-153. The Y-axis shows relative abundance, and the X-axis shows retention time in minutes, with grey shading indicating the integrated area. The integrated AUC values for each peptide ion and calculated protein concentrations are listed in Supplemental Table B2.

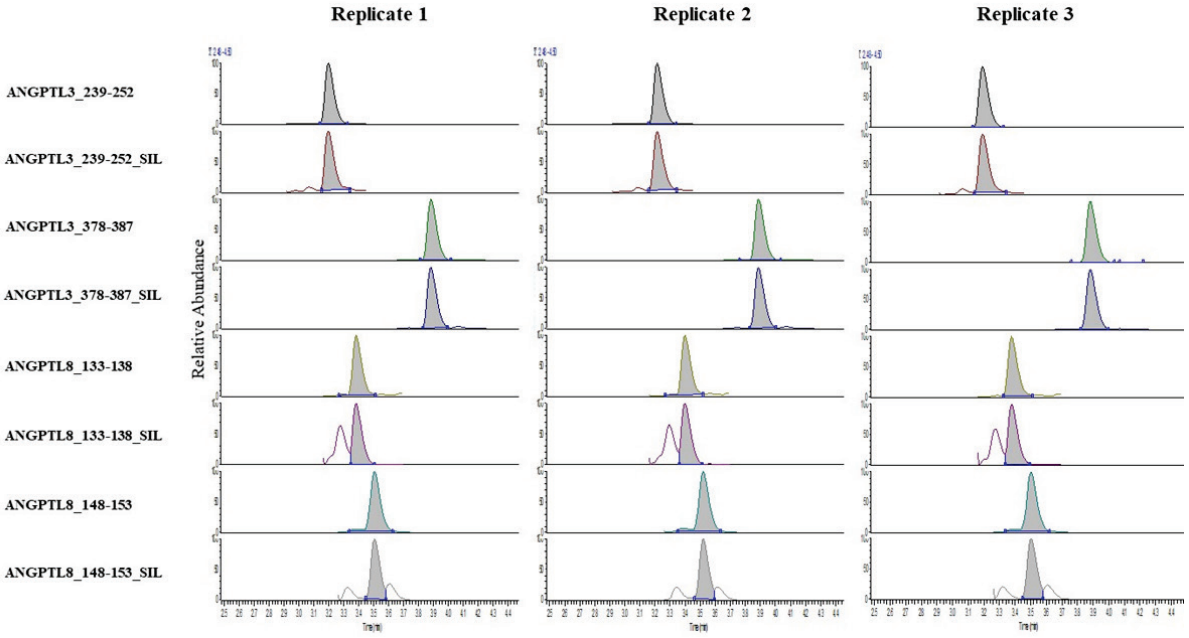

Figure A20 Chromatograms of protein ions detected in ANGPTL3 immunoprecipitation experiments.

MRM data were quantified using Thermo Xcalibur (version 4.2.47) with ICIS peak detection algorithm. The following parameters were used for peak integration: Smoothing points: 7; Baseline window: 20; Area noise factor: 5; Peak noise factor: 10. Two peptides per protein were monitored. SIL peptides (0.2 pmole) were spiked into each replicate after digestion. The ratio between endogenous peptide and the corresponding SIL peptide was calculated and the amount of protein detected was determined using the molecular weight. All analyses were performed in triplicate. The SIL peptides used for quantitation of ANGPTL3 were 239-252 and 378-387, and those used for ANGPTL8 were 133-138 and 148-153. The Y-axis shows relative abundance, and the X-axis shows retention time in minutes, with grey shading indicating the integrated area. The integrated AUC values for each peptide ion and calculated protein concentrations are listed in Supplemental Table B2.

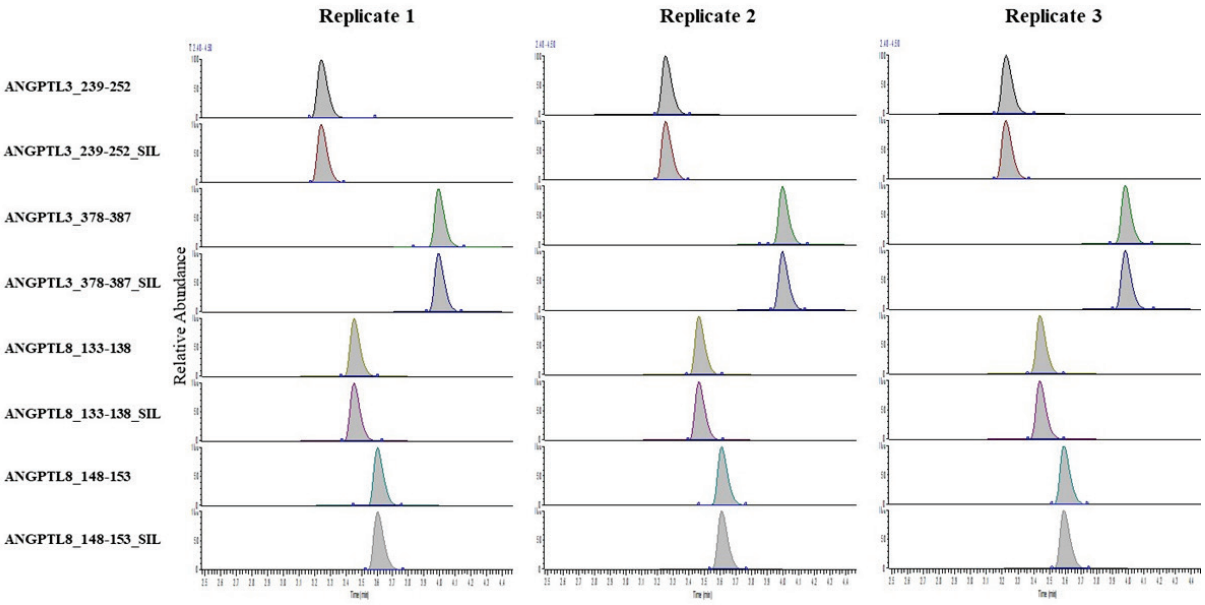

Figure A21 Chromatograms for ANGPTL protein ions from recombinant ANGPTL3/8 digest.

The peak detection methods are the same as described previously. All analyses were performed in triplicate from a single protein production preparation. Two peptides per protein were monitored. The SIL peptides used for quantitation were 239-252 and 378-387 for ANGPTL3 and 133-138 and 148-153 for ANGPTL8. The Y-axis shows the relative abundance, and the X-axis shows retention time in minutes, with grey shading indicating the integrated area. The integrated AUC values for each peptide ion and the protein ratios for the complex are listed in Supplemental Table B2.

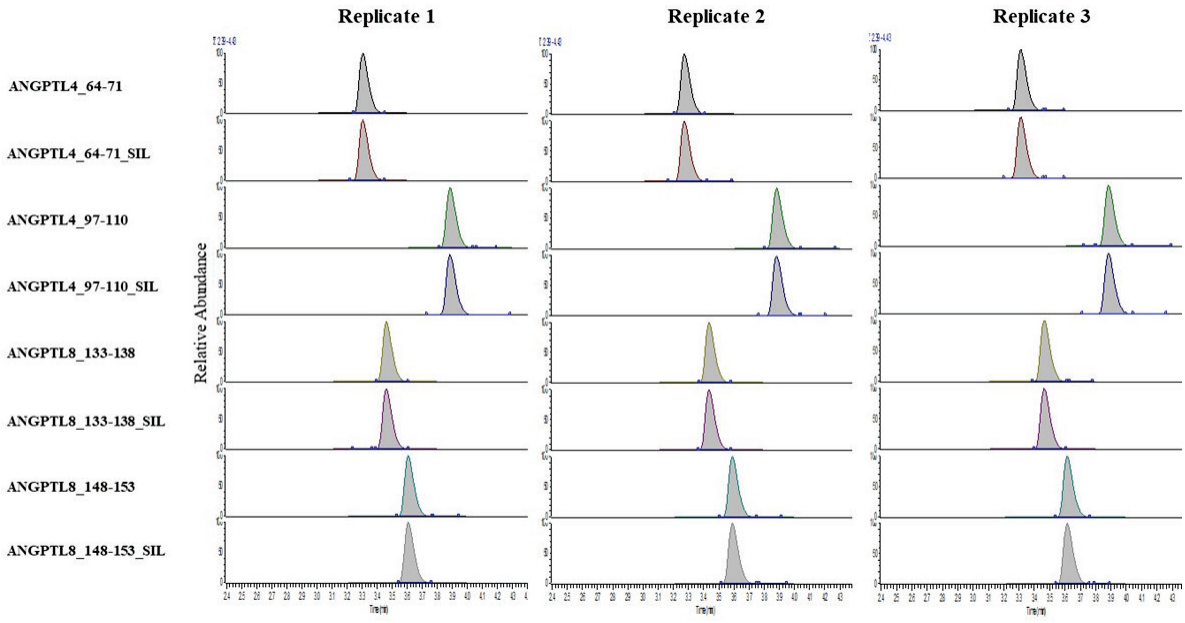

Figure A22 Chromatograms for ANGPTL protein ions from recombinant ANGPTL4/8 digest.

The peak detection methods are the same as described previously. All analyses were performed in triplicate from a single protein production preparation. Two peptides per protein were monitored. The SIL peptides used for quantitation were 64-71 and 97-110 for ANGPTL4 and 133-138 and 148-153 for ANGPTL8. The Y-axis shows the relative abundance, and the X-axis shows retention time in minutes, with grey shading indicating the integrated area. The integrated AUC values for each peptide ion and the protein ratios for the complex are listed in Supplemental Table B2.

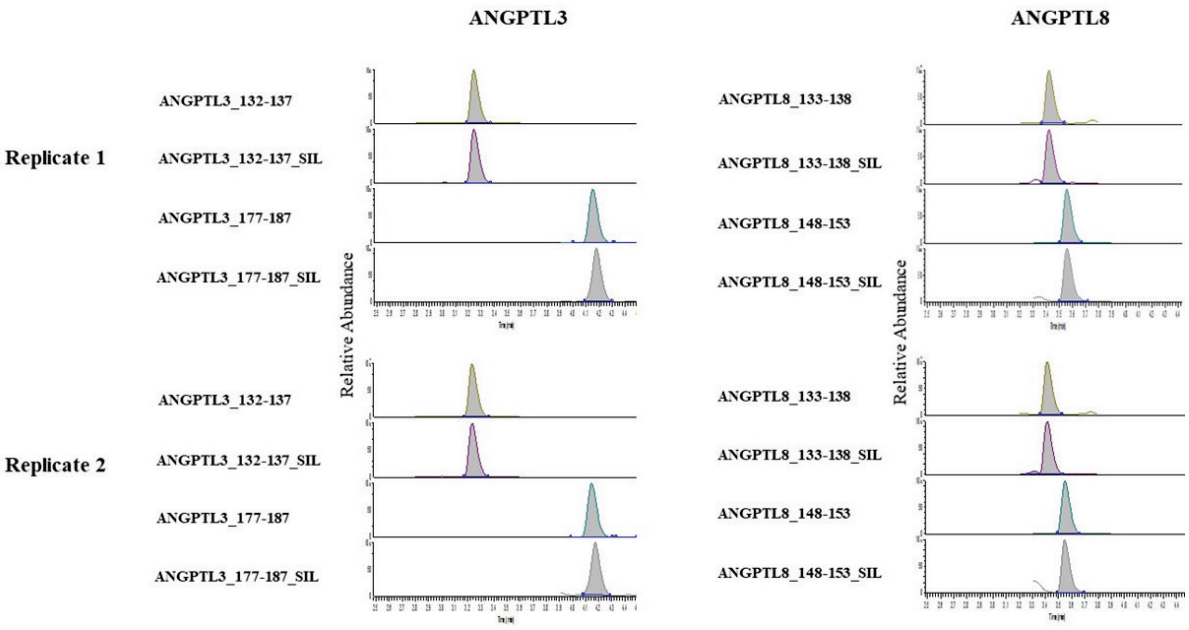

Figure A23 Chromatograms for ANGPTL protein ions from endogenous ANGPTL3/8 digest.

The peak detection methods are the same as described previously. All analyses were performed in duplicate from a sample composed of a pool of sera from 20 healthy donors. Two peptides per protein were monitored. The SIL peptides used for quantitation were 132-137 and 177-187 for ANGPTL3 and 133-138 and 148-153 for ANGPTL8. The Y-axis shows the relative abundance, and the X-axis shows retention time in minutes, with grey shading indicating the integrated area. The integrated AUC values for each peptide ion and the protein ratios for the complex are listed in Supplemental Table B2.

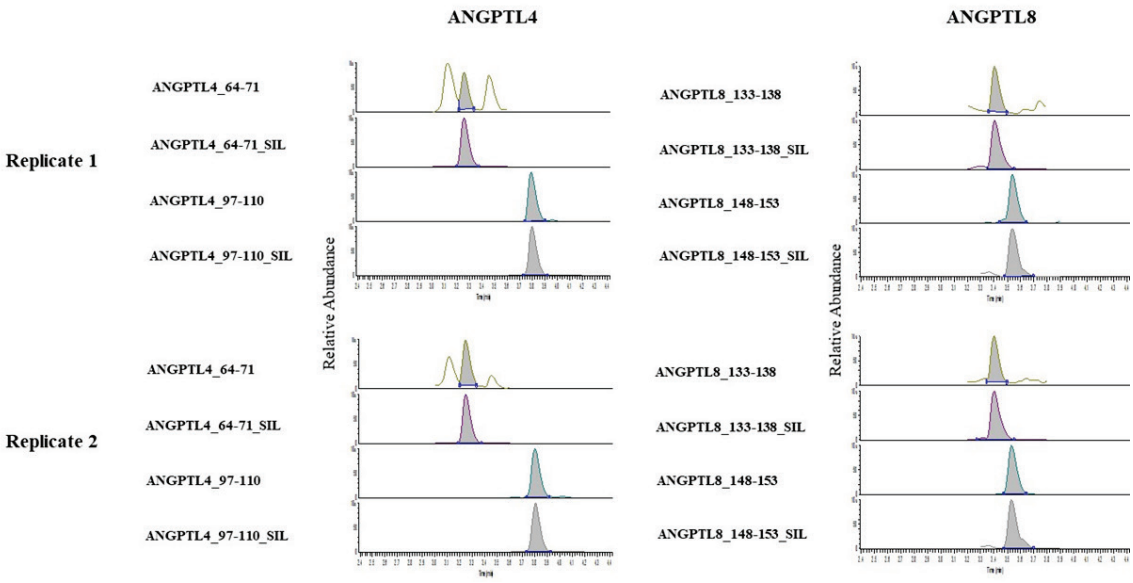

Figure A24 Chromatograms for ANGPTL protein ions from endogenous ANGPTL4/8 digest.

The peak detection methods are the same as described previously. All analyses were performed in duplicate from a sample composed of a pool of sera from 20 healthy donors. Two peptides per protein were monitored. The SIL peptides used for quantitation were 64-71 and 97-110 for ANGPTL4 and 133-138 an 148-153 for ANGPTL8. The Y-axis shows the relative abundance, and the X-axis shows retention time in minutes, with grey shading indicating the integrated area. The integrated AUC values for each peptide ion and the protein ratios for the complex are listed in Supplemental Table B2.

APPENDIX B. SUPPLEMENTAL TABLES

Table B1 ApoA5 peptide ions identified from mass spectrometry analysis & database search.

ID	Peptide	Start#	End#	z	M	Theo M	m/z	Δ M (ppm)	q-val§	AUC* ANGPTL3/8	AUC* control
1	R.KGFWDYFSQTSGDK.G	25	38	3	1664.7486	1664.7471	555.9234	-0.9	0	3.248e+6	0e+0
2	K.DSLEQDLNNM[15.9949]NK.F	58	69	2	1435.6265	1435.6249	718.8205	-1.1	0	1.118e+7	1.382e+5
3	K.LRPLSGSEAPR.L	74	84	3	1181.6516	1181.6517	394.8911	0	0.0019	4.622e+6	0e+0
4	R.LPQDPVGM[15.9949]R.R	85	93	2	1027.5135	1027.5121	514.7640	-1.4	0	2.403e+7	0e+0
5	R.RQLQEELEEVK.A	94	104	2	1399.7329	1399.7307	700.8737	-1.6	0.0255	3.015e+6	0e+0
6	R.RQLQEELEEVK.A	94	104	3	1399.7316	1399.7307	467.5844	-0.6	0	2.949e+6	0e+0
7	Y.M[15.9949]AEAHELVGWNLEGLR.Q	111	126	3	1839.8961	1839.8938	614.3059	-1.3	0	5.084e+6	1.175e+5
8	K.AQLLGGVDEAWALLQGLQSR.V	160	179	2	2124.1385	2124.1328	1063.0765	-2.7	0	5.741e+5	0e+0
9	K.AQLLGGVDEAWALLQGLQSR.V	160	179	3	2124.1372	2124.1328	709.0530	-2.1	0	2.386e+6	0e+0
10	K.ELEHPYAESLVSGIGR.H	189	204	2	1773.909	1773.905	887.9617	-2.2	0	1.954e+6	0e+0
11	K.ELEHPYAESLVSGIGR.H	189	204	3	1773.9061	1773.905	592.3093	-0.6	0	1.485e+7	0e+0
12	R.IQQNLDQLR.E	246	254	2	1126.6109	1126.6095	564.3127	-1.3	0.0024	8.237e+6	0e+0
13	R.IQQNLDQLREELSR.A	246	259	3	1740.9129	1740.9119	581.3115	-0.6	0	1.985e+7	3.981e+5
14	R.AEAGTGTEEGAGPDPQM[15.9949]LSEEVR.Q	260	282	2	2364.0553	2364.054	1183.0353	-0.6	0	3.277e+6	0e+0
15	R.AEAGTGTEEGAGPDPQM[15.9949]LSEEVR.Q	260	282	3	2364.0617	2364.054	789.0278	-3.3	0	8.651e+6	0e+0
16	R.LDDLWEDITHSLHDQGHSHLGDP.-	344	366	3	2636.2002	2636.1892	879.7406	-4.2	0	1.793e+6	0e+0
17	R.LDDLWEDITHSLHDQGHSHLGDP.-	344	366	4	2636.1935	2636.1892	660.0556	-1.7	0.0033	2.221e+7	0e+0

#: The start or end locations of the peptide in the protein sequence.
§: The false discovery rate estimate for this peptide.
* The mean AUC value from three replicates.

Table B2 ANGPTL protein MRM peptide characteristics

protein_name	Peptide location	sequence	Q1	Q3	dwelltime	Tr_original	transition_group	CE	relative_	decoy	isotype	prec_z	frg_type	frg_nr	frg_z	Frg_loss	RF Lens (V)	organism
ANGPTL3	239-252	HDGIPAEC[57]TTIYNR	549.7	423.2	11.3	3.3	1	19	0	0	Light	3	b	4	1		65	Human
ANGPTL3	239-252	HDGIPAEC[57]TTIYNR	549.7	452.2	11.3	3.3	1	10.25	0	0	Light	3	y	3	1	-36	65	Human
ANGPTL3	239-252	HDGIPAEC[57]TTIYNR	549.7	513.3	11.3	3.3	1	10.25	0	0	Light	3	MH	14	3		65	Human
ANGPTL3	239-252	HDGIPAEC[57]TTIYNR(13C6, 15N4)	553.1	423.2	11.3	3.3	2	19	0	0	Heavy	3	b	4	1		65	Human
ANGPTL3	239-252	HDGIPAEC[57]TTIYNR(13C6, 15N4)	553.1	462.2	11.3	3.3	2	10.25	0	0	Heavy	3	y	3	1		65	Human
ANGPTL3	239-252	HDGIPAEC[57]TTIYNR(13C6, 15N4)	553.1	516.7	11.3	3.3	2	10.25	0	0	Heavy	3	MH	14	3	-36	65	Human
ANGPTL3	378-387	DLVFSTWDHK	416.63	460.79	13.3	4.025	3	10.25	0	0	Light	3	y	7	2		55	Human
ANGPTL3	378-387	DLVFSTWDHK	416.63	510.32	13.3	4.025	3	10.25	0	0	Light	3	y	8	2		55	Human
ANGPTL3	378-387	DLVFSTWDHK(13C6, 15N2)	419.3	464.79	13.3	4.025	4	10.25	0	0	Heavy	3	y	7	2		55	Human
ANGPTL3	378-387	DLVFSTWDHK(13C6, 15N2)	419.3	514.32	13.3	4.025	4	10.25	0	0	Heavy	3	y	8	2		55	Human
ANGPTL3	132-137	ILLQQK	371.9	199.2	11.3	3.25	13	14	0	0	Light	2	a	2	1		59	Human
ANGPTL3	132-137	ILLQQK	371.9	227.2	11.3	3.25	13	12	0	0	Light	2	b	2	1		59	Human
ANGPTL3	132-137	ILLQQK	371.9	516.4	11.3	3.25	13	13	0	0	Light	2	y	4	1		59	Human
ANGPTL3	132-137	ILLQQK	371.9	629.4	11.3	3.25	13	13	0	0	Light	2	y	5	1		59	Human
ANGPTL3	132-137	ILLQQK(13C6, 15N2)	375.9	199.2	11.3	3.25	14	14	0	0	Heavy	2	a	2	1		59	Human
ANGPTL3	132-137	ILLQQK(13C6, 15N2)	375.9	227.2	11.3	3.25	14	12	0	0	Heavy	2	b	2	1		59	Human
ANGPTL3	132-137	ILLQQK(13C6, 15N2)	375.9	524.4	11.3	3.25	14	13	0	0	Heavy	2	y	4	1		59	Human
ANGPTL3	132-137	ILLQQK(13C6, 15N2)	375.9	637.4	11.3	3.25	14	13	0	0	Heavy	2	y	5	1		59	Human
ANGPTL3	177-187	DLLQTVEDQYK	676.5	201.2	23	4.2	15	34	0	0	Light	2	a	2	1		86	Human
ANGPTL3	177-187	DLLQTVEDQYK	676.5	229.1	23	4.2	15	24	0	0	Light	2	b	2	1		86	Human
ANGPTL3	177-187	DLLQTVEDQYK	676.5	682.3	23	4.2	15	18	0	0	Light	2	y	5	1		86	Human
ANGPTL3	177-187	DLLQTVEDQYK	676.5	882.5	23	4.2	15	20.5	0	0	Light	2	y	7	1		86	Human
ANGPTL3	177-187	DLLQTVEDQYK(13C6, 15N2)	680.5	201.2	23	4.2	16	34	0	0	Heavy	2	a	2	1		86	Human
ANGPTL3	177-187	DLLQTVEDQYK(13C6, 15N2)	680.5	229.1	23	4.2	16	24	0	0	Heavy	2	b	2	1		86	Human
ANGPTL3	177-187	DLLQTVEDQYK(13C6, 15N2)	680.5	690.3	23	4.2	16	18	0	0	Heavy	2	y	5	1		86	Human
ANGPTL3	177-187	DLLQTVEDQYK(13C6, 15N2)	680.5	890.5	23	4.2	16	20.5	0	0	Heavy	2	y	7	1		86	Human
ANGPTL4	64-71	SQLSALER	452.33	575.3	11.3	3.3	5	13.6	0	0	Light	2	y	5	1		58	Human
ANGPTL4	64-71	SQLSALER	452.33	688.4	11.3	3.3	5	12.8	0	0	Light	2	y	6	1		58	Human
ANGPTL4	64-71	SQLSALER(13C6, 15N4)	457.33	585.3	11.3	3.3	6	13.6	0	0	Heavy	2	y	5	1		58	Human
ANGPTL4	64-71	SQLSALER(13C6, 15N4)	457.33	698.4	11.3	3.3	6	12.8	0	0	Heavy	2	y	6	1		58	Human
ANGPTL4	97-110	VDPEVLHSLQTQLK	536.41	464.94	13.3	3.9	7	10.3	0	0	Light	3	y	12	3		67	Human
ANGPTL4	97-110	VDPEVLHSLQTQLK	536.41	697	13.3	3.9	7	10.3	0	0	Light	3	y	11	2		67	Human
ANGPTL4	97-110	VDPEVLHSLQTQLK(13C6, 15N2)	539.08	467.61	13.3	3.9	8	10.3	0	0	Heavy	3	y	12	3		67	Human
ANGPTL4	97-110	VDPEVLHSLQTQLK(13C6, 15N2)	539.08	701	13.3	3.9	8	10.3	0	0	Heavy	3	y	11	2		67	Human
ANGPTL8	133-138	LEVQLR	379.33	243.1	11.3	3.5	9	10.25	0	0	Light	2	b	2	1		56	Human
ANGPTL8	133-138	LEVQLR	379.33	515.27	11.3	3.5	9	10.25	0	0	Light	2	y	4	1		56	Human
ANGPTL8	133-138	LEVQLR	379.33	644.2	11.3	3.5	9	13.2	0	0	Light	2	y	5	1		56	Human
ANGPTL8	133-138	LEVQLR(13C6, 15N4)	384.33	243.05	11.3	3.5	10	10.25	0	0	Heavy	2	b	2	1		56	Human
ANGPTL8	133-138	LEVQLR(13C6, 15N4)	384.33	525.27	11.3	3.5	10	10.25	0	0	Heavy	2	y	4	1		56	Human
ANGPTL8	133-138	LEVQLR(13C6, 15N4)	384.33	654.2	11.3	3.5	10	13.2	0	0	Heavy	2	y	5	1		56	Human
ANGPTL8	148-153	EFEVLK	382.8	260.15	11.3	3.65	11	10.25	0	0	Light	2	y	2	1		55	Human
ANGPTL8	148-153	EFEVLK	382.8	388.1	11.3	3.65	11	10.25	0	0	Light	2	b	3	1	-18	55	Human
ANGPTL8	148-153	EFEVLK	382.8	487.2	11.3	3.65	11	10.25	0	0	Light	2	b	4	1	-18	55	Human
ANGPTL8	148-153	EFEVLK(13C6, 15N2)	386.8	268.15	11.3	3.65	12	10.25	0	0	Heavy	2	y	2	1		55	Human
ANGPTL8	148-153	EFEVLK(13C6, 15N2)	386.8	388.1	11.3	3.65	12	10.25	0	0	Heavy	2	b	3	1	-18	55	Human
ANGPTL8	148-153	EFEVLK(13C6, 15N2)	386.8	487.2	11.3	3.65	12	10.25	0	0	Heavy	2	b	4	1	-18	55	Human

Table B3 MRM peptide AUCs for ANGPTL protein immunoprecipitations.

Integrated AUC values for each peptide ion and calculated ANGPTL protein concentration are listed.

Integrated AUC, peptide ion ratios and calculated protein concentrations for experiments presented in Figure 1B.

	ANGPTL3_239-252			ANGPTL3_378-387			ANGPTL3		ANGPTL8_133-138			ANGPTL8_148-153			ANGPTL8		ANGPTL4_64-71			ANGPTL4_97-110			ANGPTL4	
	Unlabeled	SIL	Area ratio	Unlabeled	SIL	Area ratio	Averaged ratio	ANGTL3 (ng/ml)	Unlabeled	SIL	Area ratio	Unlabeled	SIL	Area ratio	Averaged ratio	ANGPTL8 (ng/ml)	Unlabeled	SIL	Area ratio	Unlabeled	SIL	Area ratio	Averaged ratio	ANGPTL4 (ng/ml)
Anti-ANGPTL3_IP_01	8.28E+05	4.05E+04	20.42	1.85E+06	8.26E+04	22.45	21.43	**222.5**	2.64E+05	5.07E+05	0.52	9.18E+04	1.75E+05	0.52	0.52	**2.08**								
Anti-ANGPTL3_IP_02	8.38E+05	4.54E+04	18.46	1.94E+06	8.36E+04	23.17	20.82	**216.1**	2.52E+05	5.58E+05	0.45	9.07E+04	1.70E+05	0.53	0.49	**1.96**								
Anti-ANGPTL3_IP_03	8.12E+05	4.42E+04	18.36	1.98E+06	8.65E+04	22.92	20.64	**214.3**	2.52E+05	5.44E+05	0.46	9.22E+04	1.82E+05	0.51	0.49	**1.93**								
SD			1.16			0.37	0.42	**4.3**			0.04			0.01	0.02	**0.08**								
Anti-ANGPTL8_IP_01	6.59E+04	6.48E+04	1.02	1.14E+05	9.57E+04	1.19	1.10	**11.4**	5.34E+05	5.86E+05	0.91	2.03E+05	2.23E+05	0.91	0.91	**3.63**	1.88E+04	3.73E+05	0.05	6.45E+04	7.42E+05	0.09	0.07	**0.59**
Anti-ANGPTL8_IP_02	5.47E+04	7.14E+04	0.77	1.08E+05	1.11E+05	0.97	0.87	**9.0**	4.86E+05	6.69E+05	0.73	1.79E+05	2.55E+05	0.70	0.71	**2.84**	1.75E+04	4.11E+05	0.04	6.17E+04	8.63E+05	0.07	0.06	**0.49**
Anti-ANGPTL8_IP_03	7.42E+04	7.31E+04	1.02	1.31E+05	1.04E+05	1.26	1.14	**11.8**	6.16E+05	6.36E+05	0.97	2.24E+05	2.42E+05	0.93	0.95	**3.77**	2.09E+04	4.12E+05	0.05	6.77E+04	7.96E+05	0.08	0.07	**0.58**
SD			0.14			0.15	0.14	**1.5**			0.13			0.13	0.13	**0.50**			0.005			0.01	0.01	**0.06**
Anti-ANGPTL4_IP_01									4.65E+04	5.26E+05	0.09	1.94E+04	2.19E+05	0.09	0.09	**0.35**	5.85E+04	3.56E+05	0.16	1.98E+05	8.68E+05	0.23	0.20	**1.69**
Anti-ANGPTL4_IP_02									4.25E+04	5.41E+05	0.08	1.91E+04	2.21E+05	0.09	0.08	**0.33**	5.83E+04	3.55E+05	0.16	1.95E+05	8.36E+05	0.23	0.20	**1.71**
Anti-ANGPTL4_IP_03									5.04E+04	5.54E+05	0.09	1.77E+04	2.31E+05	0.08	0.08	**0.33**	5.72E+04	3.46E+05	0.17	1.95E+05	8.39E+05	0.23	0.20	**1.71**
SD											0.01			0.01	0.00	**0.01**			0.000			0.003	0.001	**0.01**

Table B4 MRM peptide AUCs for recombinant ANGPTL3/8 & ANGPTL4/8 protein complexes.

Integrated AUC values for each peptide ion and the protein ratios for the recombinant ANGPTL3/8 and ANGPTL4/8 complexes are listed.

Integrated AUC, peptide ion ratios and proteins ratios for recombinant protein complexes presented in Table 1.

	ANGPTL3_239-252			ANGPTL3_378-387			ANGPTL3	ANGPTL8_133-138			ANGPTL8_148-153			ANGPTL8	ANGPTL4_64-71			ANGPTL4_97-110			ANGPTL4	Stoichiometry	
	Unlabeled	SIL	Area ratio	Unlabeled	SIL	Area ratio	Averaged ratio	Unlabeled	SIL	Area ratio	Unlabeled	SIL	Area ratio	Averaged ratio	Unlabeled	SIL	Area ratio	Unlabeled	SIL	Area ratio	Averaged ratio	ANGPTL3/8	ANGPTL4/8
recombinant Angptl3/8_01	8.37E+06	8.72E+05	9.60	1.75E+07	1.35E+06	12.96	11.28	2.13E+07	5.84E+06	3.64	1.09E+07	3.75E+06	2.92	3.28								**3.4**	
recombinant Angptl3/8_02	9.14E+06	9.94E+05	9.19	1.82E+07	1.32E+06	13.74	11.47	2.16E+07	5.93E+06	3.64	1.12E+07	3.70E+06	3.04	3.34								**3.4**	
recombinant Angptl3/8_03	6.57E+06	8.15E+05	8.06	1.87E+07	1.39E+06	13.45	10.75	1.92E+07	5.96E+06	3.23	1.07E+07	3.68E+06	2.92	3.08								**3.5**	
SD			0.80			0.40	0.37			0.24			0.07	0.14								0.03	
recombinant Angptl4/8_01								5.59E+06	6.31E+06	0.88	2.83E+06	3.85E+06	0.74	0.81	3.70E+06	5.20E+06	0.71	8.67E+06	1.07E+07	0.81	0.76		**0.9**
recombinant Angptl4/8_02								4.49E+06	6.61E+06	0.68	2.21E+06	3.90E+06	0.57	0.62	2.88E+06	5.36E+06	0.54	7.12E+06	1.07E+07	0.67	0.60		**1.0**
recombinant Angptl4/8_03								5.24E+06	7.07E+06	0.74	2.77E+06	4.44E+06	0.62	0.68	3.89E+06	5.71E+06	0.68	8.75E+06	9.54E+06	0.92	0.80		**1.2**
SD										0.11			0.09	0.10			0.09			0.13	0.11		0.13

Table B5 MRM peptide AUCs for endogenous ANGPTL3/8 & ANGPTL4/8 protein complexes.

Integrated AUC values for each peptide ion and the protein ratios for the endogenous ANGPTL3/8 and ANGPTL4/8 complexes are listed.

Integrated AUC, peptide ion ratios and proteins ratios for endogenous protein complexes presented in Table 1.

	ANGPTL3_132-137			ANGPTL3_177-187			ANGPTL3	ANGPTL8_133-138			ANGPTL8_148-153			ANGPTL8	ANGPTL4_64-71			ANGPTL4_97-110			ANGPTL4	Stoichiometry	
	Unlabeled	SIL	Area ratio	Unlabeled	SIL	Area ratio	Averaged ratio	Unlabeled	SIL	Area ratio	Unlabeled	SIL	Area ratio	Averaged ratio	Unlabeled	SIL	Area ratio	Unlabeled	SIL	Area ratio	Averaged ratio	ANGPTL3/8	ANGPTL4/8
Endogenous Angptl3/8_01	5.82E+05	4.57E+05	1.27	3.46E+04	2.58E+04	1.34	1.31	1.98E+05	5.40E+05	0.37	9.78E+04	2.60E+05	0.38	0.37								**3.5**	
Endogenous Angptl3/8_02	6.03E+05	4.80E+05	1.25	3.37E+04	2.66E+04	1.27	1.26	2.18E+05	5.87E+05	0.37	9.39E+04	2.64E+05	0.36	0.36								**3.4**	
SD			0.02			0.05	0.03			0.004			0.01	0.01								0.08	
Endogenous Angptl4/8_01								3.01E+04	4.83E+05	0.062	8.47E+03	1.47E+05	0.058	0.060	7.10E+03	1.75E+05	0.041	3.52E+04	6.41E+05	0.055	0.048		**0.8**
Endogenous Angptl4/8_02								2.64E+04	4.45E+05	0.059	9.18E+03	1.48E+05	0.062	0.061	1.20E+04	2.80E+05	0.043	2.99E+04	5.70E+05	0.052	0.048		**0.8**
SD										0.002			0.003	0.00			0.002			0.002	0.00		0.01

REFERENCES

1. Karantonis, H. C., T. Nomikos, and C. A. Demopoulos. 2009. Triacylglycerol metabolism. *Curr Drug Targets* **10**: 302-319.

2. Merkel, M., R. H. Eckel, and I. J. Goldberg. 2002. Lipoprotein lipase: genetics, lipid uptake, and regulation. *J Lipid Res* **43**: 1997-2006.

3. Berglund, L., J. D. Brunzell, A. C. Goldberg, I. J. Goldberg, F. Sacks, M. H. Murad, A. F. Stalenhoef, and s. Endocrine. 2012. Evaluation and treatment of hypertriglyceridemia: an Endocrine Society clinical practice guideline. *J Clin Endocrinol Metab* **97**: 2969-2989.

4. Zhang, R. 2016. The ANGPTL3-4-8 model, a molecular mechanism for triglyceride trafficking. *Open Biol* **6**: 150272.

5. Kersten, S. 2014. Physiological regulation of lipoprotein lipase. *Biochim Biophys Acta* **1841**: 919-933.

6. Chait, A., and S. Subramanian. 2000. Hypertriglyceridemia: Pathophysiology, Role of Genetics, Consequences, and Treatment. *In* Endotext. K. R. Feingold, B. Anawalt, A. Boyce, G. Chrousos, W. W. de Herder, K. Dungan, A. Grossman, J. M. Hershman, H. J. Hofland, G. Kaltsas, C. Koch, P. Kopp, M. Korbonits, R. McLachlan, J. E. Morley, M. New, J. Purnell, F. Singer, C. A. Stratakis, D. L. Trence, and D. P. Wilson, editors, South Dartmouth (MA).

7. Grundy, S. M., J. I. Cleeman, S. R. Daniels, K. A. Donato, R. H. Eckel, B. A. Franklin, D. J. Gordon, R. M. Krauss, P. J. Savage, S. C. Smith, Jr., J. A. Spertus, and C. Fernando. 2005. Diagnosis and management of the metabolic syndrome: an American Heart Association/National Heart, Lung, and Blood Institute scientific statement: Executive Summary. *Crit Pathw Cardiol* **4**: 198-203.

8. Abou Ziki, M. D., and A. Mani. 2016. Metabolic syndrome: genetic insights into disease pathogenesis. *Curr Opin Lipidol* **27**: 162-171.

9. NCEP. 2002. Third Report of the National Cholesterol Education Program (NCEP) Expert Panel on Detection, Evaluation, and Treatment of High Blood Cholesterol in Adults (Adult Treatment Panel III) final report. *Circulation* **106**: 3143-3421.

10. Freeman, A. M., and N. Pennings. 2020. Insulin Resistance. *In* StatPearls, Treasure Island (FL).

11. Grundy, S. M., B. Hansen, S. C. Smith, Jr., J. I. Cleeman, and R. A. Kahn. 2004. Clinical management of metabolic syndrome: report of the American Heart Association/National Heart, Lung, and Blood Institute/American Diabetes Association conference on scientific issues related to management. *Arterioscler Thromb Vasc Biol* **24**: e19-24.

12. Stancakova, A., and M. Laakso. 2014. Genetics of metabolic syndrome. *Rev Endocr Metab Disord* **15**: 243-252.

13. Panuganti, K. K., M. Nguyen, and R. K. Kshirsagar. 2020. Obesity. *In* StatPearls, Treasure Island (FL).

14. Peterfy, M. 2012. Lipase maturation factor 1: a lipase chaperone involved in lipid metabolism. *Biochim Biophys Acta* **1821**: 790-794.

15. Wang, H. H., D. K. Lee, M. Liu, P. Portincasa, and D. Q. Wang. 2020. Novel Insights into the Pathogenesis and Management of the Metabolic Syndrome. *Pediatr Gastroenterol Hepatol Nutr* **23**: 189-230.

16. Bansal, S., J. E. Buring, N. Rifai, S. Mora, F. M. Sacks, and P. M. Ridker. 2007. Fasting compared with nonfasting triglycerides and risk of cardiovascular events in women. *JAMA* **298**: 309-316.

17. Nordestgaard, B. G., M. Benn, P. Schnohr, and A. Tybjaerg-Hansen. 2007. Nonfasting triglycerides and risk of myocardial infarction, ischemic heart disease, and death in men and women. *JAMA* **298**: 299-308.

18. Bhatt, D. L., P. G. Steg, M. Miller, E. A. Brinton, T. A. Jacobson, S. B. Ketchum, R. T. Doyle, Jr., R. A. Juliano, L. Jiao, C. Granowitz, J. C. Tardif, and C. M. Ballantyne. 2019. Cardiovascular Risk Reduction with Icosapent Ethyl for Hypertriglyceridemia. *N Engl J Med* **380**: 11-22.

19. Yokoyama, M., H. Origasa, M. Matsuzaki, Y. Matsuzawa, Y. Saito, Y. Ishikawa, S. Oikawa, J. Sasaki, H. Hishida, H. Itakura, T. Kita, A. Kitabatake, N. Nakaya, T. Sakata, K. Shimada, and K. Shirato. 2007. Effects of eicosapentaenoic acid on major coronary events in hypercholesterolaemic patients (JELIS): a randomised open-label, blinded endpoint analysis. *Lancet* **369**: 1090-1098.

20. Eckel, R. H. 1989. Lipoprotein lipase. A multifunctional enzyme relevant to common metabolic diseases. *N Engl J Med* **320**: 1060-1068.

21. Goldberg, I. J. 1996. Lipoprotein lipase and lipolysis: central roles in lipoprotein metabolism and atherogenesis. *J Lipid Res* **37**: 693-707.

22. Mead, J. R., S. A. Irvine, and D. P. Ramji. 2002. Lipoprotein lipase: structure, function, regulation, and role in disease. *J Mol Med (Berl)* **80**: 753-769.

23. Hahn, P. F. 1943. Abolishment of alimentary lipemia following injection of heparin. *Science* **98**: 19-20.

24. Osborne, J. C., Jr., G. Bengtsson-Olivecrona, N. S. Lee, and T. Olivecrona. 1985. Studies on inactivation of lipoprotein lipase: role of the dimer to monomer dissociation. *Biochemistry* **24**: 5606-5611.

25. Iverius, P. H., and A. M. Ostlund-Lindqvist. 1976. Lipoprotein lipase from bovine milk. Isolation procedure, chemical characterization, and molecular weight analysis. *J Biol Chem* **251**: 7791-7795.

26. Kobayashi, Y., T. Nakajima, and I. Inoue. 2002. Molecular modeling of the dimeric structure of human lipoprotein lipase and functional studies of the carboxyl-terminal domain. *Eur J Biochem* **269**: 4701-4710.

27. Wong, H., D. Yang, J. S. Hill, R. C. Davis, J. Nikazy, and M. C. Schotz. 1997. A molecular biology-based approach to resolve the subunit orientation of lipoprotein lipase. *Proc Natl Acad Sci U S A* **94**: 5594-5598.

28. Zhang, L., A. Lookene, G. Wu, and G. Olivecrona. 2005. Calcium triggers folding of lipoprotein lipase into active dimers. *J Biol Chem* **280**: 42580-42591.

29. Korn, E. D. 1955. Clearing factor, a heparin-activated lipoprotein lipase. I. Isolation and characterization of the enzyme from normal rat heart. *J Biol Chem* **215**: 1-14.

30. Camps, L., M. Reina, M. Llobera, S. Vilaro, and T. Olivecrona. 1990. Lipoprotein lipase: cellular origin and functional distribution. *Am J Physiol* **258**: C673-681.

31. Holmes, R. S., J. L. Vandeberg, and L. A. Cox. 2011. Comparative studies of vertebrate lipoprotein lipase: a key enzyme of very low density lipoprotein metabolism. *Comp Biochem Physiol Part D Genomics Proteomics* **6**: 224-234.

32. van Tilbeurgh, H., A. Roussel, J. M. Lalouel, and C. Cambillau. 1994. Lipoprotein lipase. Molecular model based on the pancreatic lipase x-ray structure: consequences for heparin binding and catalysis. *J Biol Chem* **269**: 4626-4633.

33. Peterfy, M., O. Ben-Zeev, H. Z. Mao, D. Weissglas-Volkov, B. E. Aouizerat, C. R. Pullinger, P. H. Frost, J. P. Kane, M. J. Malloy, K. Reue, P. Pajukanta, and M. H. Doolittle. 2007. Mutations in LMF1 cause combined lipase deficiency and severe hypertriglyceridemia. *Nat Genet* **39**: 1483-1487.

34. Davies, B. S., A. P. Beigneux, R. H. Barnes, Y. Tu, P. Gin, M. M. Weinstein, C. Nobumori, R. Nyren, I. Goldberg, G. Olivecrona, A. Bensadoun, S. G. Young, and L. G. Fong. 2010. GPIHBP1 is responsible for the entry of lipoprotein lipase into capillaries. *Cell Metab* **12**: 42-52.

35. Young, S. G., B. S. Davies, L. G. Fong, P. Gin, M. M. Weinstein, A. Bensadoun, and A. P. Beigneux. 2007. GPIHBP1: an endothelial cell molecule important for the lipolytic processing of chylomicrons. *Curr Opin Lipidol* **18**: 389-396.

36. Sonnenburg, W. K., D. Yu, E. C. Lee, W. Xiong, G. Gololobov, B. Key, J. Gay, N. Wilganowski, Y. Hu, S. Zhao, M. Schneider, Z. M. Ding, B. P. Zambrowicz, G. Landes, D. R. Powell, and U. Desai. 2009. GPIHBP1 stabilizes lipoprotein lipase and prevents its inhibition by angiopoietin-like 3 and angiopoietin-like 4. *J Lipid Res* **50**: 2421-2429.

37. Kuwajima, M., D. W. Foster, and J. D. McGarry. 1988. Regulation of lipoprotein lipase in different rat tissues. *Metabolism* **37**: 597-601.

38. Lithell, H., J. Boberg, K. Hellsing, G. Lundqvist, and B. Vessby. 1978. Lipoprotein-lipase activity in human skeletal muscle and adipose tissue in the fasting and the fed states. *Atherosclerosis* **30**: 89-94.

39. Schoonjans, K., J. Peinado-Onsurbe, A. M. Lefebvre, R. A. Heyman, M. Briggs, S. Deeb, B. Staels, and J. Auwerx. 1996. PPARalpha and PPARgamma activators direct a distinct tissue-specific transcriptional response via a PPRE in the lipoprotein lipase gene. *EMBO J* **15**: 5336-5348.

40. Borensztajn, J., and D. S. Robinson. 1970. The effect of fasting on the utilization of chylomicron triglyceride fatty acids in relation to clearing factor lipase (lipoprotein lipase) releasable by heparin in the perfused rat heart. *J Lipid Res* **11**: 111-117.

41. Picard, F., N. Naimi, D. Richard, and Y. Deshaies. 1999. Response of adipose tissue lipoprotein lipase to the cephalic phase of insulin secretion. *Diabetes* **48**: 452-459.

42. Semenkovich, C. F., M. Wims, L. Noe, J. Etienne, and L. Chan. 1989. Insulin regulation of lipoprotein lipase activity in 3T3-L1 adipocytes is mediated at posttranscriptional and posttranslational levels. *J Biol Chem* **264**: 9030-9038.

43. Ruge, T., M. Bergo, M. Hultin, G. Olivecrona, and T. Olivecrona. 2000. Nutritional regulation of binding sites for lipoprotein lipase in rat heart. *Am J Physiol Endocrinol Metab* **278**: E211-218.

44. Shah, A. S., and D. P. Wilson. 2000. Genetic Disorders Causing Hypertriglyceridemia in Children and Adolescents. *In* Endotext. K. R. Feingold, B. Anawalt, A. Boyce, G. Chrousos, W. W. de Herder, K. Dungan, A. Grossman, J. M. Hershman, H. J. Hofland, G. Kaltsas, C. Koch, P. Kopp, M. Korbonits, R. McLachlan, J. E. Morley, M. New, J. Purnell, F. Singer, C. A. Stratakis, D. L. Trence, and D. P. Wilson, editors, South Dartmouth (MA).

45. Pimstone, S. N., S. E. Gagne, C. Gagne, P. J. Lupien, D. Gaudet, R. R. Williams, M. Kotze, P. W. Reymer, J. C. Defesche, and J. J. Kastelein. 1995. Mutations in the gene for lipoprotein lipase. A cause for low HDL cholesterol levels in individuals heterozygous for familial hypercholesterolemia. *Arterioscler Thromb Vasc Biol* **15**: 1704-1712.

46. Coleman, T., R. L. Seip, J. M. Gimble, D. Lee, N. Maeda, and C. F. Semenkovich. 1995. COOH-terminal disruption of lipoprotein lipase in mice is lethal in homozygotes, but heterozygotes have elevated triglycerides and impaired enzyme activity. *J Biol Chem* **270**: 12518-12525.

47. Santamarina-Fojo, S., and H. B. Brewer, Jr. 1991. The familial hyperchylomicronemia syndrome. New insights into underlying genetic defects. *JAMA* **265**: 904-908.

48. Weinstock, P. H., C. L. Bisgaier, K. Aalto-Setala, H. Radner, R. Ramakrishnan, S. Levak-Frank, A. D. Essenburg, R. Zechner, and J. L. Breslow. 1995. Severe hypertriglyceridemia, reduced high density lipoprotein, and neonatal death in lipoprotein lipase knockout mice. Mild hypertriglyceridemia with impaired very low density lipoprotein clearance in heterozygotes. *J Clin Invest* **96**: 2555-2568.

49. Shimada, M., H. Shimano, T. Gotoda, K. Yamamoto, M. Kawamura, T. Inaba, Y. Yazaki, and N. Yamada. 1994. Overexpression of human lipoprotein lipase in transgenic mice. Resistance to diet-induced hypertriglyceridemia and hypercholesterolemia. *J Biol Chem* **269**: 11673.

50. Shimada, M., S. Ishibashi, T. Gotoda, M. Kawamura, K. Yamamoto, T. Inaba, K. Harada, J. Ohsuga, S. Perrey, Y. Yazaki, and et al. 1995. Overexpression of human lipoprotein lipase protects diabetic transgenic mice from diabetic hypertriglyceridemia and hypercholesterolemia. *Arterioscler Thromb Vasc Biol* **15**: 1688-1694.

51. Rip, J., M. C. Nierman, C. J. Ross, J. W. Jukema, M. R. Hayden, J. J. Kastelein, E. S. Stroes, and J. A. Kuivenhoven. 2006. Lipoprotein lipase S447X: a naturally occurring gain-of-function mutation. *Arterioscler Thromb Vasc Biol* **26**: 1236-1245.

52. Havel, R. J., and R. S. Gordon, Jr. 1960. Idiopathic hyperlipemia: metabolic studies in an affected family. *J Clin Invest* **39**: 1777-1790.

53. Ross, C. J., G. Liu, J. A. Kuivenhoven, J. Twisk, J. Rip, W. van Dop, K. J. Excoffon, S. M. Lewis, J. J. Kastelein, and M. R. Hayden. 2005. Complete rescue of lipoprotein lipase-deficient mice by somatic gene transfer of the naturally occurring LPLS447X beneficial mutation. *Arterioscler Thromb Vasc Biol* **25**: 2143-2150.

54. Ference, B. A., J. J. P. Kastelein, K. K. Ray, H. N. Ginsberg, M. J. Chapman, C. J. Packard, U. Laufs, C. Oliver-Williams, A. M. Wood, A. S. Butterworth, E. Di Angelantonio, J. Danesh, S. J. Nicholls, D. L. Bhatt, M. S. Sabatine, and A. L. Catapano. 2019. Association of triglyceride-lowering LPL variants and LDL-C-lowering LDLR variants with risk of coronary heart disease. *JAMA* **321**: 364-373.

55. Hayne, C. K., M. J. Lafferty, B. J. Eglinger, J. P. Kane, and S. B. Neher. 2017. Biochemical analysis of the lipoprotein lipase truncation variant, LPL(S447X), reveals increased lipoprotein uptake. *Biochemistry* **56**: 525-533.

56. Ioka, R. X., M. J. Kang, S. Kamiyama, D. H. Kim, K. Magoori, A. Kamataki, Y. Ito, Y. A. Takei, M. Sasaki, T. Suzuki, H. Sasano, S. Takahashi, J. Sakai, T. Fujino, and T. T. Yamamoto. 2003. Expression cloning and characterization of a novel glycosylphosphatidylinositol-anchored high density lipoprotein-binding protein, GPI-HBP1. *J Biol Chem* **278**: 7344-7349.

57. Weinstein, M. M., L. Yin, A. P. Beigneux, B. S. Davies, P. Gin, K. Estrada, K. Melford, J. R. Bishop, J. D. Esko, G. M. Dallinga-Thie, L. G. Fong, A. Bensadoun, and S. G. Young. 2008. Abnormal patterns of lipoprotein lipase release into the plasma in GPIHBP1-deficient mice. *J Biol Chem* **283**: 34511-34518.

58. Mysling, S., K. K. Kristensen, M. Larsson, A. P. Beigneux, H. Gardsvoll, L. G. Fong, A. Bensadouen, T. J. Jorgensen, S. G. Young, and M. Ploug. 2016. The acidic domain of the endothelial membrane protein GPIHBP1 stabilizes lipoprotein lipase activity by preventing unfolding of its catalytic domain. *Elife* **5**: e12095.

59. Gin, P., L. Yin, B. S. Davies, M. M. Weinstein, R. O. Ryan, A. Bensadoun, L. G. Fong, S. G. Young, and A. P. Beigneux. 2008. The acidic domain of GPIHBP1 is important for the binding of lipoprotein lipase and chylomicrons. *J Biol Chem* **283**: 29554-29562.

60. Davies, B. S., H. Waki, A. P. Beigneux, E. Farber, M. M. Weinstein, D. C. Wilpitz, L. J. Tai, R. M. Evans, L. G. Fong, P. Tontonoz, and S. G. Young. 2008. The expression of GPIHBP1, an endothelial cell binding site for lipoprotein lipase and chylomicrons, is induced by peroxisome proliferator-activated receptor-gamma. *Mol Endocrinol* **22**: 2496-2504.

61. Beigneux, A. P., B. S. Davies, P. Gin, M. M. Weinstein, E. Farber, X. Qiao, F. Peale, S. Bunting, R. L. Walzem, J. S. Wong, W. S. Blaner, Z. M. Ding, K. Melford, N. Wongsiriroj, X. Shu, F. de Sauvage, R. O. Ryan, L. G. Fong, A. Bensadoun, and S. G. Young. 2007. Glycosylphosphatidylinositol-anchored high-density lipoprotein-binding protein 1 plays a critical role in the lipolytic processing of chylomicrons. *Cell Metab* **5**: 279-291.

62. Patni, N., Z. Ahmad, and D. P. Wilson. 2000. Genetics and Dyslipidemia. *In* Endotext. K. R. Feingold, B. Anawalt, A. Boyce, G. Chrousos, W. W. de Herder, K. Dungan, A. Grossman, J. M. Hershman, H. J. Hofland, G. Kaltsas, C. Koch, P. Kopp, M. Korbonits, R. McLachlan, J. E. Morley, M. New, J. Purnell, F. Singer, C. A. Stratakis, D. L. Trence, and D. P. Wilson, editors, South Dartmouth (MA).

63. Beigneux, A. P., R. Franssen, A. Bensadoun, P. Gin, K. Melford, J. Peter, R. L. Walzem, M. M. Weinstein, B. S. Davies, J. A. Kuivenhoven, J. J. Kastelein, L. G. Fong, G. M. Dallinga-Thie, and S. G. Young. 2009. Chylomicronemia with a mutant GPIHBP1 (Q115P) that cannot bind lipoprotein lipase. *Arterioscler Thromb Vasc Biol* **29**: 956-962.

64. Bergo, M., G. Olivecrona, and T. Olivecrona. 1996. Forms of lipoprotein lipase in rat tissues: in adipose tissue the proportion of inactive lipase increases on fasting. *Biochem J* **313 (Pt 3)**: 893-898.

65. Doolittle, M. H., O. Ben-Zeev, J. Elovson, D. Martin, and T. G. Kirchgessner. 1990. The response of lipoprotein lipase to feeding and fasting. Evidence for posttranslational regulation. *J Biol Chem* **265**: 4570-4577.

66. Borensztajn, J., M. S. Rone, S. P. Babirak, J. A. McGarr, and L. B. Oscai. 1975. Effect of exercise on lipoprotein lipase activity in rat heart and skeletal muscle. *Am J Physiol* **229**: 394-397.

67. Ben-Zeev, O., A. J. Lusis, R. C. LeBoeuf, J. Nikazy, and M. C. Schotz. 1983. Evidence for independent genetic regulation of heart and adipose lipoprotein lipase activity. *J Biol Chem* **258**: 13632-13636.

68. Brown, W. V., R. I. Levy, and D. S. Fredrickson. 1970. Further characterization of apolipoproteins from the human plasma very low density lipoproteins. *J Biol Chem* **245**: 6588-6594.

69. Olivecrona, G., and U. Beisiegel. 1997. Lipid binding of apolipoprotein CII is required for stimulation of lipoprotein lipase activity against apolipoprotein CII-deficient chylomicrons. *Arterioscler Thromb Vasc Biol* **17**: 1545-1549.

70. McIlhargey, T. L., Y. Yang, H. Wong, and J. S. Hill. 2003. Identification of a lipoprotein lipase cofactor-binding site by chemical cross-linking and transfer of apolipoprotein C-II-responsive lipolysis from lipoprotein lipase to hepatic lipase. *J Biol Chem* **278**: 23027-23035.

71. Larsson, M., E. Vorrsjo, P. Talmud, A. Lookene, and G. Olivecrona. 2013. Apolipoproteins C-I and C-III inhibit lipoprotein lipase activity by displacement of the enzyme from lipid droplets. *J Biol Chem* **288**: 33997-34008.

72. Conklin, D., D. Gilbertson, D. W. Taft, M. F. Maurer, T. E. Whitmore, D. L. Smith, K. M. Walker, L. H. Chen, S. Wattler, M. Nehls, and K. B. Lewis. 1999. Identification of a mammalian angiopoietin-related protein expressed specifically in liver. *Genomics* **62**: 477-482.

73. Kim, I., H. G. Kim, H. Kim, H. H. Kim, S. K. Park, C. S. Uhm, Z. H. Lee, and G. Y. Koh. 2000. Hepatic expression, synthesis and secretion of a novel fibrinogen/angiopoietin-related protein that prevents endothelial-cell apoptosis. *Biochem J* **346 Pt 3**: 603-610.

74. Koster, A., Y. B. Chao, M. Mosior, A. Ford, P. A. Gonzalez-DeWhitt, J. E. Hale, D. Li, Y. Qiu, C. C. Fraser, D. D. Yang, J. G. Heuer, S. R. Jaskunas, and P. Eacho. 2005. Transgenic angiopoietin-like (angptl)4 overexpression and targeted disruption of angptl4 and angptl3: regulation of triglyceride metabolism. *Endocrinology* **146**: 4943-4950.

75. Shimizugawa, T., M. Ono, M. Shimamura, K. Yoshida, Y. Ando, R. Koishi, K. Ueda, T. Inaba, H. Minekura, T. Kohama, and H. Furukawa. 2002. ANGPTL3 decreases very low density lipoprotein triglyceride clearance by inhibition of lipoprotein lipase. *J Biol Chem* **277**: 33742-33748.

76. Yoshida, K., T. Shimizugawa, M. Ono, and H. Furukawa. 2002. Angiopoietin-like protein 4 is a potent hyperlipidemia-inducing factor in mice and inhibitor of lipoprotein lipase. *J Lipid Res* **43**: 1770-1772.

77. Lee, E. C., U. Desai, G. Gololobov, S. Hong, X. Feng, X. C. Yu, J. Gay, N. Wilganowski, C. Gao, L. L. Du, J. Chen, Y. Hu, S. Zhao, L. Kirkpatrick, M. Schneider, B. P. Zambrowicz, G. Landes, D. R. Powell, and W. K. Sonnenburg. 2009. Identification of a new functional domain in angiopoietin-like 3 (ANGPTL3) and angiopoietin-like 4 (ANGPTL4) involved in binding and inhibition of lipoprotein lipase (LPL). *J Biol Chem* **284**: 13735-13745.

78. Ono, M., T. Shimizugawa, M. Shimamura, K. Yoshida, C. Noji-Sakikawa, Y. Ando, R. Koishi, and H. Furukawa. 2003. Protein region important for regulation of lipid metabolism in angiopoietin-like 3 (ANGPTL3): ANGPTL3 is cleaved and activated in vivo. *J Biol Chem* **278**: 41804-41809.

79. Ge, H., G. Yang, L. Huang, D. L. Motola, T. Pourbahrami, and C. Li. 2004. Oligomerization and regulated proteolytic processing of angiopoietin-like protein 4. *J Biol Chem* **279**: 2038-2045.

80. Sukonina, V., A. Lookene, T. Olivecrona, and G. Olivecrona. 2006. Angiopoietin-like protein 4 converts lipoprotein lipase to inactive monomers and modulates lipase activity in adipose tissue. *Proc Natl Acad Sci U S A* **103**: 17450-17455.

81. Ge, H., G. Yang, X. Yu, T. Pourbahrami, and C. Li. 2004. Oligomerization state-dependent hyperlipidemic effect of angiopoietin-like protein 4. *J Lipid Res* **45**: 2071-2079.

82. Ge, H., J. Y. Cha, H. Gopal, C. Harp, X. Yu, J. J. Repa, and C. Li. 2005. Differential regulation and properties of angiopoietin-like proteins 3 and 4. *J Lipid Res* **46**: 1484-1490.

83. Koishi, R., Y. Ando, M. Ono, M. Shimamura, H. Yasumo, T. Fujiwara, H. Horikoshi, and H. Furukawa. 2002. Angptl3 regulates lipid metabolism in mice. *Nat Genet* **30**: 151-157.

84. Desai, U., E. C. Lee, K. Chung, C. Gao, J. Gay, B. Key, G. Hansen, D. Machajewski, K. A. Platt, A. T. Sands, M. Schneider, I. Van Sligtenhorst, A. Suwanichkul, P. Vogel, N. Wilganowski, J. Wingert, B. P. Zambrowicz, G. Landes, and D. R. Powell. 2007. Lipid-lowering effects of anti-angiopoietin-like 4 antibody recapitulate the lipid phenotype found in angiopoietin-like 4 knockout mice. *Proc Natl Acad Sci U S A* **104**: 11766-11771.

85. Ando, Y., T. Shimizugawa, S. Takeshita, M. Ono, M. Shimamura, R. Koishi, and H. Furukawa. 2003. A decreased expression of angiopoietin-like 3 is protective against atherosclerosis in apoE-deficient mice. *J Lipid Res* **44**: 1216-1223.

86. Shimamura, M., M. Matsuda, H. Yasumo, M. Okazaki, K. Fujimoto, K. Kono, T. Shimizugawa, Y. Ando, R. Koishi, T. Kohama, N. Sakai, K. Kotani, R. Komuro, T. Ishida, K. Hirata, S. Yamashita, H. Furukawa, and I. Shimomura. 2007. Angiopoietin-like protein3 regulates plasma HDL cholesterol through suppression of endothelial lipase. *Arterioscler Thromb Vasc Biol* **27**: 366-372.

87. Mandard, S., F. Zandbergen, E. van Straten, W. Wahli, F. Kuipers, M. Muller, and S. Kersten. 2006. The fasting-induced adipose factor/angiopoietin-like protein 4 is physically associated with lipoproteins and governs plasma lipid levels and adiposity. *J Biol Chem* **281**: 934-944.

88. Lichtenstein, L., J. F. Berbee, S. J. van Dijk, K. W. van Dijk, A. Bensadoun, I. P. Kema, P. J. Voshol, M. Muller, P. C. Rensen, and S. Kersten. 2007. Angptl4 upregulates cholesterol synthesis in liver via inhibition of LPL- and HL-dependent hepatic cholesterol uptake. *Arterioscler Thromb Vasc Biol* **27**: 2420-2427.

89. Bergo, M., G. Wu, T. Ruge, and T. Olivecrona. 2002. Down-regulation of adipose tissue lipoprotein lipase during fasting requires that a gene, separate from the lipase gene, is switched on. *J Biol Chem* **277**: 11927-11932.

90. Shan, L., X. C. Yu, Z. Liu, Y. Hu, L. T. Sturgis, M. L. Miranda, and Q. Liu. 2009. The angiopoietin-like proteins ANGPTL3 and ANGPTL4 inhibit lipoprotein lipase activity through distinct mechanisms. *J Biol Chem* **284**: 1419-1424.

91. Chi, X., E. C. Britt, H. W. Shows, A. J. Hjelmaas, S. K. Shetty, E. M. Cushing, W. Li, A. Dou, R. Zhang, and B. S. J. Davies. 2017. ANGPTL8 promotes the ability of ANGPTL3 to bind and inhibit lipoprotein lipase. *Mol Metab* **6**: 1137-1149.

92. Shimamura, M., M. Matsuda, S. Kobayashi, Y. Ando, M. Ono, R. Koishi, H. Furukawa, M. Makishima, and I. Shimomura. 2003. Angiopoietin-like protein 3, a hepatic secretory factor, activates lipolysis in adipocytes. *Biochem Biophys Res Commun* **301**: 604-609.

93. Inaba, T., M. Matsuda, M. Shimamura, N. Takei, N. Terasaka, Y. Ando, H. Yasumo, R. Koishi, M. Makishima, and I. Shimomura. 2003. Angiopoietin-like protein 3 mediates hypertriglyceridemia induced by the liver X receptor. *J Biol Chem* **278**: 21344-21351.

94. Mattijssen, F., and S. Kersten. 2012. Regulation of triglyceride metabolism by Angiopoietin-like proteins. *Biochim Biophys Acta* **1821**: 782-789.

95. Kaplan, R., T. Zhang, M. Hernandez, F. X. Gan, S. D. Wright, M. G. Waters, and T. Q. Cai. 2003. Regulation of the angiopoietin-like protein 3 gene by LXR. *J Lipid Res* **44**: 136-143.

96. Inukai, K., Y. Nakashima, M. Watanabe, S. Kurihara, T. Awata, H. Katagiri, Y. Oka, and S. Katayama. 2004. ANGPTL3 is increased in both insulin-deficient and -resistant diabetic states. *Biochem Biophys Res Commun* **317**: 1075-1079.

97. Wang, Y., M. C. McNutt, S. Banfi, M. G. Levin, W. L. Holland, V. Gusarova, J. Gromada, J. C. Cohen, and H. H. Hobbs. 2015. Hepatic ANGPTL3 regulates adipose tissue energy homeostasis. *Proc Natl Acad Sci U S A* **112**: 11630-11635.

98. Mehta, N., A. Qamar, L. Qu, A. N. Qasim, N. N. Mehta, M. P. Reilly, and D. J. Rader. 2014. Differential association of plasma angiopoietin-like proteins 3 and 4 with lipid and metabolic traits. *Arterioscler Thromb Vasc Biol* **34**: 1057-1063.

99. Musunuru, K., J. P. Pirruccello, R. Do, G. M. Peloso, C. Guiducci, C. Sougnez, K. V. Garimella, S. Fisher, J. Abreu, A. J. Barry, T. Fennell, E. Banks, L. Ambrogio, K. Cibulskis, A. Kernytsky, E. Gonzalez, N. Rudzicz, J. C. Engert, M. A. DePristo, M. J. Daly, J. C. Cohen, H. H. Hobbs, D. Altshuler, G. Schonfeld, S. B. Gabriel, P. Yue, and S. Kathiresan. 2010. Exome sequencing, ANGPTL3 mutations, and familial combined hypolipidemia. *N Engl J Med* **363**: 2220-2227.

100. Romeo, S., W. Yin, J. Kozlitina, L. A. Pennacchio, E. Boerwinkle, H. H. Hobbs, and J. C. Cohen. 2009. Rare loss-of-function mutations in ANGPTL family members contribute to plasma triglyceride levels in humans. *J Clin Invest* **119**: 70-79.

101. Minicocci, I., A. Montali, M. R. Robciuc, F. Quagliarini, V. Censi, G. Labbadia, C. Gabiati, G. Pigna, M. L. Sepe, F. Pannozzo, D. Lutjohann, S. Fazio, M. Jauhiainen, C. Ehnholm, and M. Arca. 2012. Mutations in the ANGPTL3 gene and familial combined hypolipidemia: a clinical and biochemical characterization. *J Clin Endocrinol Metab* **97**: E1266-1275.

102. Dewey, F. E., V. Gusarova, R. L. Dunbar, C. O'Dushlaine, C. Schurmann, O. Gottesman, S. McCarthy, C. V. Van Hout, S. Bruse, H. M. Dansky, J. B. Leader, M. F. Murray, M. D. Ritchie, H. L. Kirchner, L. Habegger, A. Lopez, J. Penn, A. Zhao, W. Shao, N. Stahl, A. J. Murphy, S. Hamon, A. Bouzelmat, R. Zhang, B. Shumel, R. Pordy, D. Gipe, G. A. Herman, W. H. H. Sheu, I. T. Lee, K. W. Liang, X. Guo, J. I. Rotter, Y. I. Chen, W. E. Kraus, S. H. Shah, S. Damrauer, A. Small, D. J. Rader, A. B. Wulff, B. G. Nordestgaard, A. Tybjaerg-Hansen, A. M. van den Hoek, H. M. G. Princen, D. H. Ledbetter, D. J. Carey, J. D. Overton, J. G. Reid, W. J. Sasiela, P. Banerjee, A. R. Shuldiner, I. B. Borecki, T. M. Teslovich, G. D. Yancopoulos, S. J. Mellis, J. Gromada, and A. Baras. 2017. Genetic and pharmacologic inactivation of ANGPTL3 and cardiovascular disease. *N Engl J Med* **377**: 211-221.

103. Tarugi, P., S. Bertolini, and S. Calandra. 2019. Angiopoietin-like protein 3 (ANGPTL3) deficiency and familial combined hypolipidemia. *J Biomed Res* **33**: 73-81.

104. Fujimoto, K., R. Koishi, T. Shimizugawa, and Y. Ando. 2006. Angptl3-null mice show low plasma lipid concentrations by enhanced lipoprotein lipase activity. *Exp Anim* **55**: 27-34.

105. Wang, Y., V. Gusarova, S. Banfi, J. Gromada, J. C. Cohen, and H. H. Hobbs. 2015. Inactivation of ANGPTL3 reduces hepatic VLDL-triglyceride secretion. *J Lipid Res* **56**: 1296-1307.

106. Yoon, J. C., T. W. Chickering, E. D. Rosen, B. Dussault, Y. Qin, A. Soukas, J. M. Friedman, W. E. Holmes, and B. M. Spiegelman. 2000. Peroxisome proliferator-activated receptor gamma target gene encoding a novel angiopoietin-related protein associated with adipose differentiation. *Mol Cell Biol* **20**: 5343-5349.

107. Kersten, S., S. Mandard, N. S. Tan, P. Escher, D. Metzger, P. Chambon, F. J. Gonzalez, B. Desvergne, and W. Wahli. 2000. Characterization of the fasting-induced adipose factor FIAF, a novel peroxisome proliferator-activated receptor target gene. *J Biol Chem* **275**: 28488-28493.

108. Mandard, S., F. Zandbergen, N. S. Tan, P. Escher, D. Patsouris, W. Koenig, R. Kleemann, A. Bakker, F. Veenman, W. Wahli, M. Muller, and S. Kersten. 2004. The direct peroxisome proliferator-activated receptor target fasting-induced adipose factor (FIAF/PGAR/ANGPTL4) is present in blood plasma as a truncated protein that is increased by fenofibrate treatment. *J Biol Chem* **279**: 34411-34420.

109. Ntambi, J. M., M. Miyazaki, J. P. Stoehr, H. Lan, C. M. Kendziorski, B. S. Yandell, Y. Song, P. Cohen, J. M. Friedman, and A. D. Attie. 2002. Loss of stearoyl-CoA desaturase-1 function protects mice against adiposity. *Proc Natl Acad Sci U S A* **99**: 11482-11486.

110. Schmuth, M., C. M. Haqq, W. J. Cairns, J. C. Holder, S. Dorsam, S. Chang, P. Lau, A. J. Fowler, G. Chuang, A. H. Moser, B. E. Brown, M. Mao-Qiang, Y. Uchida, K. Schoonjans, J. Auwerx, P. Chambon, T. M. Willson, P. M. Elias, and K. R. Feingold. 2004. Peroxisome proliferator-activated receptor (PPAR)-beta/delta stimulates differentiation and lipid accumulation in keratinocytes. *J Invest Dermatol* **122**: 971-983.

111. Tien, E. S., J. W. Davis, and J. P. Vanden Heuvel. 2004. Identification of the CREB-binding protein/p300-interacting protein CITED2 as a peroxisome proliferator-activated receptor alpha coregulator. *J Biol Chem* **279**: 24053-24063.

112. Belanger, A. J., H. Lu, T. Date, L. X. Liu, K. A. Vincent, G. Y. Akita, S. H. Cheng, R. J. Gregory, and C. Jiang. 2002. Hypoxia up-regulates expression of peroxisome proliferator-activated receptor gamma angiopoietin-related gene (PGAR) in cardiomyocytes: role of hypoxia inducible factor 1alpha. *J Mol Cell Cardiol* **34**: 765-774.

113. Georgiadi, A., L. Lichtenstein, T. Degenhardt, M. V. Boekschoten, M. van Bilsen, B. Desvergne, M. Muller, and S. Kersten. 2010. Induction of cardiac Angptl4 by dietary fatty acids is mediated by peroxisome proliferator-activated receptor beta/delta and protects against fatty acid-induced oxidative stress. *Circ Res* **106**: 1712-1721.

114. Catoire, M., S. Alex, N. Paraskevopulos, F. Mattijssen, I. Evers-van Gogh, G. Schaart, J. Jeppesen, A. Kneppers, M. Mensink, P. J. Voshol, G. Olivecrona, N. S. Tan, M. K. Hesselink, J. F. Berbee, P. C. Rensen, E. Kalkhoven, P. Schrauwen, and S. Kersten. 2014. Fatty acid-inducible ANGPTL4 governs lipid metabolic response to exercise. *Proc Natl Acad Sci U S A* **111**: E1043-1052.

115. Kroupa, O., E. Vorrsjo, R. Stienstra, F. Mattijssen, S. K. Nilsson, V. Sukonina, S. Kersten, G. Olivecrona, and T. Olivecrona. 2012. Linking nutritional regulation of Angptl4, Gpihbp1, and Lmf1 to lipoprotein lipase activity in rodent adipose tissue. *BMC Physiol* **12**: 13.

116. Mysling, S., K. K. Kristensen, M. Larsson, O. Kovrov, A. Bensadouen, T. J. Jorgensen, G. Olivecrona, S. G. Young, and M. Ploug. 2016. The angiopoietin-like protein ANGPTL4 catalyzes unfolding of the hydrolase domain in lipoprotein lipase and the endothelial membrane protein GPIHBP1 counteracts this unfolding. *Elife* **5**: 1-18.

117. Kovrov, O., K. K. Kristensen, E. Larsson, M. Ploug, and G. Olivecrona. 2019. On the mechanism of angiopoietin-like protein 8 for control of lipoprotein lipase activity. *J Lipid Res* **60**: 783-793.

118. Lafferty, M. J., K. C. Bradford, D. A. Erie, and S. B. Neher. 2013. Angiopoietin-like protein 4 inhibition of lipoprotein lipase: evidence for reversible complex formation. *J Biol Chem* **288**: 28524-28534.

119. Dijk, W., and S. Kersten. 2016. Regulation of lipid metabolism by angiopoietin-like proteins. *Curr Opin Lipidol* **27**: 249-256.

120. Romeo, S., L. A. Pennacchio, Y. Fu, E. Boerwinkle, A. Tybjaerg-Hansen, H. H. Hobbs, and J. C. Cohen. 2007. Population-based resequencing of ANGPTL4 uncovers variations that reduce triglycerides and increase HDL. *Nat Genet* **39**: 513-516.

121. Yu, X., S. C. Burgess, H. Ge, K. K. Wong, R. H. Nassem, D. J. Garry, A. D. Sherry, C. R. Malloy, J. P. Berger, and C. Li. 2005. Inhibition of cardiac lipoprotein utilization by transgenic overexpression of Angptl4 in the heart. *Proc Natl Acad Sci U S A* **102**: 1767-1772.

122. Xu, A., M. C. Lam, K. W. Chan, Y. Wang, J. Zhang, R. L. Hoo, J. Y. Xu, B. Chen, W. S. Chow, A. W. Tso, and K. S. Lam. 2005. Angiopoietin-like protein 4 decreases blood glucose and improves glucose tolerance but induces hyperlipidemia and hepatic steatosis in mice. *Proc Natl Acad Sci U S A* **102**: 6086-6091.

123. Backhed, F., H. Ding, T. Wang, L. V. Hooper, G. Y. Koh, A. Nagy, C. F. Semenkovich, and J. I. Gordon. 2004. The gut microbiota as an environmental factor that regulates fat storage. *Proc Natl Acad Sci U S A* **101**: 15718-15723.

124. Mattijssen, F., S. Alex, H. J. Swarts, A. K. Groen, E. M. van Schothorst, and S. Kersten. 2014. Angptl4 serves as an endogenous inhibitor of intestinal lipid digestion. *Mol Metab* **3**: 135-144.

125. Iqbal, J., and M. M. Hussain. 2009. Intestinal lipid absorption. *Am J Physiol Endocrinol Metab* **296**: E1183-1194.

126. Hussain, M. M. 2014. Intestinal lipid absorption and lipoprotein formation. *Curr Opin Lipidol* **25**: 200-206.

127. Ren, G., J. Y. Kim, and C. M. Smas. 2012. Identification of RIFL, a novel adipocyte-enriched insulin target gene with a role in lipid metabolism. *Am J Physiol Endocrinol Metab* **303**: E334-351.

128. Zhang, R. 2012. Lipasin, a novel nutritionally-regulated liver-enriched factor that regulates serum triglyceride levels. *Biochem Biophys Res Commun* **424**: 786-792.

129. Quagliarini, F., Y. Wang, J. Kozlitina, N. V. Grishin, R. Hyde, E. Boerwinkle, D. M. Valenzuela, A. J. Murphy, J. C. Cohen, and H. H. Hobbs. 2012. Atypical angiopoietin-like protein that regulates ANGPTL3. *Proc Natl Acad Sci U S A* **109**: 19751-19756.

130. Fadaei, R., H. Shateri, J. K. DiStefano, N. Moradi, M. Mohammadi, F. Emami, H. Aghajani, and N. Ziamajidi. 2020. Higher circulating levels of ANGPTL8 are associated with body mass index, triglycerides, and endothelial dysfunction in patients with coronary artery disease. *Mol Cell Biochem* **469**: 29-39.

131. Fu, Z., F. Berhane, A. Fite, B. Seyoum, A. B. Abou-Samra, and R. Zhang. 2014. Elevated circulating lipasin/betatrophin in human type 2 diabetes and obesity. *Sci Rep* **4**: 5013.

132. Ebert, T., S. Kralisch, A. Hoffmann, A. Bachmann, U. Lossner, J. Kratzsch, M. Bluher, M. Stumvoll, A. Tonjes, and M. Fasshauer. 2014. Circulating angiopoietin-like protein 8 is independently associated with fasting plasma glucose and type 2 diabetes mellitus. *J Clin Endocrinol Metab* **99**: E2510-2517.

133. Fu, Z., A. B. Abou-Samra, and R. Zhang. 2014. An explanation for recent discrepancies in levels of human circulating betatrophin. *Diabetologia* **57**: 2232-2234.

134. Lee, J., S. W. Hong, S. E. Park, E. J. Rhee, C. Y. Park, K. W. Oh, S. W. Park, and W. Y. Lee. 2015. AMP-activated protein kinase suppresses the expression of LXR/SREBP-1 signaling-induced ANGPTL8 in HepG2 cells. *Mol Cell Endocrinol* **414**: 148-155.

135. Dang, F., R. Wu, P. Wang, Y. Wu, M. S. Azam, Q. Xu, Y. Chen, and Y. Liu. 2016. Fasting and feeding signals control the oscillatory expression of Angptl8 to modulate lipid metabolism. *Sci Rep* **6**: 1-13.

136. Yi, P., J. S. Park, and D. A. Melton. 2013. Betatrophin: a hormone that controls pancreatic beta cell proliferation. *Cell* **153**: 747-758.

137. Gusarova, V., C. A. Alexa, E. Na, P. E. Stevis, Y. Xin, S. Bonner-Weir, J. C. Cohen, H. H. Hobbs, A. J. Murphy, G. D. Yancopoulos, and J. Gromada. 2014. ANGPTL8/betatrophin does not control pancreatic beta cell expansion. *Cell* **159**: 691-696.

138. Wang, Y., F. Quagliarini, V. Gusarova, J. Gromada, D. M. Valenzuela, J. C. Cohen, and H. H. Hobbs. 2013. Mice lacking ANGPTL8 (Betatrophin) manifest disrupted triglyceride metabolism without impaired glucose homeostasis. *Proc Natl Acad Sci U S A* **110**: 16109-16114.

139. Fu, Z., A. B. Abou-Samra, and R. Zhang. 2015. A lipasin/Angptl8 monoclonal antibody lowers mouse serum triglycerides involving increased postprandial activity of the cardiac lipoprotein lipase. *Sci Rep* **5**: 18502.

140. Izumi, R., T. Kusakabe, M. Noguchi, H. Iwakura, T. Tanaka, T. Miyazawa, D. Aotani, K. Hosoda, K. Kangawa, and K. Nakao. 2018. CRISPR/Cas9-mediated Angptl8 knockout suppresses plasma triglyceride concentrations and adiposity in rats. *J Lipid Res* **59**: 1575-1585.

141. Peloso, G. M., P. L. Auer, J. C. Bis, A. Voorman, A. C. Morrison, N. O. Stitziel, J. A. Brody, S. A. Khetarpal, J. R. Crosby, M. Fornage, A. Isaacs, J. Jakobsdottir, M. F. Feitosa, G. Davies, J. E. Huffman, A. Manichaikul, B. Davis, K. Lohman, A. Y. Joon, A. V. Smith, M. L. Grove, P. Zanoni, V. Redon, S. Demissie, K. Lawson, U. Peters, C. Carlson, R. D. Jackson, K. K. Ryckman, R. H. Mackey, J. G. Robinson, D. S. Siscovick, P. J. Schreiner, J. C. Mychaleckyj, J. S. Pankow, A. Hofman, A. G. Uitterlinden, T. B. Harris, K. D. Taylor, J. M. Stafford, L. M. Reynolds, R. E. Marioni, A. Dehghan, O. H. Franco, A. P. Patel, Y. Lu, G. Hindy, O. Gottesman, E. P. Bottinger, O. Melander, M. Orho-Melander, R. J. Loos, S. Duga, P. A. Merlini, M. Farrall, A. Goel, R. Asselta, D. Girelli, N. Martinelli, S. H. Shah, W. E. Kraus, M. Li, D. J. Rader, M. P. Reilly, R. McPherson, H. Watkins, D. Ardissino, N. G. E. S. Project, Q. Zhang, J. Wang, M. Y. Tsai, H. A. Taylor, A. Correa, M. E. Griswold, L. A. Lange, J. M. Starr, I. Rudan, G. Eiriksdottir, L. J. Launer, J. M. Ordovas, D. Levy, Y. D. Chen, A. P. Reiner, C. Hayward, O. Polasek, I. J. Deary, I. B. Borecki, Y. Liu, V. Gudnason, J. G. Wilson, C. M. van Duijn, C. Kooperberg, S. S. Rich, B. M. Psaty, J. I. Rotter, C. J. O'Donnell, K. Rice, E. Boerwinkle, S. Kathiresan, and L. A. Cupples. 2014. Association of low-frequency and rare coding-sequence variants with blood lipids and coronary heart disease in 56,000 whites and blacks. *Am J Hum Genet* **94**: 223-232.

142. Clapham, K. R., A. Y. Chu, J. Wessel, P. Natarajan, J. Flannick, M. A. Rivas, S. Sartori, R. Mehran, U. Baber, V. Fuster, R. A. Scott, D. J. Rader, M. Boehnke, M. I. McCarthy, D. M. Altshuler, S. Kathiresan, and G. M. Peloso. 2016. A null mutation in ANGPTL8 does not associate with either plasma glucose or type 2 diabetes in humans. *BMC Endocr Disord* **16**: 7.

143. Gusarova, V., S. Banfi, C. A. Alexa-Braun, L. M. Shihanian, I. J. Mintah, J. S. Lee, Y. Xin, Q. Su, V. Kamat, J. C. Cohen, H. H. Hobbs, B. Zambrowicz, G. D. Yancopoulos, A. J. Murphy, and J. Gromada. 2017. ANGPTL8 Blockade With a Monoclonal Antibody Promotes Triglyceride Clearance, Energy Expenditure, and Weight Loss in Mice. *Endocrinology* **158**: 1252-1259.

144. Haller, J. F., I. J. Mintah, L. M. Shihanian, P. Stevis, D. Buckler, C. A. Alexa-Braun, S. Kleiner, S. Banfi, J. C. Cohen, H. H. Hobbs, G. D. Yancopoulos, A. J. Murphy, V. Gusarova, and J. Gromada. 2017. ANGPTL8 requires ANGPTL3 to inhibit lipoprotein lipase and plasma triglyceride clearance. *J Lipid Res* **58**: 1166-1173.

145. Siddiqa, A., J. Ahmad, A. Ali, R. Z. Paracha, Z. Bibi, and B. Aslam. 2016. Structural characterization of ANGPTL8 (betatrophin) with its interacting partner lipoprotein lipase. *Comput Biol Chem* **61**: 210-220.

146. Oldoni, F., H. Cheng, S. Banfi, V. Gusarova, J. C. Cohen, and H. H. Hobbs. 2020. ANGPTL8 has both endocrine and autocrine effects on substrate utilization. *JCI Insight* **5**.

147. Guo, C., Z. Zhao, X. Deng, Z. Chen, Z. Tu, and G. Yuan. 2019. Regulation of angiopoietin-like protein 8 expression under different nutritional and metabolic status. *Endocr J* **66**: 1039-1046.

148. Speakman, J. R. 2013. Evolutionary perspectives on the obesity epidemic: adaptive, maladaptive, and neutral viewpoints. *Annu Rev Nutr* **33**: 289-317.

149. Neel, J. V. 1962. Diabetes mellitus: a "thrifty" genotype rendered detrimental by "progress"? *Am J Hum Genet* **14**: 353-362.

150. Ungar, P. S., F. E. Grine, and M. F. Teaford. 2006. Diet in early Homo: a review of the evidence and a new model of adaptive versatility. *Annual Review of Anthropology* **35**: 209-228.

151. Hardy, K., J. Brand-Miller, K. D. Brown, M. G. Thomas, and L. Copeland. 2015. The importance of dietary carbohydrate in human evolution. *Q Rev Biol* **90**: 251-268.

152. Harris, D. N., I. Ruczinski, L. R. Yanek, L. C. Becker, D. M. Becker, H. Guio, T. Cui, F. H. Chilton, R. A. Mathias, and T. D. O'Connor. 2019. Evolution of hominin polyunsaturated fatty acid metabolism: from Africa to the New World. *Genome Biol Evol* **11**: 1417-1430.

153. Messer, E. 1984. Anthropological Perspectives on Diet. *Annual Review of Anthropology* **13**: 205-249.

154. Wells, J. C. 2012. The evolution of human adiposity and obesity: where did it all go wrong? *Dis Model Mech* **5**: 595-607.

155. Wells, J. C. 2006. The evolution of human fatness and susceptibility to obesity: an ethological approach. *Biol Rev Camb Philos Soc* **81**: 183-205.

156. Saklayen, M. G. 2018. The global epidemic of the metabolic syndrome. *Curr Hypertens Rep* **20**: 12.

157. Mendrick, D. L., A. M. Diehl, L. S. Topor, R. R. Dietert, Y. Will, M. A. La Merrill, S. Bouret, V. Varma, K. L. Hastings, T. T. Schug, S. G. Emeigh Hart, and F. G. Burleson. 2018. Metabolic syndrome and associated diseases: from the bench to the clinic. *Toxicol Sci* **162**: 36-42.

158. Esposito, K., P. Chiodini, A. Colao, A. Lenzi, and D. Giugliano. 2012. Metabolic syndrome and risk of cancer: a systematic review and meta-analysis. *Diabetes Care* **35**: 2402-2411.

159. Bhandari, R., G. A. Kelley, T. A. Hartley, and I. R. Rockett. 2014. Metabolic syndrome is associated with increased breast cancer risk: a systematic review with meta-analysis. *Int J Breast Cancer* **2014**: 189384.

160. O'Neill, S., and L. O'Driscoll. 2015. Metabolic syndrome: a closer look at the growing epidemic and its associated pathologies. *Obes Rev* **16**: 1-12.

161. Allott, E. H., and S. D. Hursting. 2015. Obesity and cancer: mechanistic insights from transdisciplinary studies. *Endocr Relat Cancer* **22**: R365-386.

162. Gonzalez-Muniesa, P., M. A. Martinez-Gonzalez, F. B. Hu, J. P. Despres, Y. Matsuzawa, R. J. F. Loos, L. A. Moreno, G. A. Bray, and J. A. Martinez. 2017. Obesity. *Nat Rev Dis Primers* **3**: 17034.

163. Camara, N. O., K. Iseki, H. Kramer, Z. H. Liu, and K. Sharma. 2017. Kidney disease and obesity: epidemiology, mechanisms and treatment. *Nat Rev Nephrol* **13**: 181-190.

164. Colditz, G. A., and L. L. Peterson. 2018. Obesity and cancer: evidence, impact, and future directions. *Clin Chem* **64**: 154-162.

165. Friedrich, M. J. 2017. Global obesity epidemic worsening global health. *JAMA* **318**: 603-603.

166. Seidell, J. C., and J. Halberstadt. 2016. Obesity: The obesity epidemic in the USA - no end in sight? *Nat Rev Endocrinol* **12**: 499-500.

167. Aguilar, M., T. Bhuket, S. Torres, B. Liu, and R. J. Wong. 2015. Prevalence of the metabolic syndrome in the United States, 2003-2012. *JAMA* **313**: 1973-1974.

168. Nolan, P. B., G. Carrick-Ranson, J. W. Stinear, S. A. Reading, and L. C. Dalleck. 2017. Prevalence of metabolic syndrome and metabolic syndrome components in young adults: A pooled analysis. *Prev Med Rep* **7**: 211-215.

169. Gurka, M. J., S. L. Filipp, and M. D. DeBoer. 2018. Geographical variation in the prevalence of obesity, metabolic syndrome, and diabetes among US adults. *Nutr Diabetes* **8**: 14.

170. Jensen, M. D., D. H. Ryan, C. M. Apovian, J. D. Ard, A. G. Comuzzie, K. A. Donato, F. B. Hu, V. S. Hubbard, J. M. Jakicic, R. F. Kushner, C. M. Loria, B. E. Millen, C. A. Nonas, F. X. Pi-Sunyer, J. Stevens, V. J. Stevens, T. A. Wadden, B. M. Wolfe, and S. Z. Yanovski. 2014. 2013 AHA/ACC/TOS guideline for the management of overweight and obesity in adults: a report of the American College of Cardiology/American Heart Association Task Force on Practice Guidelines and The Obesity Society. *J Am Coll Cardiol* **63**: 2985-3023.

171. von Bibra, H., S. Saha, A. Hapfelmeier, G. Muller, and P. E. H. Schwarz. 2017. Impact of the triglyceride/high-density lipoprotein cholesterol ratio and the hypertriglyceremic-waist phenotype to predict the metabolic syndrome and insulin resistance. *Horm Metab Res* **49**: 542-549.

172. Marotta, T., B. F. Russo, and L. A. Ferrara. 2010. Triglyceride-to-HDL-cholesterol ratio and metabolic syndrome as contributors to cardiovascular risk in overweight patients. *Obesity (Silver Spring)* **18**: 1608-1613.

173. Bitzur, R., H. Cohen, Y. Kamari, A. Shaish, and D. Harats. 2009. Triglycerides and HDL cholesterol: stars or second leads in diabetes? *Diabetes Care* **32 Suppl 2**: S373-377.

174. Gastaldelli, A., M. Gaggini, and R. A. DeFronzo. 2017. Role of adipose tissue insulin resistance in the natural history of Type 2 Diabetes: results from the San Antonio Metabolism Study. *Diabetes* **66**: 815-822.

175. Frayn, K. N. 2001. Adipose tissue and the insulin resistance syndrome. *Proc Nutr Soc* **60**: 375-380.

176. Sachs, S., S. Zarini, D. E. Kahn, K. A. Harrison, L. Perreault, T. Phang, S. A. Newsom, A. Strauss, A. Kerege, J. A. Schoen, D. H. Bessesen, T. Schwarzmayr, E. Graf, D. Lutter, J. Krumsiek, S. M. Hofmann, and B. C. Bergman. 2019. Intermuscular adipose tissue directly modulates skeletal muscle insulin sensitivity in humans. *Am J Physiol Endocrinol Metab* **316**: E866-E879.

177. DeFronzo, R. A., and D. Tripathy. 2009. Skeletal muscle insulin resistance is the primary defect in type 2 diabetes. *Diabetes Care* **32 Suppl 2**: S157-163.

178. Smith, U., and B. B. Kahn. 2016. Adipose tissue regulates insulin sensitivity: role of adipogenesis, de novo lipogenesis and novel lipids. *J Intern Med* **280**: 465-475.

179. Zhou, J., and G. Qin. 2012. Adipocyte dysfunction and hypertension. *Am J Cardiovasc Dis* **2**: 143-149.

180. Yiannikouris, F., M. Gupte, K. Putnam, S. Thatcher, R. Charnigo, D. L. Rateri, A. Daugherty, and L. A. Cassis. 2012. Adipocyte deficiency of angiotensinogen prevents obesity-induced hypertension in male mice. *Hypertension* **60**: 1524-1530.

181. Patel, J. V., H. S. Lim, E. A. Hughes, and G. Y. Lip. 2007. Adiponectin and hypertension: a putative link between adipocyte function and atherosclerotic risk? *J Hum Hypertens* **21**: 1-4.

182. Oriowo, M. A. 2015. Perivascular adipose tissue, vascular reactivity and hypertension. *Med Princ Pract* **24 Suppl 1**: 29-37.

183. Ferrannini, E. 1992. The haemodynamics of obesity: a theoretical analysis. *J Hypertens* **10**: 1417-1423.

184. Stapleton, P. A., M. E. James, A. G. Goodwill, and J. C. Frisbee. 2008. Obesity and vascular dysfunction. *Pathophysiology* **15**: 79-89.

185. Abu-Farha, M., J. Abubaker, I. Al-Khairi, P. Cherian, F. Noronha, S. Kavalakatt, A. Khadir, K. Behbehani, M. Alarouj, A. Bennakhi, and N. Elkum. 2016. Circulating angiopoietin-like protein 8 (betatrophin) association with HsCRP and metabolic syndrome. *Cardiovasc Diabetol* **15**: 25.

186. Zhang, R., and A. B. Abou-Samra. 2013. Emerging roles of Lipasin as a critical lipid regulator. *Biochem Biophys Res Commun* **432**: 401-405.

187. He, P. P., T. Jiang, X. P. OuYang, Y. Q. Liang, J. Q. Zou, Y. Wang, Q. Q. Shen, L. Liao, and X. L. Zheng. 2018. Lipoprotein lipase: Biosynthesis, regulatory factors, and its role in atherosclerosis and other diseases. *Clin Chim Acta* **480**: 126-137.

188. Beigneux, A. P., C. M. Allan, N. P. Sandoval, G. W. Cho, P. J. Heizer, R. S. Jung, K. L. Stanhope, P. J. Havel, G. Birrane, M. Meiyappan, J. E. t. Gill, M. Murakami, K. Miyashita, K. Nakajima, M. Ploug, L. G. Fong, and S. G. Young. 2019. Lipoprotein lipase is active as a monomer. *Proc Natl Acad Sci U S A* **116**: 6319-6328.

189. Chappell, D. A., G. L. Fry, M. A. Waknitz, L. E. Muhonen, M. W. Pladet, P. H. Iverius, and D. K. Strickland. 1993. Lipoprotein lipase induces catabolism of normal triglyceride-rich lipoproteins via the low density lipoprotein receptor-related protein/alpha 2-macroglobulin receptor in vitro. A process facilitated by cell-surface proteoglycans. *J Biol Chem* **268**: 14168-14175.

190. Young, S. G., L. G. Fong, A. P. Beigneux, C. M. Allan, C. He, H. Jiang, K. Nakajima, M. Meiyappan, G. Birrane, and M. Ploug. 2019. GPIHBP1 and Lipoprotein Lipase, Partners in Plasma Triglyceride Metabolism. *Cell Metab* **30**: 51-65.

191. Gusarova, V., C. A. Alexa, Y. Wang, A. Rafique, J. H. Kim, D. Buckler, I. J. Mintah, L. M. Shihanian, J. C. Cohen, H. H. Hobbs, Y. Xin, D. M. Valenzuela, A. J. Murphy, G. D. Yancopoulos, and J. Gromada. 2015. ANGPTL3 blockade with a human monoclonal antibody reduces plasma lipids in dyslipidemic mice and monkeys. *J Lipid Res* **56**: 1308-1317.

192. Aryal, B., N. L. Price, Y. Suarez, and C. Fernandez-Hernando. 2019. ANGPTL4 in Metabolic and Cardiovascular Disease. *Trends Mol Med* **25**: 723-734.

193. Dijk, W., and S. Kersten. 2014. Regulation of lipoprotein lipase by Angptl4. *Trends Endocrinol Metab* **25**: 146-155.

194. Gutgsell, A. R., S. V. Ghodge, A. A. Bowers, and S. B. Neher. 2019. Mapping the sites of the lipoprotein lipase (LPL)-angiopoietin-like protein 4 (ANGPTL4) interaction provides mechanistic insight into LPL inhibition. *J Biol Chem* **294**: 2678-2689.

195. Dijk, W., S. Schutte, E. O. Aarts, I. M. C. Janssen, L. Afman, and S. Kersten. 2018. Regulation of angiopoietin-like 4 and lipoprotein lipase in human adipose tissue. *J Clin Lipidol* **12**: 773-783.

196. Cushing, E. M., X. Chi, K. L. Sylvers, S. K. Shetty, M. J. Potthoff, and B. S. J. Davies. 2017. Angiopoietin-like 4 directs uptake of dietary fat away from adipose during fasting. *Mol Metab* **6**: 809-818.

197. Liu, J., H. Afroza, D. J. Rader, and W. Jin. 2010. Angiopoietin-like protein 3 inhibits lipoprotein lipase activity through enhancing its cleavage by proprotein convertases. *J Biol Chem* **285**: 27561-27570.

198. Ahmad, Z., P. Banerjee, S. Hamon, K. C. Chan, A. Bouzelmat, W. J. Sasiela, R. Pordy, S. Mellis, H. Dansky, D. A. Gipe, and R. L. Dunbar. 2019. Inhibition of Angiopoietin-like protein 3 with a monoclonal antibody reduces triglycerides in hypertriglyceridemia. *Circulation* **140**: 470-486.

199. Stitziel, N. O., A. V. Khera, X. Wang, A. J. Bierhals, A. C. Vourakis, A. E. Sperry, P. Natarajan, D. Klarin, C. A. Emdin, S. M. Zekavat, A. Nomura, J. Erdmann, H. Schunkert, N. J. Samani, W. E. Kraus, S. H. Shah, B. Yu, E. Boerwinkle, D. J. Rader, N. Gupta, P. M. Frossard, A. Rasheed, J. Danesh, E. S. Lander, S. Gabriel, D. Saleheen, K. Musunuru, S. Kathiresan, Promis, and M. I. G. Consortium. 2017. ANGPTL3 deficiency and protection against coronary artery disease. *J Am Coll Cardiol* **69**: 2054-2063.

200. Noto, D., A. B. Cefalu, V. Valenti, F. Fayer, E. Pinotti, M. Ditta, R. Spina, G. Vigna, P. Yue, S. Kathiresan, P. Tarugi, and M. R. Averna. 2012. Prevalence of ANGPTL3 and APOB gene mutations in subjects with combined hypolipidemia. *Arterioscler Thromb Vasc Biol* **32**: 805-809.

201. Oteng, A. B., A. Bhattacharya, S. Brodesser, L. Qi, N. S. Tan, and S. Kersten. 2017. Feeding Angptl4(-/-) mice trans fat promotes foam cell formation in mesenteric lymph nodes without leading to ascites. *J Lipid Res* **58**: 1100-1113.

202. Lichtenstein, L., F. Mattijssen, N. J. de Wit, A. Georgiadi, G. J. Hooiveld, R. van der Meer, Y. He, L. Qi, A. Koster, J. T. Tamsma, N. S. Tan, M. Muller, and S. Kersten. 2010. Angptl4 protects against severe proinflammatory effects of saturated fat by inhibiting fatty acid uptake into mesenteric lymph node macrophages. *Cell Metab* **12**: 580-592.

203. Bailetti, D., L. Bertoccini, R. M. Mancina, I. Barchetta, D. Capoccia, E. Cossu, A. Pujia, A. Lenzi, F. Leonetti, M. G. Cavallo, S. Romeo, and M. G. Baroni. 2019. ANGPTL4 gene E40K variation protects against obesity-associated dyslipidemia in participants with obesity. *Obes Sci Pract* **5**: 83-90.

204. Smart-Halajko, M. C., A. Kelley-Hedgepeth, M. C. Montefusco, J. A. Cooper, A. Kopin, J. M. McCaffrey, A. Balasubramanyam, H. J. Pownall, D. M. Nathan, I. Peter, P. J. Talmud, G. S. Huggins, and A. S. Look. 2011. ANGPTL4 variants E40K and T266M are associated with lower fasting triglyceride levels in Non-Hispanic White Americans from the Look AHEAD Clinical Trial. *BMC Med Genet* **12**: 89.

205. Dewey, F. E., V. Gusarova, C. O'Dushlaine, O. Gottesman, J. Trejos, C. Hunt, C. V. Van Hout, L. Habegger, D. Buckler, K. M. Lai, J. B. Leader, M. F. Murray, M. D. Ritchie, H. L. Kirchner, D. H. Ledbetter, J. Penn, A. Lopez, I. B. Borecki, J. D. Overton, J. G. Reid, D. J. Carey, A. J. Murphy, G. D. Yancopoulos, A. Baras, J. Gromada, and A. R. Shuldiner. 2016. Inactivating variants in ANGPTL4 and risk of coronary artery disease. *N Engl J Med* **374**: 1123-1133.

206. Lim, G. B. 2016. Genetics: Polymorphisms in ANGPTL4 link triglycerides with CAD. *Nat Rev Cardiol* **13**: 245.

207. Gusarova, V., C. O'Dushlaine, T. M. Teslovich, P. N. Benotti, T. Mirshahi, O. Gottesman, C. V. Van Hout, M. F. Murray, A. Mahajan, J. B. Nielsen, L. Fritsche, A. B. Wulff, D. F. Gudbjartsson, M. Sjogren, C. A. Emdin, R. A. Scott, W. J. Lee, A. Small, L. C. Kwee, O. P. Dwivedi, R. B. Prasad, S. Bruse, A. E. Lopez, J. Penn, A. Marcketta, J. B. Leader, C. D. Still, H. L. Kirchner, U. L. Mirshahi, A. H. Wardeh, C. M. Hartle, L. Habegger, S. N. Fetterolf, T. Tusie-Luna, A. P. Morris, H. Holm, V. Steinthorsdottir, P. Sulem, U. Thorsteinsdottir, J. I. Rotter, L. M. Chuang, S. Damrauer, D. Birtwell, C. M. Brummett, A. V. Khera, P. Natarajan, M. Orho-Melander, J. Flannick, L. A. Lotta, C. J. Willer, O. L. Holmen, M. D. Ritchie, D. H. Ledbetter, A. J. Murphy, I. B. Borecki, J. G. Reid, J. D. Overton, O. Hansson, L. Groop, S. H. Shah, W. E. Kraus, D. J. Rader, Y. I. Chen, K. Hveem, N. J. Wareham, S. Kathiresan, O. Melander, K. Stefansson, B. G. Nordestgaard, A. Tybjaerg-Hansen, G. R. Abecasis, D. Altshuler, J. C. Florez, M. Boehnke, M. I. McCarthy, G. D. Yancopoulos, D. J. Carey, A. R. Shuldiner, A. Baras, F. E. Dewey, and J. Gromada. 2018. Genetic inactivation of ANGPTL4 improves glucose homeostasis and is associated with reduced risk of diabetes. *Nat Commun* **9**: 2252.

208. Samnegard, A., A. Silveira, P. Lundman, S. Boquist, J. Odeberg, J. Hulthe, W. McPheat, P. Tornvall, L. Bergstrand, C. G. Ericsson, A. Hamsten, and P. Eriksson. 2005. Serum matrix metalloproteinase-3 concentration is influenced by MMP-3 -1612 5A/6A promoter genotype and associated with myocardial infarction. *J Intern Med* **258**: 411-419.

209. Mannila, M. N., P. Eriksson, P. Lundman, A. Samnegard, S. Boquist, C. G. Ericsson, P. Tornvall, A. Hamsten, and A. Silveira. 2005. Contribution of haplotypes across the fibrinogen gene cluster to variation in risk of myocardial infarction. *Thromb Haemost* **93**: 570-577.

210. Silveira, A., D. Scanavini, S. Boquist, C. G. Ericsson, M. L. Hellenius, K. Leander, U. de Faire, J. Ohrvik, B. Woodhams, J. H. Morrissey, and A. Hamsten. 2012. Relationships of plasma factor VIIa-antithrombin complexes to manifest and future cardiovascular disease. *Thromb Res* **130**: 221-225.

211. Medh, J. D., G. L. Fry, S. L. Bowen, S. Ruben, H. Wong, and D. A. Chappell. 2000. Lipoprotein lipase- and hepatic triglyceride lipase- promoted very low density lipoprotein degradation proceeds via an apolipoprotein E-dependent mechanism. *J Lipid Res* **41**: 1858-1871.

212. Henry, R. R., S. Mudaliar, T. P. Ciaraldi, D. A. Armstrong, P. Burke, J. Pettus, P. Garhyan, S. L. Choi, S. J. Jacober, M. P. Knadler, E. C. Lam, M. J. Prince, N. Bose, N. Porksen, V. P. Sinha, and H. Linnebjerg. 2014. Basal insulin peglispro demonstrates preferential hepatic versus peripheral action relative to insulin glargine in healthy subjects. *Diabetes Care* **37**: 2609-2615.

213. Ginsberg, H., B. Cariou, T. Orchard, L. Chen, J. Luo, E. J. Bastyr, 3rd, J. Bue-Valleskey, A. M. Chang, T. Ivanyi, S. J. Jacober, and B. J. Hoogwerf. 2016. Lipid changes during basal insulin peglispro, insulin glargine, or NPH treatment in six IMAGINE trials. *Diabetes Obes Metab* **18**: 1089-1092.

214. Luo, M., and D. Peng. 2018. ANGPTL8: An Important Regulator in Metabolic Disorders. *Front Endocrinol (Lausanne)* **9**: 169.

215. Nidhina Haridas, P. A., J. Soronen, S. Sadevirta, R. Mysore, F. Quagliarini, A. Pasternack, J. Metso, J. Perttila, M. Leivonen, C. M. Smas, P. Fischer-Posovszky, M. Wabitsch, C. Ehnholm, O. Ritvos, M. Jauhiainen, V. M. Olkkonen, and H. Yki-Jarvinen. 2015. Regulation of Angiopoietin-Like Proteins (ANGPTLs) 3 and 8 by Insulin. *J Clin Endocrinol Metab* **100**: E1299-1307.

216. Troutt, J. S., R. W. Siegel, J. Chen, J. H. Sloan, M. A. Deeg, G. Cao, and R. J. Konrad. 2011. Dual-monoclonal, sandwich immunoassay specific for glucose-dependent insulinotropic peptide1-42, the active form of the incretin hormone. *Clin Chem* **57**: 849-855.

217. Su, X., and D. Q. Peng. 2018. New insights into ANGPLT3 in controlling lipoprotein metabolism and risk of cardiovascular diseases. *Lipids Health Dis* **17**: 12.

218. Staiger, H., C. Haas, J. Machann, R. Werner, M. Weisser, F. Schick, F. Machicao, N. Stefan, A. Fritsche, and H.-U. Häring. 2009. Muscle-Derived Angiopoietin-Like Protein 4 Is Induced by Fatty Acids via Peroxisome Proliferator–Activated Receptor (PPAR)-δ and Is of Metabolic Relevance in Humans. *Diabetes* **58**: 579-589.

219. Williams, S. E., I. Inoue, H. Tran, G. L. Fry, M. W. Pladet, P. H. Iverius, J. M. Lalouel, D. A. Chappell, and D. K. Strickland. 1994. The carboxyl-terminal domain of lipoprotein lipase binds to the low density lipoprotein receptor-related protein/alpha 2-macroglobulin receptor (LRP) and mediates binding of normal very low density lipoproteins to LRP. *J Biol Chem* **269**: 8653-8658.

220. Beisiegel, U., W. Weber, and G. Bengtsson-Olivecrona. 1991. Lipoprotein lipase enhances the binding of chylomicrons to low density lipoprotein receptor-related protein. *Proc Natl Acad Sci U S A* **88**: 8342-8346.

221. Takahashi, S., J. Suzuki, M. Kohno, K. Oida, T. Tamai, S. Miyabo, T. Yamamoto, and T. Nakai. 1995. Enhancement of the binding of triglyceride-rich lipoproteins to the very low density lipoprotein receptor by apolipoprotein E and lipoprotein lipase. *J Biol Chem* **270**: 15747-15754.

222. Loeffler, B., J. Heeren, M. Blaeser, H. Radner, D. Kayser, B. Aydin, and M. Merkel. 2007. Lipoprotein lipase-facilitated uptake of LDL is mediated by the LDL receptor. *J Lipid Res* **48**: 288-298.

223. Wung, S. F., M. V. Kulkarni, C. R. Pullinger, M. J. Malloy, J. P. Kane, and B. E. Aouizerat. 2006. The lipoprotein lipase gene in combined hyperlipidemia: evidence of a protective allele depletion. *Lipids Health Dis* **5**: 19.

224. Adachi, H., T. Kondo, G. Y. Koh, A. Nagy, Y. Oike, and E. Araki. 2011. Angptl4 deficiency decreases serum triglyceride levels in low-density lipoprotein receptor knockout mice and streptozotocin-induced diabetic mice. *Biochem Biophys Res Commun* **409**: 177-180.

225. Chen, Y. Q., T. G. Pottanat, R. W. Siegel, M. Ehsani, Y. W. Qian, E. Y. Zhen, A. Regmi, W. C. Roell, H. Guo, M. J. Luo, R. E. Gimeno, F. Van't Hooft, and R. J. Konrad. 2020. Angiopoietin-like protein 8 differentially regulates ANGPTL3 and ANGPTL4 during postprandial partitioning of fatty acids. *J Lipid Res* **61**: 1203-1220.

226. Wolska, A., M. Reimund, and A. T. Remaley. 2020. Apolipoprotein C-II: the re-emergence of a forgotten factor. *Curr Opin Lipidol* **31**: 147-153.

227. Larsson, M., C. M. Allan, R. S. Jung, P. J. Heizer, A. P. Beigneux, S. G. Young, and L. G. Fong. 2017. Apolipoprotein C-III inhibits triglyceride hydrolysis by GPIHBP1-bound LPL. *J Lipid Res* **58**: 1893-1902.

228. Pennacchio, L. A., M. Olivier, J. A. Hubacek, J. C. Cohen, D. R. Cox, J. C. Fruchart, R. M. Krauss, and E. M. Rubin. 2001. An apolipoprotein influencing triglycerides in humans and mice revealed by comparative sequencing. *Science* **294**: 169-173.

229. van der Vliet, H. N., M. G. Sammels, A. C. Leegwater, J. H. Levels, P. H. Reitsma, W. Boers, and R. A. Chamuleau. 2001. Apolipoprotein A-V: a novel apolipoprotein associated with an early phase of liver regeneration. *J Biol Chem* **276**: 44512-44520.

230. van der Vliet, H. N., F. G. Schaap, J. H. Levels, R. Ottenhoff, N. Looije, J. G. Wesseling, A. K. Groen, and R. A. Chamuleau. 2002. Adenoviral overexpression of apolipoprotein A-V reduces serum levels of triglycerides and cholesterol in mice. *Biochem Biophys Res Commun* **295**: 1156-1159.

231. Pennacchio, L. A., and E. M. Rubin. 2003. Apolipoprotein A5, a newly identified gene that affects plasma triglyceride levels in humans and mice. *Arterioscler Thromb Vasc Biol* **23**: 529-534.

232. Baroukh, N., E. Bauge, J. Akiyama, J. Chang, V. Afzal, J. C. Fruchart, E. M. Rubin, J. Fruchart-Najib, and L. A. Pennacchio. 2004. Analysis of apolipoprotein A5, c3, and plasma triglyceride concentrations in genetically engineered mice. *Arterioscler Thromb Vasc Biol* **24**: 1297-1302.

233. Pennacchio, L. A., M. Olivier, J. A. Hubacek, R. M. Krauss, E. M. Rubin, and J. C. Cohen. 2002. Two independent apolipoprotein A5 haplotypes influence human plasma triglyceride levels. *Hum Mol Genet* **11**: 3031-3038.

234. Evans, D., A. Buchwald, and F. U. Beil. 2003. The single nucleotide polymorphism -1131T>C in the apolipoprotein A5 (APOA5) gene is associated with elevated triglycerides in patients with hyperlipidemia. *J Mol Med (Berl)* **81**: 645-654.

235. Kao, J. T., H. C. Wen, K. L. Chien, H. C. Hsu, and S. W. Lin. 2003. A novel genetic variant in the apolipoprotein A5 gene is associated with hypertriglyceridemia. *Hum Mol Genet* **12**: 2533-2539.

236. Horinek, A., M. Vrablik, R. Ceska, V. Adamkova, R. Poledne, and J. A. Hubacek. 2003. T-1131-->C polymorphism within the apolipoprotein AV gene in hypertriglyceridemic individuals. *Atherosclerosis* **167**: 369-370.

237. Prieur, X., H. Coste, and J. C. Rodriguez. 2003. The human apolipoprotein AV gene is regulated by peroxisome proliferator-activated receptor-alpha and contains a novel farnesoid X-activated receptor response element. *J Biol Chem* **278**: 25468-25480.

238. Vu-Dac, N., P. Gervois, H. Jakel, M. Nowak, E. Bauge, H. Dehondt, B. Staels, L. A. Pennacchio, E. M. Rubin, J. Fruchart-Najib, and J. C. Fruchart. 2003. Apolipoprotein A5, a crucial determinant of plasma triglyceride levels, is highly responsive to peroxisome proliferator-activated receptor alpha activators. *J Biol Chem* **278**: 17982-17985.

239. Schultze, A. E., W. E. Alborn, R. K. Newton, and R. J. Konrad. 2005. Administration of a PPARalpha agonist increases serum apolipoprotein A-V levels and the apolipoprotein A-V/apolipoprotein C-III ratio. *J Lipid Res* **46**: 1591-1595.

240. Wong, K., and R. O. Ryan. 2007. Characterization of apolipoprotein A-V structure and mode of plasma triacylglycerol regulation. *Curr Opin Lipidol* **18**: 319-324.

241. Sharma, V., R. O. Ryan, and T. M. Forte. 2012. Apolipoprotein A-V dependent modulation of plasma triacylglycerol: a puzzlement. *Biochim Biophys Acta* **1821**: 795-799.

242. Forte, T. M., and R. O. Ryan. 2015. Apolipoprotein A5: Extracellular and Intracellular Roles in Triglyceride Metabolism. *Curr Drug Targets* **16**: 1274-1280.

243. O'Brien, P. J., W. E. Alborn, J. H. Sloan, M. Ulmer, A. Boodhoo, M. D. Knierman, A. E. Schultze, and R. J. Konrad. 2005. The novel apolipoprotein A5 is present in human serum, is associated with VLDL, HDL, and chylomicrons, and circulates at very low concentrations compared with other apolipoproteins. *Clin Chem* **51**: 351-359.

244. Alborn, W. E., M. G. Johnson, M. J. Prince, and R. J. Konrad. 2006. Definitive N-terminal protein sequence and further characterization of the novel apolipoprotein A5 in human serum. *Clin Chem* **52**: 514-517.

245. Kirchgessner, T. G., P. Sleph, J. Ostrowski, J. Lupisella, C. S. Ryan, X. Liu, G. Fernando, D. Grimm, P. Shipkova, R. Zhang, R. Garcia, J. Zhu, A. He, H. Malone, R. Martin, K. Behnia, Z. Wang, Y. C. Barrett, R. J. Garmise, L. Yuan, J. Zhang, M. D. Gandhi, P. Wastall, T. Li, S. Du, L. Salvador, R. Mohan, G. H. Cantor, E. Kick, J. Lee, and R. J. Frost. 2016. Beneficial and adverse effects of an LXR agonist on human lipid and lipoprotein metabolism and circulating neutrophils. *Cell Metab* **24**: 223-233.

246. Jakel, H., M. Nowak, E. Moitrot, H. Dehondt, D. W. Hum, L. A. Pennacchio, J. Fruchart-Najib, and J. C. Fruchart. 2004. The liver X receptor ligand T0901317 down-regulates APOA5 gene expression through activation of SREBP-1c. *J Biol Chem* **279**: 45462-45469.

247. Beigneux, A. P., B. S. Davies, A. Bensadoun, L. G. Fong, and S. G. Young. 2009. GPIHBP1, a GPI-anchored protein required for the lipolytic processing of triglyceride-rich lipoproteins. *J Lipid Res* **50 Suppl**: S57-62.

248. Joseph, S. B., E. McKilligin, L. Pei, M. A. Watson, A. R. Collins, B. A. Laffitte, M. Chen, G. Noh, J. Goodman, G. N. Hagger, J. Tran, T. K. Tippin, X. Wang, A. J. Lusis, W. A. Hsueh, R. E. Law, J. L. Collins, T. M. Willson, and P. Tontonoz. 2002. Synthetic LXR ligand inhibits the development of atherosclerosis in mice. *Proc Natl Acad Sci U S A* **99**: 7604-7609.

249. Bradley, M. N., C. Hong, M. Chen, S. B. Joseph, D. C. Wilpitz, X. Wang, A. J. Lusis, A. Collins, W. A. Hseuh, J. L. Collins, R. K. Tangirala, and P. Tontonoz. 2007. Ligand activation of LXR beta reverses atherosclerosis and cellular cholesterol overload in mice lacking LXR alpha and apoE. *J Clin Invest* **117**: 2337-2346.

250. Grefhorst, A., B. M. Elzinga, P. J. Voshol, T. Plosch, T. Kok, V. W. Bloks, F. H. van der Sluijs, L. M. Havekes, J. A. Romijn, H. J. Verkade, and F. Kuipers. 2002. Stimulation of lipogenesis by pharmacological activation of the liver X receptor leads to production of large, triglyceride-rich very low density lipoprotein particles. *J Biol Chem* **277**: 34182-34190.

251. Parikh, M., K. Patel, S. Soni, and T. Gandhi. 2014. Liver X receptor: a cardinal target for atherosclerosis and beyond. *J Atheroscler Thromb* **21**: 519-531.

252. Chen, G., G. Liang, J. Ou, J. L. Goldstein, and M. S. Brown. 2004. Central role for liver X receptor in insulin-mediated activation of Srebp-1c transcription and stimulation of fatty acid synthesis in liver. *Proc Natl Acad Sci U S A* **101**: 11245-11250.

253. Nowak, M., A. Helleboid-Chapman, H. Jakel, G. Martin, D. Duran-Sandoval, B. Staels, E. M. Rubin, L. A. Pennacchio, M. R. Taskinen, J. Fruchart-Najib, and J. C. Fruchart. 2005. Insulin-mediated down-regulation of apolipoprotein A5 gene expression through the phosphatidylinositol 3-kinase pathway: role of upstream stimulatory factor. *Mol Cell Biol* **25**: 1537-1548.

254. Sun, X., M. E. Haas, J. Miao, A. Mehta, M. J. Graham, R. M. Crooke, J. P. Pais de Barros, J. G. Wang, M. Aikawa, D. Masson, and S. B. Biddinger. 2016. Insulin Dissociates the Effects of Liver X Receptor on Lipogenesis, Endoplasmic Reticulum Stress, and Inflammation. *J Biol Chem* **291**: 1115-1122.

255. Repa, J. J., and D. J. Mangelsdorf. 2002. The liver X receptor gene team: potential new players in atherosclerosis. *Nat Med* **8**: 1243-1248.

256. Komati, R., D. Spadoni, S. Zheng, J. Sridhar, K. E. Riley, and G. Wang. 2017. Ligands of Therapeutic Utility for the Liver X Receptors. *Molecules* **22**.

257. Mutemberezi, V., O. Guillemot-Legris, and G. G. Muccioli. 2016. Oxysterols: From cholesterol metabolites to key mediators. *Prog Lipid Res* **64**: 152-169.

258. Guillemot-Legris, O., V. Mutemberezi, and G. G. Muccioli. 2016. Oxysterols in Metabolic Syndrome: From Bystander Molecules to Bioactive Lipids. *Trends Mol Med* **22**: 594-614.

259. Haas, J. T., J. Miao, D. Chanda, Y. Wang, E. Zhao, M. E. Haas, M. Hirschey, B. Vaitheesvaran, R. V. Farese, Jr., I. J. Kurland, M. Graham, R. Crooke, F. Foufelle, and S. B. Biddinger. 2012. Hepatic insulin signaling is required for obesity-dependent expression of SREBP-1c mRNA but not for feeding-dependent expression. *Cell Metab* **15**: 873-884.

260. Tobin, K. A., S. M. Ulven, G. U. Schuster, H. H. Steineger, S. M. Andresen, J. A. Gustafsson, and H. I. Nebb. 2002. Liver X receptors as insulin-mediating factors in fatty acid and cholesterol biosynthesis. *J Biol Chem* **277**: 10691-10697.

261. Zierler, K. 1999. Whole body glucose metabolism. *Am J Physiol* **276**: E409-426.

262. Chawla, A., J. J. Repa, R. M. Evans, and D. J. Mangelsdorf. 2001. Nuclear receptors and lipid physiology: opening the X-files. *Science* **294**: 1866-1870.

263. Cha, J. Y., and J. J. Repa. 2007. The liver X receptor (LXR) and hepatic lipogenesis. The carbohydrate-response element-binding protein is a target gene of LXR. *J Biol Chem* **282**: 743-751.

264. Lazar, M. A., and T. M. Willson. 2007. Sweet dreams for LXR. *Cell Metab* **5**: 159-161.

265. Denechaud, P. D., P. Bossard, J. M. Lobaccaro, L. Millatt, B. Staels, J. Girard, and C. Postic. 2008. ChREBP, but not LXRs, is required for the induction of glucose-regulated genes in mouse liver. *J Clin Invest* **118**: 956-964.

266. Shiota, M., and M. A. Magnuson. 2008. Hepatic glucose sensing: does flux matter? *J Clin Invest* **118**: 841-844.

267. Repa, J. J., G. Liang, J. Ou, Y. Bashmakov, J. M. Lobaccaro, I. Shimomura, B. Shan, M. S. Brown, J. L. Goldstein, and D. J. Mangelsdorf. 2000. Regulation of mouse sterol regulatory element-binding protein-1c gene (SREBP-1c) by oxysterol receptors, LXRalpha and LXRbeta. *Genes Dev* **14**: 2819-2830.

268. Schultz, J. R., H. Tu, A. Luk, J. J. Repa, J. C. Medina, L. Li, S. Schwendner, S. Wang, M. Thoolen, D. J. Mangelsdorf, K. D. Lustig, and B. Shan. 2000. Role of LXRs in control of lipogenesis. *Genes Dev* **14**: 2831-2838.

269. Yoshikawa, T., H. Shimano, M. Amemiya-Kudo, N. Yahagi, A. H. Hasty, T. Matsuzaka, H. Okazaki, Y. Tamura, Y. Iizuka, K. Ohashi, J. Osuga, K. Harada, T. Gotoda, S. Kimura, S. Ishibashi, and N. Yamada. 2001. Identification of liver X receptor-retinoid X receptor as an activator of the sterol regulatory element-binding protein 1c gene promoter. *Mol Cell Biol* **21**: 2991-3000.

270. Hasty, A. H., H. Shimano, N. Yahagi, M. Amemiya-Kudo, S. Perrey, T. Yoshikawa, J. Osuga, H. Okazaki, Y. Tamura, Y. Iizuka, F. Shionoiri, K. Ohashi, K. Harada, T. Gotoda, R. Nagai, S. Ishibashi, and N. Yamada. 2000. Sterol regulatory element-binding protein-1 is regulated by glucose at the transcriptional level. *J Biol Chem* **275**: 31069-31077.

271. Mitro, N., P. A. Mak, L. Vargas, C. Godio, E. Hampton, V. Molteni, A. Kreusch, and E. Saez. 2007. The nuclear receptor LXR is a glucose sensor. *Nature* **445**: 219-223.

272. Joseph, S. B., B. A. Laffitte, P. H. Patel, M. A. Watson, K. E. Matsukuma, R. Walczak, J. L. Collins, T. F. Osborne, and P. Tontonoz. 2002. Direct and indirect mechanisms for regulation of fatty acid synthase gene expression by liver X receptors. *J Biol Chem* **277**: 11019-11025.

273. Svensson, S., T. Ostberg, M. Jacobsson, C. Norstrom, K. Stefansson, D. Hallen, I. C. Johansson, K. Zachrisson, D. Ogg, and L. Jendeberg. 2003. Crystal structure of the heterodimeric complex of LXRalpha and RXRbeta ligand-binding domains in a fully agonistic conformation. *EMBO J* **22**: 4625-4633.

274. Hu, X., S. Li, J. Wu, C. Xia, and D. S. Lala. 2003. Liver X receptors interact with corepressors to regulate gene expression. *Mol Endocrinol* **17**: 1019-1026.

275. Huuskonen, J., P. E. Fielding, and C. J. Fielding. 2004. Role of p160 coactivator complex in the activation of liver X receptor. *Arterioscler Thromb Vasc Biol* **24**: 703-708.

276. Lee, S., J. Lee, S. K. Lee, and J. W. Lee. 2008. Activating signal cointegrator-2 is an essential adaptor to recruit histone H3 lysine 4 methyltransferases MLL3 and MLL4 to the liver X receptors. *Mol Endocrinol* **22**: 1312-1319.

277. Kim, S. W., K. Park, E. Kwak, E. Choi, S. Lee, J. Ham, H. Kang, J. M. Kim, S. Y. Hwang, Y. Y. Kong, K. Lee, and J. W. Lee. 2003. Activating signal cointegrator 2 required for liver lipid metabolism mediated by liver X receptors in mice. *Mol Cell Biol* **23**: 3583-3592.

278. Kim, G. H., K. Park, S. Y. Yeom, K. J. Lee, G. Kim, J. Ko, D. K. Rhee, Y. H. Kim, H. K. Lee, H. W. Kim, G. T. Oh, K. U. Lee, J. W. Lee, and S. W. Kim. 2009. Characterization of ASC-2 as an antiatherogenic transcriptional coactivator of liver X receptors in macrophages. *Mol Endocrinol* **23**: 966-974.

279. Son, Y. L., and Y. C. Lee. 2010. Molecular determinants of the interactions between SRC-1 and LXR/RXR heterodimers. *FEBS Lett* **584**: 3862-3866.

280. Anthonisen, E. H., L. Berven, S. Holm, M. Nygard, H. I. Nebb, and L. M. Gronning-Wang. 2010. Nuclear receptor liver X receptor is O-GlcNAc-modified in response to glucose. *J Biol Chem* **285**: 1607-1615.

281. Foretz, M., C. Guichard, P. Ferre, and F. Foufelle. 1999. Sterol regulatory element binding protein-1c is a major mediator of insulin action on the hepatic expression of glucokinase and lipogenesis-related genes. *Proc Natl Acad Sci U S A* **96**: 12737-12742.

282. Foretz, M., C. Pacot, I. Dugail, P. Lemarchand, C. Guichard, X. Le Liepvre, C. Berthelier-Lubrano, B. Spiegelman, J. B. Kim, P. Ferre, and F. Foufelle. 1999. ADD1/SREBP-1c is required in the activation of hepatic lipogenic gene expression by glucose. *Mol Cell Biol* **19**: 3760-3768.

283. Koo, S. H., and H. C. Towle. 2000. Glucose regulation of mouse S(14) gene expression in hepatocytes. Involvement of a novel transcription factor complex. *J Biol Chem* **275**: 5200-5207.

284. Shimomura, I., Y. Bashmakov, S. Ikemoto, J. D. Horton, M. S. Brown, and J. L. Goldstein. 1999. Insulin selectively increases SREBP-1c mRNA in the livers of rats with streptozotocin-induced diabetes. *Proc Natl Acad Sci U S A* **96**: 13656-13661.

285. Yamashita, H., M. Takenoshita, M. Sakurai, R. K. Bruick, W. J. Henzel, W. Shillinglaw, D. Arnot, and K. Uyeda. 2001. A glucose-responsive transcription factor that regulates carbohydrate metabolism in the liver. *Proc Natl Acad Sci U S A* **98**: 9116-9121.

286. Uyeda, K., and J. J. Repa. 2006. Carbohydrate response element binding protein, ChREBP, a transcription factor coupling hepatic glucose utilization and lipid synthesis. *Cell Metab* **4**: 107-110.

287. Dentin, R., J. Girard, and C. Postic. 2005. Carbohydrate responsive element binding protein (ChREBP) and sterol regulatory element binding protein-1c (SREBP-1c): two key regulators of glucose metabolism and lipid synthesis in liver. *Biochimie* **87**: 81-86.

288. Zhang, Z., H. Wu, L. Dai, Y. Yuan, Y. Zhu, Z. Ma, X. Ruan, and X. Guo. 2020. ANGPTL8 enhances insulin sensitivity by directly activating insulin-mediated AKT phosphorylation. *Gene* **749**: 144707.

289. Harris, R. B. 2014. Direct and indirect effects of leptin on adipocyte metabolism. *Biochim Biophys Acta* **1842**: 414-423.

290. Sinha, R. A., B. K. Singh, and P. M. Yen. 2018. Direct effects of thyroid hormones on hepatic lipid metabolism. *Nat Rev Endocrinol* **14**: 259-269.

291. Speakman, J. R. 2008. Thrifty genes for obesity, an attractive but flawed idea, and an alternative perspective: the 'drifty gene' hypothesis. *Int J Obes (Lond)* **32**: 1611-1617.

292. Raal, F. J., R. S. Rosenson, L. F. Reeskamp, G. K. Hovingh, J. J. P. Kastelein, P. Rubba, S. Ali, P. Banerjee, K. C. Chan, D. A. Gipe, N. Khilla, R. Pordy, D. M. Weinreich, G. D. Yancopoulos, Y. Zhang, D. Gaudet, and E. H. Investigators. 2020. Evinacumab for Homozygous Familial Hypercholesterolemia. *N Engl J Med* **383**: 711-720.

293. Graham, M. J., R. G. Lee, T. A. Brandt, L. J. Tai, W. Fu, R. Peralta, R. Yu, E. Hurh, E. Paz, B. W. McEvoy, B. F. Baker, N. C. Pham, A. Digenio, S. G. Hughes, R. S. Geary, J. L. Witztum, R. M. Crooke, and S. Tsimikas. 2017. Cardiovascular and Metabolic Effects of ANGPTL3 Antisense Oligonucleotides. *N Engl J Med* **377**: 222-232.

294. Basu, D., J. Manjur, and W. Jin. 2011. Determination of lipoprotein lipase activity using a novel fluorescent lipase assay. *J Lipid Res* **52**: 826-832.

295. Hale, J. E., J. P. Butler, V. Gelfanova, J. S. You, and M. D. Knierman. 2004. A simplified procedure for the reduction and alkylation of cysteine residues in proteins prior to proteolytic digestion and mass spectral analysis. *Anal Biochem* **333**: 174-181.

296. Higgs, R. E., J. P. Butler, B. Han, and M. D. Knierman. 2013. Quantitative Proteomics via High Resolution MS Quantification: Capabilities and Limitations. *Int J Proteomics* **2013**: 674282.

VITA

Education

Purdue University – Indianapolis	PhD Biology	2016-2020
Purdue University – Indianapolis	Non-Thesis Masters	2008-2009
Indiana University – Bloomington	BA Biology	2004-2008
Indiana University – Bloomington	BA Biochemistry	2004-2008
Indiana University – Bloomington	Political Science Minor	2004-2008

Professional Experience

2007-2007 Research Intern – Nutritional Analytical Protein Sciences, Bristol Myers Squibb

2009-2014 Senior Scientist, Immunogenicity and Biomarker Assay Development, Laboratory for Experimental Medicine, Eli Lilly & Company

2014-2016 Associate Consultant Scientist, Immunogenicity & Biomarker Assay Development, Laboratory for Experimental Medicine, Eli Lilly & Company

2016-Current Consultant Scientist, Scientific Implementation, Laboratory for Experimental Medicine

Research Experience

2003-2003 Basic Science Research, Indiana University School of Medicine, Department of Cellular and Integrative Physiology

Elucidation of Ca^{2+} involvement in ROS induced vascular contraction

2004-2005 Basic Science Research, Indiana University, Department of Psychology

Cerebellar timing deficits in relation to improper sensory gating in schizophrenia

2007-2008 Basic Science Research, Indiana University, Department of Psychology

Effects of MK-801 in reversing effects of Fetal Alcohol Syndrome

2016-2020 PhD Candidate, Purdue University, Department of Biology

Effects of ANGPTL proteins on triglyceride metabolism

Publications

Bivi N, Swearingen CA, Shockley T, Sloan JH, Pottanat TG, et al. Development and validation of a novel immunogenicity assay to detect anti-drug and anti-PEG antibodies simultaneously with high sensitivity. J Immunol Methods. 2020;112856. doi:10.1016/j.jim.2020.112856

Chen YQ*, Pottanat TG*, Siegel RW, et al. Angiopoietin-like protein 8 differentially regulates ANGPTL3 and ANGPTL4 during postprandial partitioning of fatty acids. J Lipid Res. 2020;jlr.RA120000781. doi:10.1194/jlr.RA120000781 (**Co-First Author Publication)*

Jin Y, Smith CL, Hu L, Coutant DE, Whitehurst K, Phipps K1, McNearney TA, Yang XY, Ackermann BL, Pottanat TG, Landschulz W. "LY3127760, a Selective Prostaglandin E 4 (EP4) Receptor Antagonist, Demonstrated a Similar Pharmacological Profile as Celecoxib*." Clin Transl Sci.* 2018 Jan;11(1):46-53

John H Sloan, Richard G Conway, Thomas G Pottanat, Jason S Troutt, Richard E Higgs, Robert J Konrad, Yue-Wei Qian. "An innovative and highly drug-tolerant approach for detecting neutralizing antibodies directed to therapeutic antibodies." *Bioanalysis*, Vol. 8, No. 20, Pages 2157-2168

Chen YQ, Pottanat TG, Carter QL, Troutt JS, Konrad RJ, Sloan JH, "Affinity capture elution bridging assay: A novel immunoassay format for detection of anti-therapeutic protein antibodies." *J Immunol Methods*. 2016 Apr; 431:45-51

Thomas G. Pottanat, Guoqing Cao, Robert J. Konrad, Jason S. Troutt. "Biological and Analytical Considerations for PCSK9; a Key Target for LDL-Cholesterol Lowering." *Current Topics in Biochemical Research* 13.2 (2011): 1 - 11.

Thomas G. Pottanat, Carolyn A. Cook, Robert J. Konrad. "ATP Stimulates the Secretion of Caspase-1 from Human Peripheral Blood Cells through a Mechanism Involving the Purinergic Receptor P2x7." *Current Topics in Biochemical Research* 13.2 (2011): 57 - 66.

"The Development and Validation of High Sensitivity CGRP Assays Using Meso Scale Discovery and Quanterix Platforms" Xiyun Chai, Jing Xu, Kirk W. Johnson, Thomas George Pottanat, Robert I. Osborne, Karen Cox, Robert J. Benschop, Jeffrey L. Dage, Kalpana Merchant, Lisa Adams, Jayne Talbot, Bradley B. Miller.

Presented at: 5th European Headache and Migraine Trust International Congress (EHMTIC), 15-18Sept2016, Glasgow, UK.

Presented at: 58th Annual Scientific Meeting American Headache Society. 9-12June2016 San Diego, CA

Selected Awards

2002 *Finalist at Intel International Science and Engineering Fair,* Louisville, KY

- Based on work conducted under Mark Graves MD

2004 *Finalist at Intel International Science and Engineering Fair,* Portland, OR

- Based on work conducted under Subah Packer PhD

2004 *3rd Place Indiana's Most Outstanding Junior Scientist Award*

- Based on work conducted under Subah Packer PhD

2004 *Cecil B. Raymond Award & Castle High School Crest Award,*

- Recognition of Academic & Community Leadership, of personal achievement, and of significant contribution to Castle High School

2004 *Herman B Wells Scholarship, Indiana University,* Bloomington Indiana

- Offered to 18 incoming freshmen based on merit
- https://newsinfo.iu.edu/news/page/normal/1558.html
- Award Accepted

2004 *Presidential Scholarship, Saint Louis University,* Saint Louis, Missouri

- Award Declined

2016 *Lilly Innovator Award*

- Improvement of Immunogenicity Assay Reagents

2019 *Eli Lilly Multicultural Leadership Development Program*

2020 *Eli Lilly Emerson Award*

- Development of novel therapeutic: lipid lowering antibody

JOURNAL OF LIPID RESEARCH ASBMB

✥ Author's Choice

Angiopoietin-like protein 8 differentially regulates ANGPTL3 and ANGPTL4 during postprandial partitioning of fatty acids

Yan Q. Chen,[1,*] Thomas G. Pottanat,[1,*] Robert W. Siegel,[*] Mariam Ehsani,[*] Yue-Wei Qian,[*] Eugene Y. Zhen,[*] Ajit Regmi,[*] William C. Roell,[*] Haihong Guo,[*] M. Jane Luo,[*] Ruth E. Gimeno,[*] Ferdinand van't Hooft,[†] and Robert J. Konrad[2,*]

Lilly Research Laboratories,[*] Eli Lilly and Company, Indianapolis, IN; Division of Cardiovascular Medicine,[†] Department of Medicine Solna, Karolinska Institutet Karolinska University Hospital Solna, Stockholm, Sweden

Abstract Angiopoietin-like protein (ANGPTL)8 has been implicated in metabolic syndrome and reported to regulate adipose FA uptake through unknown mechanisms. Here, we studied how complex formation of ANGPTL8 with ANGPTL3 or ANGPTL4 varies with feeding to regulate LPL. In human serum, ANGPTL3/8 and ANGPTL4/8 complexes both increased postprandially, correlated negatively with HDL, and correlated positively with all other metabolic syndrome markers. ANGPTL3/8 also correlated positively with LDL-C and blocked LPL-facilitated hepatocyte VLDL-C uptake. LPL-inhibitory activity of ANGPTL3/8 was >100-fold more potent than that of ANGPTL3, and LPL-inhibitory activity of ANGPTL4/8 was >100-fold less potent than that of ANGPTL4. Quantitative analyses of inhibitory activities and competition experiments among the complexes suggested a model in which localized ANGPTL4/8 blocks the LPL-inhibitory activity of both circulating ANGPTL3/8 and localized ANGPTL4, allowing lipid sequestration into fat rather than muscle during the fed state. Supporting this model, insulin increased ANGPTL3/8 secretion from hepatocytes and ANGPTL4/8 secretion from adipocytes. These results suggest that low ANGPTL8 levels during fasting enable ANGPTL4-mediated LPL inhibition in fat tissue to minimize adipose FA uptake. During feeding, increased ANGPTL8 increases ANGPTL3 inhibition of LPL in muscle via circulating ANGPTL3/8, while decreasing ANGPTL4 inhibition of LPL in adipose tissue through localized ANGPTL4/8, thereby increasing FA uptake into adipose tissue. Excessive caloric intake may shift this system toward the latter conditions, possibly predisposing to metabolic syndrome.**—Chen, Y. Q., T. G. Pottanat, R. W. Siegel, M. Ehsani, Y-W. Qian, E. Y. Zhen, A. Regmi, W. C. Roell, H. Guo, M. J. Luo, R. E. Gimeno, F. van't Hooft, and R. J. Konrad. **Angiopoietin-like protein 8 differentially regulates ANGPTL3 and ANGPTL4 during postprandial partitioning of fatty acids.** *J. Lipid Res.* **2020. 61: 1203–1220.**

Supplementary key words lipoprotein lipase • adipose tissue • muscle • triglycerides • metabolic syndrome • angiopoietin-like protein 3 • angiopoietin-like protein 4 • lipid metabolism • obesity • postprandial condition

As humans evolved, the greatest survival threat was insufficient caloric intake (1–5). Our predecessors therefore relied on mechanisms that during times of starvation could direct FAs toward skeletal muscle to provide energy to hunt for food. Similarly, they relied on mechanisms that, during relatively rare periods of caloric availability, could reduce FA uptake into skeletal muscle and shift FA toward adipose tissue for storage as TGs to prepare for future periods of famine. These mechanisms allowed hominids to survive food scarcity. In a modern world of caloric abundance, however, the result is an unprecedented increase in metabolic syndrome and its related comorbidities (6–9).

Metabolic syndrome includes elevated TG, decreased HDL, obesity, hypertension, and insulin resistance/impaired glucose tolerance (9). This constellation of abnormalities predisposes not only to type 2 diabetes and increased cardiovascular disease but also to an increased risk of peripheral vascular disease, nonalcoholic fatty liver disease, and several types of cancer (10–17). It is currently estimated that two-thirds of the US population is overweight, and that one-third suffers from metabolic syndrome (18–23). At its most basic level, metabolic syndrome manifests as

This work was supported by Eli Lilly and Company. The authors declare that they have no conflicts of interest with the contents of this article.

Manuscript received 25 March 2020 and in revised form 9 May 2020.

Published, JLR Papers in Press, June 2, 2020
DOI https://doi.org/10.1194/jlr.RA120000781

Abbreviations: ANGPTL, angiopoietin-like protein; BIL, basal insulin peglispro; CTDC, C-terminal domain-containing; GIP, glucose-dependent insulinotropic peptide; HSA, human serum albumin; MRM, multiple reaction monitoring; MSD, Meso Scale Discovery; Ni-NTA, nickel-nitrilotriacetic acid; PECF, 1,2-dioleoyl-*sn*-glycero-3-phosphoethanolamine-*N*-carboxyfluorescein; PL, phospholipid; SEC, size exclusion chromatography; SIL, stable-isotope-labeled.

[1] Y. Q. Chen and T. G. Pottanat contributed equally to this work and are listed in alphabetical order.

[2] To whom correspondence should be addressed.
e-mail: konrad_robert@lilly.com

The online version of this article (available at https://www.jlr.org) contains a supplement.